

TSUNAMI RISK ASSESSMENT USING GIS-BASED MULTI CRITERIA
DECISION ANALYSIS AT BAKIRKÖY, İSTANBUL

A THESIS SUBMITTED TO
THE GRADUATE SCHOOL OF NATURAL AND APPLIED SCIENCES
OF
MIDDLE EAST TECHNICAL UNIVERSITY

BY

DUYGU TÜFEKÇİ

IN PARTIAL FULFILLMENT OF THE REQUIREMENTS
FOR
THE DEGREE OF MASTER OF SCIENCE
IN
GEOLOGICAL ENGINEERING

AUGUST 2016

Approval of the thesis:

**TSUNAMI RISK ASSESSMENT USING GIS-BASED MULTI CRITERIA
DECISION ANALYSIS AT BAKIRKÖY, İSTANBUL**

submitted by **DUYGU TÜFEKÇİ** in partial fulfillment of the requirements for the degree of **Master of Science in Geological Engineering Department, Middle East Technical University** by,

Prof. Dr. Gülbin Dural Ünver
Dean, Graduate School of **Natural and Applied Sciences**

Prof. Dr. Erdin Bozkurt
Head of Department, **Geological Engineering**

Prof. Dr. M. Lütfi Süzen
Supervisor, **Geological Engineering Dept., METU**

Prof. Dr. Ahmet Cevdet Yalçiner
Co-Supervisor, **Civil Engineering Dept., METU**

Examining Committee Members

Prof. Dr. Nurkan Karahanoğlu
Geological Engineering Dept., METU

Prof. Dr. M. Lütfi Süzen
Geological Engineering Dept., METU

Prof. Dr. Ahmet Cevdet Yalçiner
Civil Engineering Dept., METU

Assoc. Prof. Dr. Bekir Taner San
Geological Engineering Dept, Akdeniz University

Assist. Prof. Dr. A. Arda Özacar
Geological Engineering Dept., METU

Date:

22.08.2016

I hereby declare that all information in this document has been obtained and presented in accordance with academic rules and ethical conduct. I also declare that, as required by these rules and conduct, I have fully cited and referenced all material and results that are not original to this work.

Name, Last name: Duygu Tüfekçi

Signature:

ABSTRACT

TSUNAMI RISK ASSESSMENT USING GIS-BASED MULTI CRITERIA DECISION ANALYSIS AT BAKIRKÖY, İSTANBUL

Tüfekçi, Duygu

M.Sc., Department of Geological Engineering

Supervisor: Prof. Dr. M. Lütfi Süzen

Co-Supervisor: Prof. Dr. Ahmet Cevdet Yalçın

August 2016, 118 pages

Northern coast of the Sea of Marmara hosts many of coastal facilities. Bakırköy is one of the most critical coastal districts of İstanbul with the importance of air and marine transportation. There are many other coastal facilities and structures in Bakırköy district such as marinas, small scaled craft harbors, water front roads and business centers that are prone to suffer from the marine disasters. In the history, the Sea of Marmara has experienced numerous earthquakes and associated tsunamis. Therefore, risk assessment is essential for Bakırköy district, as well as for other parts of İstanbul.

In this study, a new methodology for tsunami risk assessment is further developed and applied to Bakırköy district of İstanbul. For determination of the worst case hazard scenario, simulations are performed on the tsunami numerical model NAMI DANCE. Human vulnerability assessments are realized by using GIS-based Multi Criteria Decision Analysis (MCDA). Among MCDA methods, Analytical Hierarchy Process (AHP) is selected. Vulnerability at location and evacuation resilience are the main elements in the hierarchical structure of AHP. Hazard and human vulnerability

assessments are integrated to obtain the tsunami risk assessments for Bakırköy district. In the risk relation, the preparedness and awareness level of the community is also considered. The hazard, vulnerability and risk assessments are also evaluated according to the neighborhoods of Bakırköy district and the population.

The tsunami simulations revealed that the maximum inundation distance is over 350 m on land and water penetrates almost 1700 m along Ayamama Stream. Inundation is observed in eleven neighborhoods of Bakırköy district. In the inundation zone, maximum flow depth is found to be over 5.7 meters. The inundated area forms 4.2% of whole Bakırköy district and 62 buildings are located in the inundation zone. According to the human vulnerability assessment, Sakızağacı and Ataköy 2-5-6 are the locationally most vulnerable neighborhoods while Yenimahalle is the one where the evacuation is most resilient. The risk assessments showed that the Ataköy 2-5-6 neighborhood is the one where the risk is very high and it is followed by Sakızağacı neighborhood.

Keywords: Tsunami Risk Assessment (TVA), Geographic Information Systems (GIS), Multi Criteria Decision Analysis (MCDA), Analytical Hierarchy Process (AHP), Tsunami Vulnerability Assessment (TVA)

ÖZ

COĞRAFİ BİLGİ SİSTEMLERİNE DAYALI ÇOK ÖLÇÜTLÜ KARAR ANALİZİYLE TSUNAMİ RİSK DEĞERLENDİRMESİ, BAKIRKÖY, İSTANBUL

Tüfekçi, Duygu

Yüksek Lisans, Jeoloji Mühendisliği Bölümü

Tez Yöneticisi: Prof. Dr. M. Lütfi Süzen

Ortak Tez Yöneticisi: Prof. Dr. Ahmet Cevdet Yalçın

Ağustos 2016, 118 sayfa

Marmara Denizi'nin kuzey kıyısı, büyük bir kısmı mega şehir İstanbul'un sınırları içinde bulunan birçok kıyı tesisine ev sahipliği yapmaktadır. Bakırköy ise İstanbul'un ilçeleri arasında hava ve deniz taşımacılığı ile önemli bir yere sahip olmakla birlikte, denizel afetlerden etkilenebilecek, marinalar, küçük çaplı limanlar, sahile yakın yollar ve iş merkezleri gibi diğer birçok kıyı tesisi ile donatılmıştır. Tarihsel verilere göre İstanbul, birçok deprem ve buna bağlı tsunami olaylarına maruz kalmıştır. Bu sebeple Bakırköy ve diğer İstanbul ilçelerinin tsunami risk değerlendirmelerinin yapılması gereklidir.

Bu çalışmada, tsunami risk değerlendirmesi için yeni bir yöntem geliştirilmiş ve İstanbul'un Bakırköy ilçesine uygulanmıştır. Tsunami afetine yönelik en kötü durum senaryosunun belirlenmesi için farklı tsunami kaynaklarına ait parametrelerin tsunami sayısal modeli NAMI DANCE ile benzetimleri gerçekleştirilmiş ve buna yönelik afet değerlendirmesi yapılmıştır. Tsunami insani zarar görülebilirlik analizleri için Coğrafi

Bilgi Sistemleri (CBS) tabanlı Çok Ölçütlü Karar Analizi (ÇÖKA) yöntemleri kullanılmıştır. ÇÖKA yöntemleri arasında Analitik Hiyerarşi İşlemi (AHI) seçilmiştir. Mekansal hasar görebilirlik ve tahliye esnekliği AHI için oluşturulan hiyerarşinin temel unsurlarıdır. Tsunami risk değerlendirmesi, afet değerlendirmesi ve insani zarar görebilirlik değerlendirmeleri oluşturulan bir denklem ile birleştirilerek elde edilmiştir. Oluşturulan risk denkleminde halkın farkındalık derecesi de dikkate alınmıştır. Çalışma kapsamında, Bakırköy ilçesinin mahallelerini ve nüfusunu da göz önüne alarak afet, zarar görebilirlik ve risk analizleri, yerel olarak da değerlendirilmiştir.

Tsunami benzetimleri maksimum su basma mesafesinin karada 350 m'yi aştığını, bunu yanı sıra Ayamama Deresi boyunca ise yaklaşık 1700 m ilerlediğini göstermektedir. Bakırköy ilçesinin 11 mahallesinde tsunami kaynaklı su basması gözlenmiş ve maksimum su derinliğinin 5.7 metreyi aştığı görülmüştür. Su basmasının görüldüğü alan Bakırköy ilçesinin %4.2'sini kaplamaktadır ve 62 bina bu alanın içinde bulunmaktadır. Hasar görebilirlik değerlendirmeleri sonucunda, Sakızağacı ve Ataköy 2-5-6 mahalleleri mekansal zarar görebilirliği en yüksek olan mahalleler olarak, Yanimahalle ise tahliye esnekliğinin en yüksek olduğu mahalle olarak belirlenmiştir. Risk değerlendirmeleri ise sırasıyla Ataköy 2-5-6 ve Sakızağacı mahallelerinin en yüksek riskin en yüksek olduğu mahalleler olduğunu göstermiştir.

Anahtar Kelimeler: Tsunami Risk Değerlendirmesi, Coğrafi Bilgi Sistemleri (CBS), Çok Ölçütlü Karar Analizi (ÇÖKA), Analitik Hiyerarşi İşlemi (AHI), Tsunami Hasar Görebilirlik Değerlendirmesi

To my beloved family,

ACKNOWLEDGEMENTS

I would like to express my deepest gratitude to Prof. Dr. M. Lütfi Süzen, first of all for accepting me as his student, being a great mentor, and sharing his valuable knowledge with me during my studies. I am very thankful to him for supporting me from the beginning of my thesis study until the end, giving endless recommendations, comments and encouragement with appreciated patience.

I am hugely indebted to my co-supervisor, Prof. Dr. Ahmet Cevdet Yalçiner for his endless and valuable contributions to my thesis and my vision of life. I am thankful to him for spending limitless hours for my studies and supporting and encouraging me at my very first academic accomplishments.

Besides my supervisor and co-supervisor, I also would like to thank to the members of my thesis committee, Prof. Dr. Nurkan Karahanoğlu, Assoc. Prof. Dr. Taner San and Assist. Prof. Dr. Arda Özacar for evaluating and supporting guidance to improve my thesis.

I am also extremely grateful to Dr. Çağıl Kolat. Her kindness and very helpful guidance during my presence in the RS-GIS Laboratory and throughout my thesis is immeasurable.

I dedicate my special thanks to Onur Enginar, for his precious presence in my life, for encouraging me diligently, making all the stages of this study more joyous and making everything more beautiful.

Lastly, even the words would not be enough, I would like to thank my great family, who support me endlessly from the beginning of my life and literally accepting me who I am. I would like to express the deepest gratefulness to my parents, Kadem Tüfekçi and Aynur Tüfekçi for their warm and comforting presence and unconditional love. My very special gratitude is for my brother, Kerem Tüfekçi, who knows me more than anyone else, for being the greatest support of me all the time and for cheering me up whenever I need.

TABLE OF CONTENTS

ABSTRACT	v
ÖZ	vii
ACKNOWLEDGEMENTS	x
TABLE OF CONTENTS	xi
LIST OF TABLES	xiv
LIST OF FIGURES	xvi
LIST OF ABBREVIATIONS	xx
CHAPTERS	
1 INTRODUCTION	1
1.1 Purpose and Scope	3
1.2 Study Area.....	3
1.2.1 The Sea of Marmara and Bakırköy District	3
1.2.2 Geology of the Area	7
1.2.3 Seismicity of Marmara	9
1.3 Available Datasets and Methodology	11
1.3.1 Available Datasets.....	11
1.3.2 Methodology	12
1.4 Hazard, Vulnerability, Risk Concepts and Implementation	15
2 LITERATURE SURVEY	17
2.1 Tsunami History of Marmara.....	17
2.2 Literature Survey on GIS-based Tsunami Vulnerability Assessment	22
3 TSUNAMI HAZARD ASSESSMENT	33

3.1	Tsunami Numerical Modeling	33
3.1.1	Theoretical Background for Tsunamis and the Computational Tool NAMI DANCE	34
3.2	Application of NAMI DANCE to Study Area	36
3.2.1	Selection of Tsunami Source Parameters	36
3.2.2	Domain Selection for Numerical Model	40
3.2.3	Development of High Resolution Topographic and Bathymetric Data for Tsunami Simulations	42
3.2.4	Tsunami Simulations for Hazard Assessment for Bakırköy District ...	44
3.2.4.1	Single Domain Simulations for Worst Case Scenario Selection ..	44
3.2.4.2	Nested Domain Simulations for the Tsunami Source YAN	46
4	METROPOLITAN TSUNAMI HUMAN VULNERABILITY ASSESSMENT (MeTHuVA) WITH GIS BASED MCDA	49
4.1	GIS-based MCDA	50
4.1.1	Analytical Hierarchy Process – AHP	51
4.2	Production of Parameter Maps and Datasets	54
4.3	Assumptions for Vulnerability analysis of Bakırköy District	55
4.4	Application of Analytical Hierarchy Process for MeTHuVA	56
4.4.1	Vulnerability at Location	57
4.4.1.1	Parameter Maps of Vulnerability at Location	58
4.4.1.1.1	Metropolitan Use Layer	58
4.4.1.1.2	Geology	61
4.4.1.1.3	Landslide Scarp Density	63
4.4.1.1.4	Distance from Shoreline	65
4.4.1.1.5	Elevation	67
4.4.1.2	Final Map of Vulnerability at Location Produced by Application of AHP	69

4.4.2	Evacuation Resilience	72
4.4.2.1	Parameter Maps of Evacuation Resilience	72
4.4.2.1.1	Distance to Buildings	72
4.4.2.1.2	Distance to Road Network	75
4.4.2.1.3	Perpendicular Road Density.....	76
4.4.2.1.4	Slope.....	79
4.4.2.2	Final Map of Evacuation Resilience Produced by Application of AHP	81
4.5	Vulnerability at Location and Evacuation Resilience Ratio: MeTHuVA..	84
5	TSUNAMI RISK ASSESSMENT.....	85
5.1	Tsunami Risk Analysis	85
5.2	The Parameter of Awareness and Preparedness of the Community	86
5.3	Tsunami Risk at Bakırköy District.....	86
5.4	Neighborhood Based Evaluation of Hazard, Vulnerability and Risk	87
6	DISCUSSION	99
7	CONCLUSION.....	105
	REFERENCES.....	109

LIST OF TABLES

TABLES

Table 2.1 List of the historical tsunami events occurred in the Sea of Marmara with their date, source coordinates, resulting earthquake magnitude, Tsunami Intensity (TI) and reliability according to historical documents. (modified from Altınok et al., 2011)	18
Table 3.1 List of tsunamigenic faults located in the Sea of Marmara and their characteristics	37
Table 3.2 Estimated rupture parameters and initial wave amplitudes for tsunami source YAN (modified from Ayça, 2012)	38
Table 3.3 Estimated rupture parameters of initial wave amplitudes for tsunami source CMN (modified from Ayça, 2012)	39
Table 3.4 Estimated rupture parameters and initial wave amplitudes for tsunami source PIN (modified from Ayça, 2012)	40
Table 3.5 Coordinates of Nested Domains.....	41
Table 4.1 Saaty’s scale of relative importance.....	52
Table 4.2 Classification of the buildings of Bakırköy according to their utilization type	58
Table 4.3 Classification and ranking of the metropolitan use layer.....	60
Table 4.4 Classification and ranking the geology layer	63
Table 4.5 Classification and ranking of the landslide density layer.....	65
Table 4.6 Classification and ranking of distance from shoreline layer	66

Table 4.7 Classification and ranking of elevation layer.....	68
Table 4.8 Pairwise comparison matrix for Vulnerability at Location map.....	70
Table 4.9 Computed weights of parameters of vulnerability at location	71
Table 4.10 Classification and ranking of distance to buildings layer	74
Table 4.11 Classification and ranking of distance to road network layer.....	76
Table 4.12 Classification and ranking of perpendicular road density layer.....	78
Table 4.13 Classification and ranking of slope layer.....	80
Table 4.14 Pairwise comparison matrix for Evacuation Resilience map.....	81
Table 4.15 Computed weights of parameters of evacuation resilience.....	83
Table 5.1 Amount of inundated area of each neighborhood and whole Bakırköy district	92

LIST OF FIGURES

FIGURES

Figure 1.1 a. General map of Turkey, b. Google Earth image of the Sea of Marmara and c. Google Earth image of Bakırköy, İstanbul with district boundary.....	5
Figure 1.2 Digital Elevation Model of the Bakırköy district of İstanbul	6
Figure 1.3 The simplified geological map of İstanbul. Study area is shown with red rectangle (modified from Özgül et al., 2011).....	7
Figure 1.4 Generalized stratigraphic section of İstanbul region (modified from OYO, IMM, 2015)	9
Figure 1.5 Tectonic setting of Turkey (Gürer et al., 2002)	10
Figure 1.6 Bathymetry and active faults in the north basin of Sea of Marmara, including three recent earthquake magnitude and dates. (Modified from Armijo et al., 2005).....	11
Figure 1.7 Flowchart of the methodology	14
Figure 3.1 A cross sectional view of the tsunami parameters (modified from Yalçiner and Aytöre, 2012).....	35
Figure 3.2 Setting distribution and parameters of the faults in the Sea of Marmara .	37
Figure 3.3 Initial wave condition of tsunami source YAN	38
Figure 3.4 Initial wave condition of tsunami source CMN.....	39
Figure 3.5 Initial wave condition resulted by tsunami source PIN	40
Figure 3.6 Selected domains for the simulations in NAMI DANCE. (a) Domain B, (b) Domain C, including Domain D with green and Domain E with orange	41

Figure 3.7 Integrated elevation dataset	43
Figure 3.8 The tsunami sources and maximum water elevation distributions according to the single domain 60 minute simulations that has been performed in NAMI DANCE. (a) Tsunami source YAN, (b) Tsunami source CMN and (c) Tsunami source PIN..	45
Figure 3.9 Time history of water level changes at the southern border of domain C resulting simulations of tsunami sources PIN, YAN and CMN.	46
Figure 3.10 The flowdepth (hazard) map of the simulated tsunami event according to the tsunami source YAN	47
Figure 4.1 An example of hierarchical structure of GIS-based AHP model. A_1 , A_2 and A_3 are decision alternatives, <i>Obj.</i> is objectives, <i>Att.</i> is attributes and the numbers are showing standardized attributes values for each level of hierarchy (Malczewski and Rinner 2015).	52
Figure 4.2 The hierarchical structure used in the vulnerability analysis.....	56
Figure 4.3 The parameter map of the metropolitan use layer	59
Figure 4.4 Ranked map of metropolitan use layer	60
Figure 4.5 Geological map of southern European side of Istanbul (IMM, 2007). Study area, Bakırköy district, is shown with the red rectangle.	61
Figure 4.6 Digitized geological map of Bakırköy district	62
Figure 4.7 Ranked map of geology layer	63
Figure 4.8 Digitized landslide scarp map.....	64
Figure 4.9 Parameter map of landslide scarp density layer	64
Figure 4.10 Ranked map of landslide density layer.....	65
Figure 4.11 Parameter map of distance from shoreline layer	66
Figure 4.12 Ranked map of distance from shoreline layer	67

Figure 4.13 Parameter map of elevation layer	68
Figure 4.14 Ranked map of elevation layer	69
Figure 4.15 The final map of vulnerability at location	72
Figure 4.16 Parameter map of distance to buildings layer	73
Figure 4.17 Ranked map of distance to buildings layer	74
Figure 4.18 Parameter map of distance to road network layer.....	75
Figure 4.19 Ranked map of distance to road network layer.....	76
Figure 4.20 Baselines for the selection of perpendicular roads	77
Figure 4.21 Parameter map of perpendicular road density layer	78
Figure 4.22 Ranked map of perpendicular road density layer	79
Figure 4.23 Parameter map of slope layer.....	80
Figure 4.24 Ranked map of slope layer.....	81
Figure 4.25 The final map of evacuation resilience	83
Figure 4.26 VL/RE (MeTHuVA) distribution of Bakırköy district. Lighter colors showing higher vulnerability scores.....	84
Figure 5.1 The risk map of Bakırköy district calculated with proposed equation with inputs of Hazard (H), awareness level of community (n) Vulnerability at Location (VL) and Evacuation Resilience (RE).....	87
Figure 5.2 Neighborhoods of Bakırköy District.....	88
Figure 5.3 (a) Locational vulnerability (VL) map, (b) Evacuation resilience (RE) map, (c) VL/RE map, lighter colors represent more vulnerable locations.....	89
Figure 5.4 (a) Neighborhood based comparison of locational vulnerability, (b) Neighborhood based comparison of evacuation resilience, (c) Neighborhood based comparison of VL/RE	90

Figure 5.5 (a) Hazard map, (b) Sum of hazard scores of the neighborhoods normalized by the area	93
Figure 5.6 (a) Risk map, (b) Sum of risk scores of the neighborhoods normalized by the area	94
Figure 5.7 (a) Chart of population density by neighborhood, (b) Chart of hazard related population density	96
Figure 5.8 (a) Chart of exposed buildings by neighborhoods, (b) Percent of exposed building for each area.....	97

LIST OF ABBREVIATIONS

<i>AHP:</i>	<i>: Analytical Hierarchy Process</i>
<i>BTV:</i>	<i>: Building Tsunami Vulnerability</i>
<i>BV:</i>	<i>: Building Vulnerability</i>
<i>CMN:</i>	<i>: Central Marmara Normal Fault</i>
<i>CSZ:</i>	<i>: Cascadia Subduction Zone</i>
<i>CVI:</i>	<i>: Composite Vulnerability Index</i>
<i>DEM:</i>	<i>: Digital Elevation Model</i>
<i>EAfZ:</i>	<i>: East Anatolian Fault Zone</i>
<i>GEBCO:</i>	<i>: General Bathymetric Charts of the Oceans</i>
<i>GIS:</i>	<i>: Geographic Information Systems</i>
<i>HV:</i>	<i>: Human Vulnerability</i>
<i>IMM:</i>	<i>: Istanbul Metropolitan Municipality</i>
<i>IOT:</i>	<i>: Indian Ocean Tsunami</i>
<i>MCDA:</i>	<i>: Multi Criteria Decision Analysis</i>
<i>MeTHuVA:</i>	<i>: METU Tsunami Human Vulnerability Assessment</i>
<i>NAF:</i>	<i>: North Anatolian Fault</i>
<i>NAFZ:</i>	<i>: North Anatolian Fault Zone</i>
<i>NSWE:</i>	<i>: Nonlinear Shallow Water Equations</i>
<i>PIN:</i>	<i>: Prince Islands Normal Fault</i>
<i>PML:</i>	<i>: Probable Maximum Loss</i>
<i>PTHA:</i>	<i>: Probabilistic Tsunami Hazard Assessments</i>

<i>PTVA:</i>	<i>: Papathoma Tsunami Vulnerability Assessment</i>
<i>PVI:</i>	<i>: Physical Vulnerability Index</i>
<i>RE:</i>	<i>: Evacuation Resilience</i>
<i>RVI:</i>	<i>: Relative Vulnerability Index</i>
<i>SV:</i>	<i>: Structural Vulnerability</i>
<i>SVI:</i>	<i>: Structural Vulnerability Index</i>
<i>TI:</i>	<i>: Tsunami Intensity</i>
<i>TNM:</i>	<i>: Tsunami Numerical Modeling</i>
<i>TVA:</i>	<i>: Tsunami Vulnerability Analysis</i>
<i>VL:</i>	<i>: Vulnerability at Location</i>
<i>WV:</i>	<i>: Vulnerability that caused by Water</i>
<i>YAN:</i>	<i>: Yalova Normal Fault</i>

CHAPTER 1

INTRODUCTION

Throughout the history of mankind, there had been many instances that natural hazards are so devastating that they have been believed to be created by the gods to punish the civil society. However, with the advance of positive sciences, the mechanisms behind these natural processes are becoming more clear. In late 80's to early 90's the increase in accessibility of low cost personal computers by researchers yield in a milestone in generation of numerical models that try to understand the behavior of these natural phenomena. In coherence with this accessibility, spatial science had evolved in such a way that both Geographical Information Systems (GIS) and Multi Criteria Decision Analysis (MCDA) methods were evolved from the necessity to assist Decision Support Systems (DSS). Especially, in the new millennia, not only the numerical models, but also the concepts of hazard, vulnerability, resilience and risk were developed and broadly understood (Alexander, 2000; Wisner et al., 2004), while being integrated to Geographical Information Systems. Integration of these concepts to GIS were applied for different natural hazards in many studies (Fischer et al., 2002; Gambolati et al., 2002; Cheung et al., 2003).

Despite the rare occurrence, tsunamis can be listed as one of the most devastating events among all the natural hazards. Its disastrous impacts on the shores mostly rules out its rarity. Especially after the major recent tsunami events, 2004 Indian Ocean Tsunami (IOT) and 2011 Tohoku Earthquake Tsunami, the importance of tsunami events has raised among the society and the scientific fields. Scientists made a great effort to develop the understanding of the mechanism of tsunami waves. Beyond that, after these events, the hazard, vulnerability and risk concepts were also clarified for the tsunami natural event and many studies to assess the level of hazard, vulnerability and risk have been performed (Papathoma et al., 2003; Papathoma and Dominey-

Howes, 2003b; Ghobarah et al., 2006; Dominey-Howes and Papathoma, 2007; Reese et al., 2007; Dall'Osso et al., 2009a; Dall'Osso et al., 2009b; Hart and Knight, 2009; Wood, 2009; Dall'Osso et al., 2010; Dominey-Howes et al., 2010; Omira et al., 2010; Atillah et al., 2011; Leone et al., 2011; Murthy et al., 2011; Sinaga et al., 2011; Eckert et al., 2012; Ismail et al., 2012; Santos et al., 2012; Tarbotton et al., 2012; Usha et al., 2012; Benchekroun et al., 2015).

Since all the coastal areas around the globe are prone to suffer from a possible tsunami event, it is a need to have early warning systems, hazard, vulnerability and risk assessments for land use zoning and planning, emergency response actions, evacuation routes, disaster planning and insurance premiums (Tüfekci, 1995; Jenkins, 2000; Dominey-Howes and Papathoma, 2007), as realized and further confirmed after the recent major tsunami events.

The analysis of these needs requires operations on a big amount of spatial data. The process of the integration of such amount of spatial data reveals the need of use the GIS-based methods. As approved by many of the above mentioned studies, GIS tools are able to deal with the hazard related assessments. Therefore, in this study these tools are used for producing hazard, vulnerability and risk models for Bakırköy district of İstanbul considering tsunami hazard.

This thesis is composed of seven chapters. This chapter continues with the aims and scope of this study and presentation of the study area. Chapter 2 is a review of a literature on historical tsunami events in the study region and tsunami vulnerability assessment methods around the world. In Chapter 3, simulations of tsunami numerical model and the hazard assessment method are presented. Chapter 4 focuses on the vulnerability of the study area. In chapter 5, the risk assessment method that was improved is explained, also a neighborhood based analysis is performed. In Chapter 6 the outcomes and the result of this study is discussed. Lastly in Chapter 7 the concluding remarks and recommendations for further studies are stated.

1.1 Purpose and Scope

Considering the need of the hazard, vulnerability and risk assessments, this study aims to further develop the tsunami vulnerability and risk analysis methodologies by bringing new insights combined with GIS-based Multi Criteria Decision Analysis (MCDA) methods while applying developed methodologies to the Bakırköy district of İstanbul.

The ultimate aimed output of the study is a high resolution tsunami risk assessment of the Bakırköy district. The process of the risk assessment requires the calculation of hazard and human vulnerability analysis.

For accurate and realistic worst case hazard assessment scenarios it is aimed to develop a high resolution topography model including the building and stream topographies with sea bathymetry in order to use as input in tsunami numerical model.

Vulnerability assessment is intended to include the conditions of human beings by using MCDA methods. For the assessments of human vulnerability, locational vulnerability and evacuation resilience for whole Bakırköy district is proposed within a hierarchical structure of MCDA.

Furthermore, for a detailed analysis of human exposure to tsunami hazard and risk based on scenario, a neighborhood based evaluation is aimed to be done.

1.2 Study Area

1.2.1 The Sea of Marmara and Bakırköy District

Turkey is surrounded by seas in three sides and addition to that, hosts an inland sea, the Sea of Marmara. This intercontinental sea is located at 40.0° and 41.1° latitude north and 26.2° and 29.9° longitude east (Figure 1.1). The Sea of Marmara connects Black Sea to the Aegean Sea and separates the Asian and European parts of Turkey. It covers an ellipsoid area of 11,350 km² with a 280 km major axis in E-W and a minor axis of 80 km in N-S direction. The Bosphorus strait connects it to the Black Sea and Dardanelles strait to the Aegean Sea. To the south Marmara Sea has broad shallow

shelf whereas to the north there are series of sub-basins (Smith et al., 1995; Yalçiner et al., 2002). The maximum depth of the sea reaches up to 1370 m around these basins.

Marmara Sea Region is the most populated area of Turkey which is over 23 million according to the 2015 census (Wikipedia, 2015). In this region there are seven cities that has coasts to the Sea of Marmara, that have industrial, trading and agricultural importance. Among these cities, İstanbul is the economically most significant and most densely populated city not only of the Marmara region but also of Turkey. Besides the economic importance, İstanbul hosts many historical and touristic places.



(a)



(b)



(c)

Figure 1.1 a. General map of Turkey, b. Google Earth image of the Sea of Marmara and c. Google Earth image of Bakırköy, İstanbul with district boundary

Bakırköy is a coastal district of İstanbul (Figure 1.1.c) and located on the European side. Its history goes back to Roman Empire, when it was called as ‘Hebdomon’, which means the seventh, since it is located on the seventh Roman mile from the Milion of Constantinople (Wikipedia, 2016).

Bakırköy is bounded by Küçükçekmece district at the west and Zeytinburnu district at the east. It is separated from Güngören and Bahçelievler districts by E-5 highway at the north and the bounded by the Sea of Marmara at the south. There are three different streams which passes through the borders of Bakırköy district: (i) Çırpıcı stream separates Bakırköy district from Zeytinburnu district at the east, (ii) Siyavuşpaşa stream passes at the eastern part of the district and its length within the borders of Bakırköy is 2400 m, and (iii) Ayamama stream is the longest and largest stream of Bakırköy, located at the east of airport and its length in Bakırköy borders is about 3500 m. Addition to these rivers, at the west, Bakırköy is partly bounded by a marine related branch of Küçükçekmece Lake. The elevation values of Bakırköy reaches up to 80 m above sea level. The higher elevation values are seen at the north-western and north-eastern part of the district, while the lowest elevations reaching to the valleys of above mentioned rivers from the shoreline (Figure 1.2).

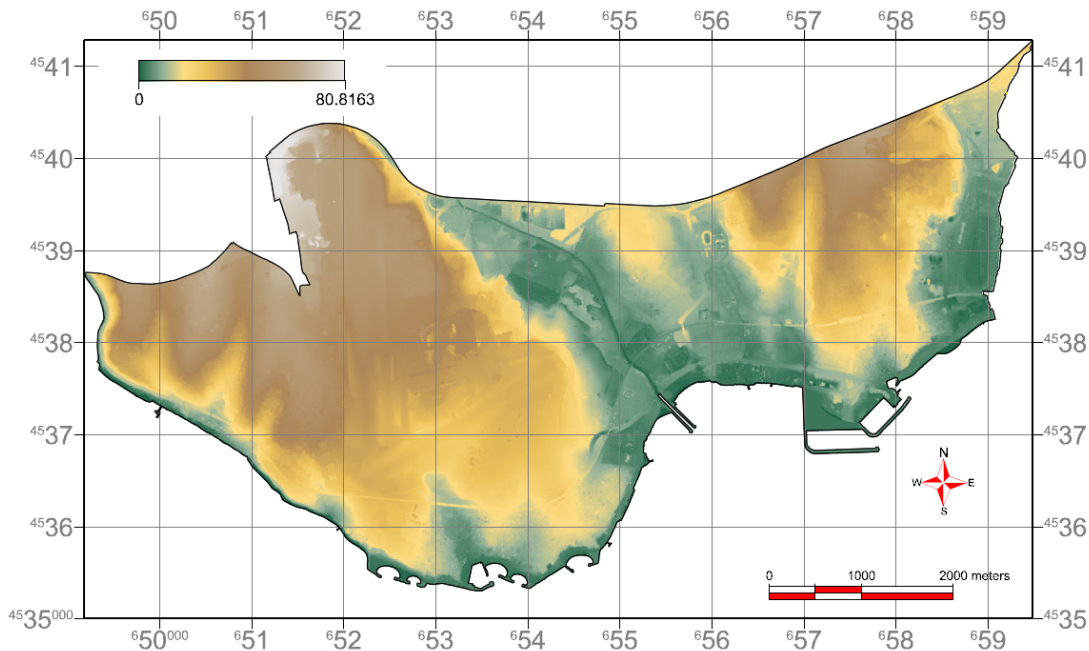


Figure 1.2 Digital Elevation Model of the Bakırköy district of İstanbul

Nowadays, Bakırköy is an important district of İstanbul and its population is 223,248 according to the 2015 census, and is composed of 15 neighborhoods (Wikipedia, 2016). Bakırköy hosts Atatürk Airport of İstanbul (the first airport in İstanbul and has the densest passenger traffic among the airports of Turkey), Veli Efendi Racecourse (the largest and oldest in Turkey), the Bakırköy Psychiatric Hospital (the largest in İstanbul with large green space around), shopping malls and many coastal facilities like marinas and small scale ports. Bakırköy is also one of the wealthiest places of Turkey where the land, air and sea transportation is developed.

1.2.2 Geology of the Area

İstanbul is located in a tectonically very active and complex area. There are many different rock units formed from Early Paleozoic to Recent. Within the borders of İstanbul, two large rock-stratigraphy units are dominant: (i) Istranca Massive with metamorphic characteristics and (ii) non-metamorphic İstanbul Massive. These two units are separated by a great tectonic line. Istranca Massive is exposed on the northwestern parts of the İstanbul province. İstanbul Massive covers all the other areas located at the two sides of the Bosphorus (Özgül et al., 2011). A simplified geological map can be seen in Figure 1.3.

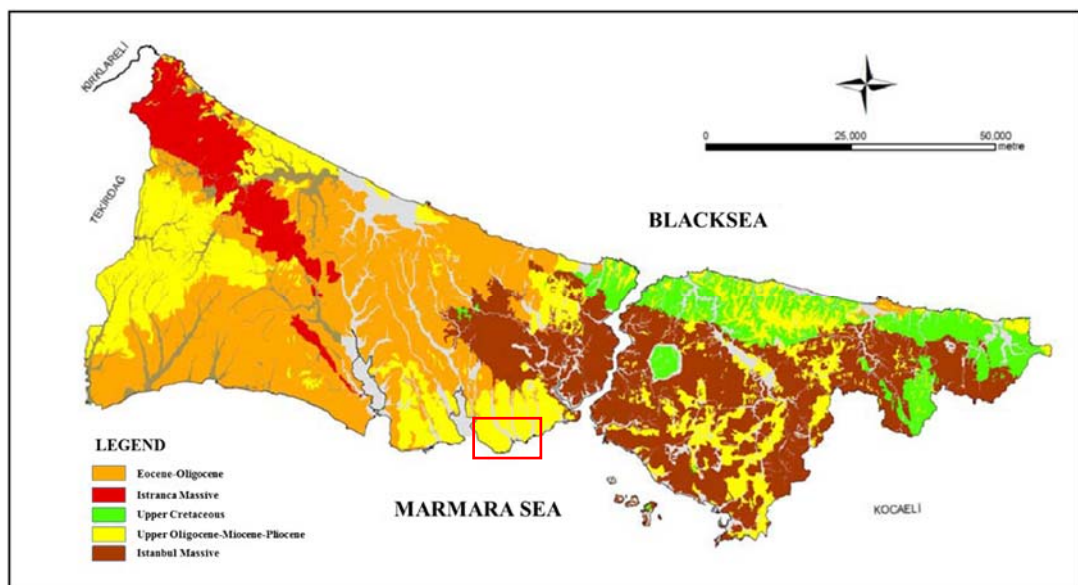


Figure 1.3 The simplified geological map of İstanbul. Study area is shown with red rectangle (modified from Özgül et al., 2011)

The European side of İstanbul consist of Carboniferous, Eocene, Oligocene, Miocene and Quaternary sedimentary rocks of İstanbul Massive. Additionally, near to coastal areas and along riverbeds, anthropogenic rock fill or consolidated fill is present.

The dominant rock units in the European side of İstanbul are Carboniferous Trakya Formation which consist of siltstone, claystone, sandstone that cross-cut by andesite and diabase dykes and lensed limestone. Trakya formation was affected by dense tectonism and has fault, fold, fracture and joint systems in different directions at in every few meters. Trakya Formation has a thickness over 1000 m and it is overlain by 150 m thick Eocene Kırklareli Formation. Kırklareli Formation is composed of thick-bedded, micritic, fossiliferous and porous limestone, marl and calcareous claystone. Over Kırklareli Formation there is over 700 m thick Oligocene Gürpınar Formation consisting claystone with tight sandstone lenses. This formation is followed by Miocene formations, where the oldest Miocene formation is 25 m thick Çukurçeşme Formation that is composed of barely consolidated to unconsolidated gravel-sand and clay layers. Güngören Formation follows the Çukurçeşme Formation and composed of greenish-grey, fair brown clay layers that includes thin sand lenses. The last and the youngest formation that can be differentiated in the Miocene sequence is the Bakırköy Formation with a thickness of 20 m. This formation composed of thin-bedded, mainly white and partly greenish-grey clay, marl and limestone. The Miocene sequenced is followed by yellow-brown sand and silty clay alluvial deposits and 35 m thick silty clay estuary deposits. Over this deposits there are antique and recent anthropogenic fill with a thickness of approximately 30 m (Dalgıç et al., 2009). A generalized stratigraphic section of İstanbul region can be observed in the Figure 1.4.

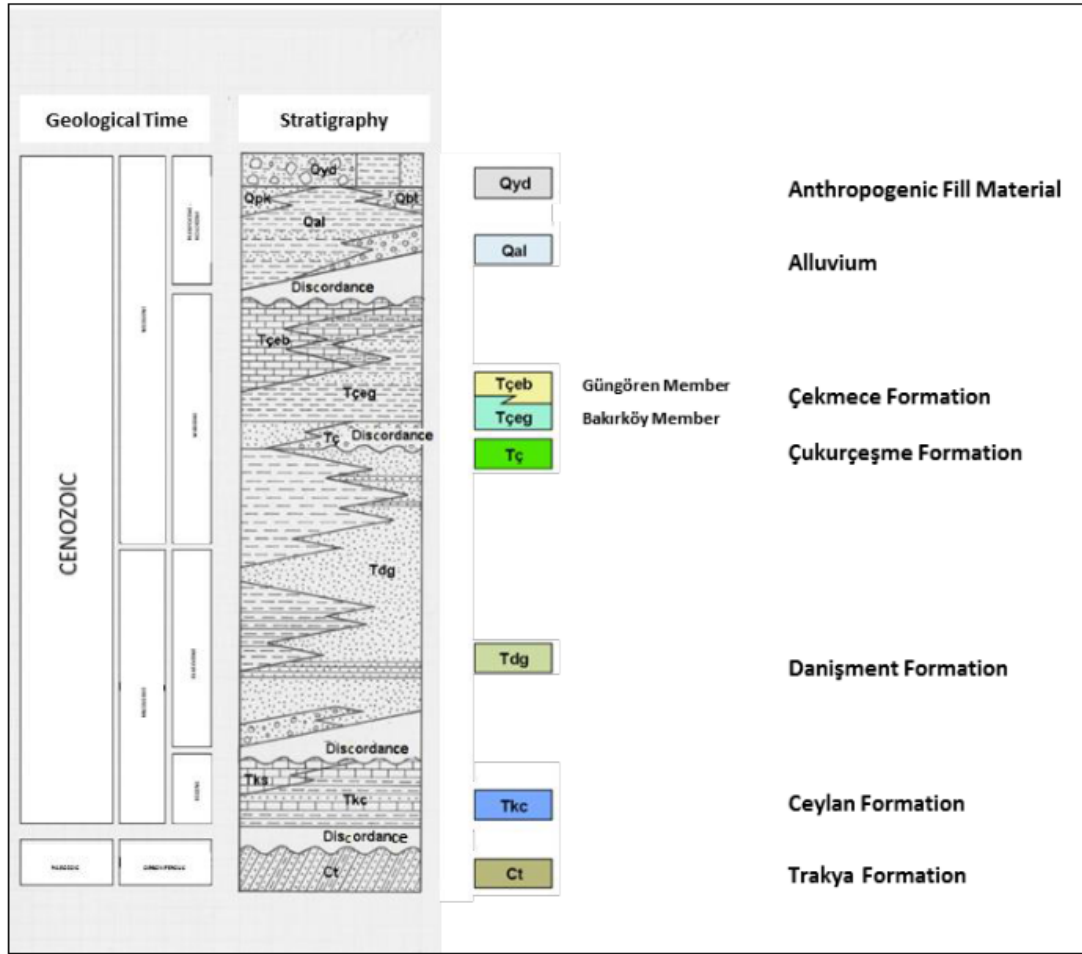


Figure 1.4 Generalized stratigraphic section of İstanbul region (modified from OYO, IMM, 2008)

1.2.3 Seismicity of Marmara

Tukey is located in one the most seismically active regions of the world and it is controlled by four major structures (Figure 1.5); North Anatolian Fault Zone (NAFZ), East Anatolian Fault Zone (EAFZ), Hellenic Arc and Dead Sea Fault Zone (DSFZ). The first two are intercontinental strike-slip faults meeting in Karlıova at the north-east of Turkey and moving the Anatolian Plate 20 mm/year westward (Bozkurt, 2001).

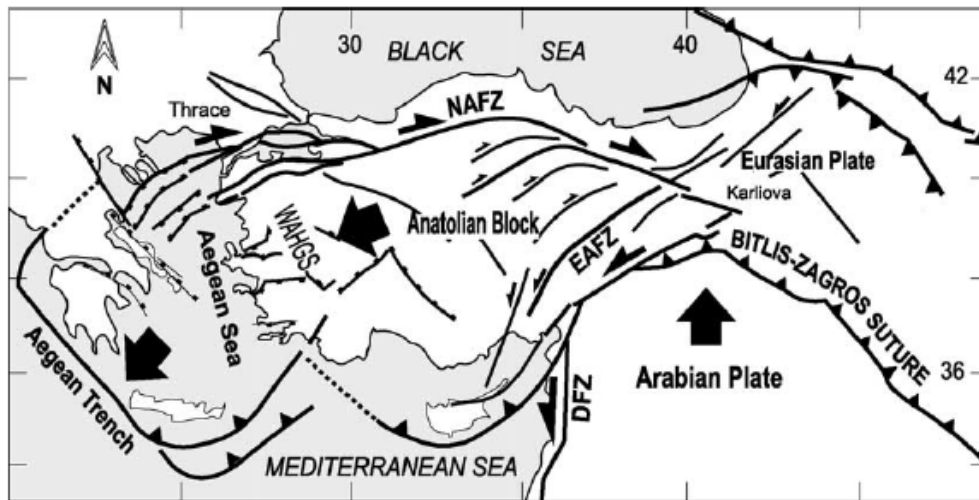


Figure 1.5 Tectonic setting of Turkey (Gürer et al., 2002)

North Anatolian Fault (NAF) is one of the well-known strike-slip faults in the world because of its active seismicity and well developed surface expression. NAF is a dextral fault with a length of approximately 1500 m (Bozkurt, 2001). At the east of Marmara Sea around 30.8° E longitude NAFZ splits into two branches (Gürer et al., 2003). When the northern branch dives to the Sea of Marmara it further splits into sub-branches and form a distributed deformation zone more than 120 km wide (Şengör et al., 1985, Barka and Kadinsky-Cade, 1988; Gürer et al., 2003). Eventually, by the geoscientists who made a detailed study about NAF, it is devoted that, in the Marmara region NAF is composed of 3 major branches. The northern branch extends in the Sea of Marmara and Gulf of Saros connecting the North Aegean through (Figure). Middle branch follows the southern coastline of the Sea of Marmara. The southern branch continues on the land along Bursa (Mercier et al., 1989; Yalçiner et al., 2002).

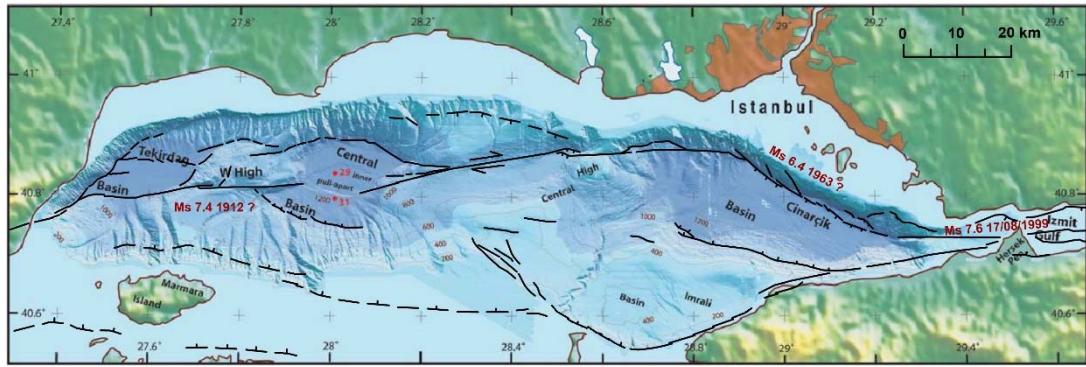


Figure 1.6 Bathymetry and active faults in the north basin of Sea of Marmara, including three recent earthquake magnitude and dates. (Modified from Armijo et al., 2005)

Morphologically the Sea of Marmara can be divided into two parts; (i) southern part with a broad shelf, (ii) northern part with a negative flower structure which is controlled by the northern branch of NAFZ (Figure 1.6). Additionally, there are four sub-basins in the Sea of Marmara that are produced by distributed deformation zone (Alpar and Yaltrak, 2002).

Therefore, NAFZ plays an important role in the tectonic and morphologic evolution of the Sea of Marmara and makes the region one of the most seismically active regions of the world. Between 2100 BC and AD 1900, there are more than 300 earthquakes that were reported for this region and some of these were followed by related tsunami events (Soysal et al., 1981; Yalçiner et al., 2002). Beyond those events, the most recent devastating event is the 1999 İzmit earthquake, which also lead the generation of tsunami waves.

1.3 Available Datasets and Methodology

1.3.1 Available Datasets

At the beginning of the study there were seven different datasets were available. These were raw datasets and they have been improved and modified if necessary in order to use for the accomplishment of the study. The raw datasets and the sources of them are listed below;

- 1:25.000 scaled Geological Map of the southern European side of İstanbul obtained from İstanbul Metropolitan Municipality (IMM)
- Digital Elevation Model (DEM) of whole İstanbul region with 5 m spatial resolution obtained from İstanbul Metropolitan Municipality (IMM)
- 30'' bathymetry dataset obtained from General Bathymetric Charts of the Oceans (GEBCO)
- 1:5.000 scaled Nautical Charts obtained from Navigation, Hydrography and Oceanography Department of Turkish Naval Forces.
- Vector dataset of almost all structures and infrastructures located in Bakırköy district of İstanbul obtained from IMM
- Vector elevation dataset of Ayamama Stream obtained from IMM
- Population statistical data of İstanbul obtained from Turkish Statistical Institute.

Since the spatial datasets are obtained from different sources, the initial datum and projection systems of those data were different from each other. In order to handle the datasets easier and all together while using GIS tools, all the used datasets have been projected to Universal Transverse Mercator (Zone 35 North) with a datum of WGS 1984. After all modifications and improvement of the spatial data, the high resolution topographic and bathymetric data has been reprojected to Geographic latitude and longitude coordinated in WGS84 (World Geodetic System 1984) datum, since this is the supported coordinate system by NAMIDANCE, the tsunami numerical model code, used in this thesis.

1.3.2 Methodology

The methodology that has been developed and followed throughout the study includes three major steps (Figure 1.7). The following chapters of the thesis includes detailed information about each major and minor steps. To give a glance about the outline of the study the three major steps are as summarized below;

- i. Tsunami Numerical Modeling (TNM) and Hazard Assessment;** After selection of the study area and data processing, the final high resolution bathymetric and topographic data have been used as input for the Tsunami numerical model NAMIDANCE for calculation of necessary parameters such

as flow depth and inundation distance, that will be caused by the selected tsunami source.

- ii. Metropolitan Tsunami Human Vulnerability Assessment (MeTHuVA) with GIS-based MCDA;** by using the developed high resolution topography and vector dataset of whole region, many parameter maps were developed in order to use in the hierarchical structure of the Multi Criteria Decision Analysis (MCDA) method. With the application of the MCDA final vulnerability and resilience maps were produced.
- iii. Tsunami Risk Assessment;** the outputs of the former two steps were utilized for the final calculation of risk. For the risk assessment, a new formula was developed and applied. The proposed risk formula involves hazard, vulnerability and resilience of the region, and awareness and preparedness of the community living in that area.

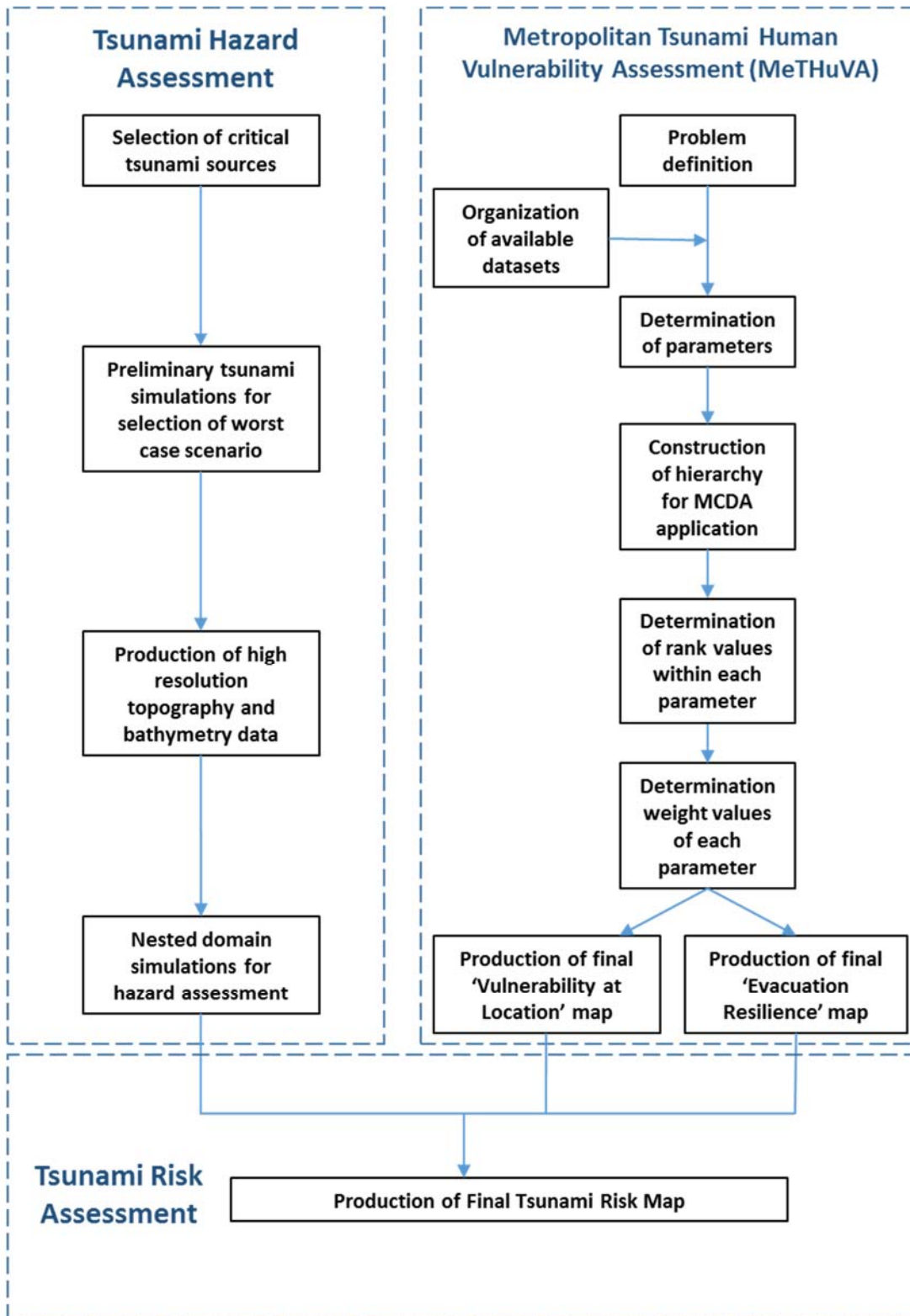


Figure 1.7 Flowchart of the methodology

1.4 Hazard, Vulnerability, Risk Concepts and Implementation

Throughout this study the terms hazard, vulnerability and risk were the main concerns and in each chapter one of them has been approached considering the natural event; tsunami.

Risk term is described as the product of the interaction between hazard and vulnerability (Birkmann, 2006). Risk is also defined as the probability and the amount of harmful consequences or expected losses resulting from interactions between natural or human induced hazards and vulnerable conditions (UNISDR, 2009). By some studies exposure and the preparedness has been added to the risk definition, additionally (Villigrán de León, 2004; Suppasri et al, 2015).

Although the terms hazard and risk are thought to have the meanings, currently it is widely excepted that hazard is a component of the risk (Cordona et al., 2012). Hazard is described as the possible, future occurrence of natural or human-induced events which may have negative impacts on exposed elements (Birkmann, 2006; Cordona et al., 2012).

The term vulnerability has also defined by many authors and many different definitions are present in the terminology (Thywissen, 2006; Manyena, 2006). Vulnerability is assumed to be distinctive form the hazard for this study and it has been calculated for each location of Bakırköy district regardless of the hazard level or exposure. In the concept of vulnerability, locational vulnerability and evacuation resilience for human have been considered together.

As mentioned earlier exposure within the risk definition, is a necessary determinant, but not a sufficient one. Therefore, in this study, exposure is involved within the hazard assessment part of this study.

Additionally, the level of awareness and preparedness of the community has been considered as a determinant of the risk.

CHAPTER 2

LITERATURE SURVEY

2.1 Tsunami History of Marmara

Tsunami phenomenon is an event with rare occurrences, especially when the level of destructiveness is taken into account. Turkey is surrounded by water at three sides and as discussed earlier located in an active seismic zone that controlled by NAFZ, EAFZ, DSFZ and Hellenic Arc. Being in a very active seismic zone with coastline over 8000 km increases the possibility of tsunami occurrences and its highly destructive impacts. Yet there isn't any modern tsunami event occurred except one event, which happened in 17 August 1999 after the devastating İzmit Earthquake. However, the 1999 Earthquake was so destructive it overshadowed the tsunami occurrence and the damage aftermath for both the community and government.

Even there aren't any awareness of the community yet about tsunami occurrences along Turkish coasts, the valuable scientific studies and historical records reveal the information about tsunami events that happened in the history (Altınok and Ersoy, 2000; Altınok, 2006; Altınok et al., 2011; Papadopoulos et al., 2014).

According to Altınok et al. (2011) there are 134 tsunami event that has impacts on the Turkish coasts in the last 3500 years. Among these events, there are 35 events are reported to be in the vicinity of the Sea of Marmara between 123 AD and 17 August 1999. The catalogue that produced by Altınok et al. (2011) is generated by using the all possible historical, literal and scientific documents including the catalogues prepared within the scope of GITEC (Genesis and Impact of Tsunamis on the European Coasts) and TRANSFER (Tsunami Risk And Strategies For the European Region) projects. The details about these events is presented in Table 2.1.

Table 2.1 List of the historical tsunami events occurred in the Sea of Marmara with their date, source coordinates, resulting earthquake magnitude, Tsunami Intensity (TI) and reliability according to historical documents. (modified from Altınok et al., 2011)

No	Year	Source Coordinates	Earthquake Magnitude	TI	Reliability
1	123	40.7N-29.1E	7.2	2	3
2	358	40.75N-29.96E	7.4	-	4
3	368	40.4N-29.7E	6.4	-	1-2
4	407	-	6.6	3-4	2
5	447	40.7N-28.2E	7.2	4	4
6	478	40.8N-29.0E	7.3	-	4
7	488	40.8N-29.6E	-	-	1
8	542	-	6.5	-	1
9	543	40.35N-27.8E	6.6	4	3
10	549	-	-	-	2-3
11	553	40.75N-29.10E	7.0	-	4
12	555	-	-	-	1
13	557	40.9N-28.8E	7.0	4	4
14	740	40.7N-28.7E	7.1	3	4
15	989	40.8N-28.7E	7.2	-	4
16	1039	41.02N-28.5E	-	4	1
17	1064	40.8N-27.4E	7.4	-	1
18	1265	40.7N-27.4E	6.6	-	4
19	1332	40.9N-28.9E	6.8	3+	3
20	1343	40.9N-28.0E	7.0	-	4
21	1419	40.9N-28.9E	6.6	-	2
22	1509	40.75N-29.0E	7.2	3+	4
23	1577	-	-	-	1
24	1648	-	6.4	3-4	4
25	1751	-	-	-	1-2
26	1754	40.8N-29.2E	6.8	-	2-3
27	1766	40.8N-29.0E	7.1	2	4
28	1829	-	7.3	2	1
29	1857	-	-	-	1
30	1878	40.7N-30.2E	5.9	3	4
31	1894	40.6N-28.7E	7.3	3	4
32	1912	40.75N-27.2E	7.3	3-4	4
33	1935	40.64N-27.51E	6.4	2-3	4
34	1963	40.64N-29.13E	6.3	-	4
35	1999	40.73N-29.88E	7.4	3	4

The table gives information about the 35 tsunami event occurred in the Sea of Marmara since the year 123. Within the table there are information about the year when the event occurs, the coordinates of the source of tsunami, the magnitude of triggering earthquake which is estimated according to the damage level, determined by the evaluation of historical and literal records, the Tsunami Intensity (TI) according to the Sieberg-Ambraseys Scale (Ambraseys, 1962) and reliability of the event according to the available resources.

Sieberg-Ambraseys Tsunami Intensity Scale is a 6- point intensity scale where, 1: very light, 2 light, 3: rather strong, 4: strong, 5: very strong and 6: disastrous. The reliability score is given according to the GITEC Catalogue criteria (Tinti et al., 2001; UNESCO/IOC Global Tsunami Website), where, 0: very improbable, 1: improbable, 2: questionable, 3: probable and 4: definite tsunami. According to the survey of Altınok et al. (2011), among the 35 historical tsunamis, 18 tsunami events are catalogued as definite. According to Ambraseys (2002), 6 of them were damaging. The most reliable historical events will be detailed in the following paragraphs.

In the year 358 an earthquake and related landslide in the Sea of Marmara triggered a tsunami which effects İzmit (Yalçınır et al., 2002; Ambraseys, 2002; Altınok et al., 2011).

In 447 an earthquake with great magnitude occurred and İzmit and its surroundings were affected and landslides were triggered by the earthquake. A tsunami occurred and according to some historical documents the city ‘...sank underground and into the sea...’ and ‘...the sea threw up dead fish, and many islands in the sea were submerged. Ship were seen on dry land when the sea having retreated...’ (Guidoboni et al., 1994; Ambraseys, 2002 and Altınok et al., 2011).

A great earthquake occurred in 25 September 478, İzmit, İstanbul, Çanakkale and Bozcaada were damaged. In historical documents it is mentioned that a tsunami occurred in İstanbul and the sea became very wild, rushed right in, engulfed a part of what had formerly been land, and destroyed several houses (Soysal et al., 1981; Ambraseys and Finkel, 1991; Yalçınır et al., 2002; Altınok et al., 2011).

On August 553 an earthquake effected İstanbul and Gulf of İzmit and triggered a tsunami resulting 3000m inundation inland (Soysal, 1985; Altınok et al., 2011).

In December 557 an earthquake caused many damage in İstanbul. According to historical documents the inundation distance was 5000m. The place where this amount of inundation occurs is thought to be in ancient Theodosian Harbour in Yenikapı, İstanbul according to recent archaeological findings (Soysal, 1985; Yalçınır et al., 2002; Altınok et al., 2011).

The earthquake of 26 October 740 lead to many casualties at the east part of Marmara Sea. As stated in some historical records the sea receded from its original position. This could indicate a tsunami redraw or it can be evaluated as an uplift of the affected region (Ambraseys and Finkel, 1991; Guidoboni et al., 1994; Ambraseys, 2002; Yalçınır et al., 2002; Altınok et al., 2011).

On 25 October 989 a great magnitude earthquake has happened in the evening and affected İstanbul, Gulf of İzmit and coasts of Marmara Sea. The Earthquake create waves in the sea and hit the coasts of Thrace, İstanbul and İzmit (Guidoboni et al., 1994; Ambraseys, 2002; Yalçınır et al., 2002; Altınok et al., 2011).

At the midnight of 11 august 1265, a big piece of land mass failed in Marmara island, probably due to the ground shaking. When mass entered to the water, a giant wave was generated and hit the shore and swallow up the area of Marmara Island (Guidoboni and Comastri 2005; Altınok et al., 2011).

Two consequent earthquakes occurred on 18 October 1343 and caused a large damage at the north coasts of Marmara Sea. The sea inundated the land up to 2000 m. The wave dragged the ships at the harbor. İstanbul and several other cities in Thrace were distracted by the giant wave. The tsunami wave reached to the Straight of İstanbul and affected Beylerbeyi. When the sea receded mud and dead fish was left behind (Papadopoulos, 1993; Soloviev et al., 2000; Altınok et al., 2011; Ambraseys, 2011;).

The earthquake happened on 10 September 1509 was the most damaging earthquake of the last 5 centuries in İstanbul. The tsunami caused by this great earthquake lead the destruction of the shipyard in İzmit. In İstanbul, the waves exceeded the height of walls in Galata and flooded in Yenikapı and Aksaray. The recent archaeological findings in

Yenikapı revealed that the inundation distance was 500-600 m in this region (Oztin and Bayulke, 1991; Ambraseys, 2002; Altınok et al., 2011).

According to the historical documents the 1648 earthquake caused a tsunami and 136 ships were destroyed by the wave when it moves towards the land (Soysal, 1985; Soloviev, 2000; Altınok et al., 2011).

In 22 May 1766 an earthquake happened in the Sea of Marmara and caused heavy damage and casualties. The tsunami wave occurred after the earthquake hit İstanbul and İzmit. Waves were observed in the coastal villages of Beşiktaş and inner parts of the straits whereas it created more destructive damage on the eastern parts of Marmara. Uninhabited islands in the Marmara Sea were said to half sunk into the sea (Ambraseys, 2002; Yalçiner, 2002; Altınok et al., 2011).

A damaging earthquake occurred on 19 April 1878. The quake generated a small tsunami that propagate to western side of Gulf of İzmit. The earthquake was felt on the ships and the associating rather strong tsunami, according to Tsunami Intensity (TI) scale, was observed in İzmit (Ambraseys, 2002; Altınok et al., 2011).

On 10 July 1894 a tsunami occurred after the earthquake was observed. The sea receded 50 m and when it hit the land the inundation distance was about 200 m in Büyükçekmece and Kartal and around Prince Islands. In Yeşilköy the 3 row of houses were inundated (Oztin and Bayulke, 1991; Ambraseys, 2002; Yalçiner et al., 2002; Altınok et al., 2011).

On 9 August 1912, a high water was observed in the Strait of İstanbul and destroyed some the anchored yachts. The sea was receded carrying the anchored boats, when the wave propagates to the land it brings the boats at a height of 2.7m (Ambraseys and Finkel, 1987; Altınok et al., 2011).

After the earthquake occurred on 4 January 1935 and the rocks of Hayırsız Island collapsed on three sides. This mass failure caused tsunami (Yalçiner et al., 2002; Altınok et al., 2011).

On 18 September 1963 the earthquake with magnitude of 6.3 occurred and the epicenter of it was located in the sea. This earthquake caused to water to boil. After the event shells and molluscs were observed at the coast of Mudanya indicating waves

reached a height of 1m (Kuran and Yalçiner, 1993; Özçiçek, 1996; Yalçiner et al., 2002; Altınok et al., 2011).

The last and the most recent tsunami event occurred in the Sea of Marmara is 17 August 1999 event. The magnitude of this destructive earthquake was 7.4 and it caused 18850 casualties. The resulted tsunami revealed itself as receding of the sea at the northern and southern coastlines especially in the central sub-basin of İzmit Bay to the east of Hersek Delta (Altınok et al., 1999, 2001). Sediment slumping at İzmit Bay generated tsunami waves in addition to tectonic displacements (Yalçiner et al., 2002). The maximum run-up heights were measured as 2.66 m along the north coast (Tütünciftlik to Hereke) and 2.9 m at the south coast (Değirmendere to Karamürsel) of the bay. Local peaks were observed for the maximum run-up heights, which were thought to be produced as a result of underwater sediment failures near offshore Değirmendere, Halidere and Ulaşlı (Yalçiner, 1999; Yalçiner et al., 2001). According to observations the maximum inundation distance in Kavaklı was more than 300 m (Altınok et al., 2011).

2.2 Literature Survey on GIS-based Tsunami Vulnerability Assessment

Similar to the understanding of the impacts of tsunami event, vulnerability and risk assessments were not the main interest of scientists until the great Indian Ocean Tsunami in 2004 except a few studies. Despite the devastating side, the 2004 Indian Ocean event and the following 2011 Tohoku Tsunami event led scientist to lean over to the tsunami phenomena more.

Since the tsunami event could cause severe damages to the places far from the source, all coastal areas around the globe are under risk by the effects of this phenomena. Increasing awareness after the 21th century events lead many studies about the hazard, vulnerability and risk assessments for different coastal areas.

The very first attempt of GIS Based Tsunami Vulnerability Analysis was studied by Wood and Stein (2001) for Cascadia Subduction Zone. Until then, there were attempts to understand tsunami hazard, but no comprehensive vulnerability assessment to community level were established yet. Only the vulnerability of few specific critical

buildings were assessed throughout the literature. In their paper they firstly define the terms such as Hazard, Exposure, Vulnerability and Risk for reaching to a consensus within natural hazard community. Then they create GIS model composing 4 main areas; (i) Portray the natural and human environment, (ii) Assess earthquake and tsunami hazards, (iii) Identify various resources exposed to hazards (societal, built environment, critical resource, infrastructure, economic and environmental), (iv) Assess community vulnerability (pre-event conditions, response issue, recovery issue).

In 2003, Papathoma et al., realized the past studies was made by thinking all structures and people within this flood area are uniformly at risk of damage. But in fact, population and infrastructure are not uniformly at risk within a tsunami inundation zone. Because risk (the probability for damage) is intimately related to vulnerability (the potential for damage) (Alexander, 2000). Therefore, Papathoma et al. (2003), stated the necessity and presence of complex set of factors that varies spatially and temporally to produce a pattern of vulnerability. They present a new methodology for tsunami vulnerability assessment constructed and presented within a GIS environment, which incorporates multiple factors and applied this methodology on coastal segment in Crete, Greece.

This pioneering study was composed of 4 steps; (i) Identification of field site; chosen area with a long and reliable historical tsunami record to yield tsunami wave heights and inundation distances, (ii) Estimation of worst case scenario, according to the historical tsunami events, the most extreme inundation zones and highest recorded tsunami waves were identified, (iii) Identification of parameters that may contribute to vulnerability (built environment, sociological data, economic data, environmental/physical data), (iv) Establishing the GIS base map and generation of the primary database (to be used by local authorities, disaster planners, insurance companies). They pointed out the usefulness of using GIS for tsunami disaster managements, due to its dynamic nature instead of producing static map.

Papathoma and Dominey-Howes (2003), outlined the hazard probability for Gulf of Corinth considering the return periods of tsunami events according to their Intensity Scale (Ambraseys, 1962), then selected the 7th February 1963 tsunami (a submarine landslide tsunami triggered by a small earthquake with a H(m) max of +5m and a

tsunami intensity of Ko IV) as the worst case scenario. Then applied the first version of 'Papathoma Tsunami Vulnerability Assessment' (PTVA-1) for two villages in the region, considering the non-uniform and dynamic form of risk within the inundated area using a number of parameters.

In PTVA method applied to the study area, the followed steps are; (i) Identification of the Inundation Zone and Inundation Depth Zones, (ii) Identification of factors that affect the vulnerability of buildings/people and collection of data, (iii) Calculation of the vulnerability of individual buildings within the inundation zone using a Simple Additive Weighing scheme among Multi criteria evaluation methods, (iv) Present Building Vulnerability (BV) and Human Vulnerability (HV)

In their study they calculate the inundation zone according to the historical data and separate the inundation depth zones according to the vertical run-up of tsunami wave from ground elevation. They neither did consider any specific source of tsunami nor use any bathymetry data for calculations. The identification of vulnerability factors in the methodology was based on building vulnerability, such as construction material, number of floors, condition of the ground floor, presence of sea defense in front of the building. They also calculate a human vulnerability for each building which is in a direct relationship of building vulnerability and the population present in the building

After calculation of BV they used the number and percentage of businesses and services within inundated buildings for each village and each classification made according to BV to obtain an economical vulnerability. According to the outcomes of the vulnerability assessments authors made recommendations to end-users and stakeholders.

Since every model require validation, Dominey-Howes and Papathoma (2007) used the post-tsunami surveys from the Maldives after the 2004 Indian Ocean Tsunami. According their evaluation, they figured out some of the attributes of PTVA-1 are significantly important and others are moderately important for assessing vulnerability. They modified the model and proposed a revised version of PTVA (PTVA-2).

In 2009, Dall'Osso et al. revised the Papathoma Tsunami Vulnerability Method and provide an enhanced version of the method (PTVA-3) which takes account some new factors that affect building vulnerability. In the PTVA-3 Method, Analytical Hierarchy Process (AHP) has been used to avoid subjective ranking of the attributes in the previous versions of the model. They have applied the modified model to Maroubra, Sydney, Australia, where they calculated a score for each building under tsunami inundation, Relative Vulnerability Index (RVI). RVI is related with structural vulnerability (SV) and WV, whereas SV was the core of the previous versions of PTVA, and the vulnerability of building elements due to their contact with water (WV) was the vulnerability of building elements due to their contact with water, formed the new part of the PTVA-3. WV parameter that considers the level of building inundated by water which will require repair or replace after the event. Any probabilistic tsunami scenarios were not made until this paper for the region therefore authors made a deterministic approach by assuming the maximum run-up of the tsunami wave as +5 m above sea level (Dall'Osso et al., 2009a).

Dall'Osso et al. (2009b) used the recently revised PTVA-3 method for a submarine landslide triggered tsunami scenario for Manly area in Australia. It was assumed that a submarine sediment slide occurs off-shore of Sydney without an earthquake occurrence and inundated the area during an astronomical high tide with maximum run-up 7 m above mean sea level. According to this scenario a Relative Vulnerability Index (RVI) was calculated for each building in that area to determine potential damage after tsunami event. The main purpose of this study was to provide a conservative and detailed building vulnerability assessment to the local governmental authorities while probabilistic approaches were being developed.

Hart et al. (2009) aimed a distinct objective and they employed GIS for assessments of the vulnerability of an open-coast dune system to tsunami hazards and protective function of those open-coast dunes. As they stated, the Indian Ocean Tsunami reveals the value of coastal barriers to tsunami run-up. Even in the areas exposed to a similar wave effect from a tsunami event experienced very different levels of property damage and casualties because of difference between the present natural coastal defenses. In the study high resolution LIDAR topographic data of the study area Christchurch, New Zealand were used, therefore collection of highly accurate coastal elevation data

including three-dimensional dune morphology was possible. According to the analysis the vulnerability of the vegetated dune system to tsunami inundation has two characteristics; (i) elevation of dune crest, (ii) the continuity of its longshore profile (lack of gaps). By using these characteristics authors developed a relative vulnerability classification of dunes and assumed that the presence of vegetated, continuous and high dunes offers the best form of natural shore protection on temperate sandy open coasts. Additionally, it was stated other natural barriers like mangrove forests, and reefs have been shown to reduce tsunami wave energy, reducing the impacts of run-up on the coastal zone and adjacent communities. Dune sections where the profile is low and/or discontinuous, with patchy vegetation, are vulnerable to tsunami inundation and require the most immediate planning and management attention.

Dall’Osso et al. (2010) applied the PTVA-3 Model to the Aeolian Islands, Italy to assess the vulnerability of the buildings in the area. That area is prone to effect by tsunami events due to its geological characteristics. The most recent event was occurred in 2002, triggered by two successive landslides. This event caused damage to the building especially in the island of Stromboli with 11 m maximum run-up. The aim of the study was both to assess the vulnerability of the area in the case of occurrence a similar event and validate the PTVA-3 Model by using the data from the 2002 event. They used the database of the buildings and calculate the Relative Vulnerability Index (RVI) for each building and validate the results of the model with the building conditions after 2002 event obtained from the photographs taken after the tsunami damage.

After the establishment of a probabilistic tsunami hazard assessment (PTHA) framework for Cascadia Subduction Zone (CSZ) by Tsunami Pilot Working Group in 2006, Dominey-Howes et al. (2010) calculated the Probable Maximum Loss (PML), according to this probabilistic approach which is associated with a 1:500 year tsunami flood. The former studies for that area (Wood, 2002; Wood and Good, 2004) were acknowledged as ‘issues identification tool’ but not a quantification of PML. In the absence of fully-developed and tested tsunami building fragility-damage assessment tools, PTVA model provides a framework capable of generating high-resolution first order assessments of building vulnerability and PML. In this study authors examine vulnerability deterministically based upon the probabilistic 1:500 year flood layer. The

PTVA method was applied to the Seaside region, northwest coast of Oregon, aiming;

(i) mapping and quantifying the exposure of one-story residential buildings and commercial buildings that located in the 1:500 year tsunami flood hazard zone, (ii) quantifying the vulnerability level of these structures using PTVA model, (iii) providing a preliminary estimate of PMLs for those buildings. The loss estimation tool was thought to be useful to emergency management and local government officials in prioritizing disaster mitigation efforts.

In another model offered by Omira et al. (2010), a different approach was proposed, where they used the combination of tsunami inundation numerical modelling, field survey and geographical information systems. This model was created to determine the tsunami impact and vulnerability assessment for Casablanca harbor and surrounding area in Morocco, which have an enormous tourist influx during high season, great economic importance due to the harbour, coastal facilities, historical and cultural sites. In this study they select the 1755 Lisbon tsunami event as the scenario, which has a run-up of 5 to 15 m according to historical records. For that particular region this study was the first attempt of a tsunami vulnerability assessment and the output of the map was required for preventing the community resilience and emergency planning for tsunami hazards.

The study was composed of two parts (i) tsunami hydrodynamic modelling and inundation mapping, (ii) tsunami vulnerability calculation model for assessment of building vulnerability. The parameters that has been used for the final calculation of building tsunami vulnerability (BTV) were building condition, inundation zone and quality of sea defense. For mapping the inundation, modified version of Cornell Multigrid Coupled Tsunami Model (COMCOT) has been used by using 3 nested grid layers. The worst case scenario was taken for the study. Authors stated that the data of historical 1755 event was not available; therefore, a validation of the model could not be possible. However, the use of tsunami inundation modeling made the method flexible to be applied in the areas where tsunami events are infrequent or there is no data available from the historical events.

Ismail et al. (2012) proposed a methodology of assessing various levels of tsunami vulnerability. Assessment was conducted in 3 stages; macro-scale, local-scale and micro-scale. On the macro-scale possible tsunami sources are determined and different scenarios were selected with the historical information for the computer modelling of the tsunami propagation which will affect the largest region of the study, Straits of Melaka. For the tsunami numerical modeling TUNA-M2 was used to simulate inundation. Verification of the numerical model was made by comparing the results of the same sources from COMCOT and TUNAMI-N2 models. From the macro-scale stage of the study a Tsunami Impact Classification Maps were created. The selected worst case scenario was from the same sources of 26 December 2004 event. At the second stage (local-scale) the most affected coastal areas taken from the worst case scenario of the first stage were determined and used for development of Tsunami Physical Vulnerability Index (PVI). The output from COMCOT model used as input in the TELEMAC-2D model, which is a hydrodynamic model that designed to simulate physical processes associated with rivers, estuaries, coastal and ocean waters. For the calculation of PVI following variables were used for divided regions of the area; geomorphology, geologic materials, coastal slope, tsunami wave height and inundation distance.

At the last stage (micro-scale) the most vulnerable areas of the second stage was used as selected areas. For that areas an exposure database was created which includes physical and structural states of buildings. In this stage a revised version of PTVA-3 was used for assessment of the building vulnerability. A Structural Vulnerability Index (SVI) was calculated for each building. According to the results recommendations has been made to the local authorities.

Santos et al. (2012) used the same historical event (1755 Lisbon Tsunami) and calculated risk for the area Figueira da Foz, Portugal. The main objective of the study was to value the presence of sand dunes and protective structures on the tsunami risk. To calculate the risk for both cases (with and without protective structures) they used tsunami hazard map determined by using non-linear shallow water equations (tsunami numerical modelling) and population data. Since these structures are prone to be damaged during a tsunami event, the case without those structures were assumed to be the worst case scenario.

Santos et al. (2012) also considered the arrival time of the tsunami wave. Tsunami hazard matrix was established by using classification based on tsunami travel times and classification of tsunami inundation depth. After establishing inundation hazard maps for the cases with and without protective structures (worst case scenario), authors calculate the tsunami risk assessment by using the population data for the region. According to the calculations the population at risk was 0.68 % with the existence of spurs and sand dunes. However, when these structures are completely destroyed the affected population increases up to 4.6 %.

Tarbotton et al. (2012), reviewed the Tsunami Vulnerability Assessment models up to that date to outline the required improvements. Authors reviewed the PTVA models more specifically and pointed out the lack of fragility curves of buildings to tsunami events and the complimentary side of qualitative PTVA methods to the absence of any quantitative data. PTVA model describe the vulnerability of a building as 'vulnerability score' which is a combination of inundation results of a potential tsunami scenario with measurable attributes of buildings such as condition, design and surroundings. The most important limitation that PTVA model is the static 'bathtub' approach for the tsunami hazard calculations. Authors indicated that the presence of a hydrodynamic model integrated to PTVA could offer a number of improvements such as; (i) integration of the protective structures to the model, (ii) improving building exposure by using the flow components (flow velocity, direction etc.), (iii) probabilistic approaches to vulnerability assessments.

Another study based on 1755 Lisbon Tsunami was made by Barros et al. (2015). In this study authors applied their methodology to two distinctive coastal areas with urban and rural context considering social, structural and morphological components of buildings for tsunami vulnerability assessment. Considering social vulnerability was the distinctive part of this study among previous studies.

After calculating morphological, structural and social vulnerability a Composite Vulnerability Index (CVI) was calculated by integrating the three components. Morphological and structural vulnerabilities was calculated as weighted sum of the parameters, where social vulnerability was calculated by using factor analysis. As a result, it is concluded that the dominant parameters can vary according to the rurality

degree of the region for the tsunami risk assessment. In the urban area selected for this study was fundamentally influenced by morphological characteristics. However, in the rural area the major component of the CVI was socioeconomic components.

A more recent tsunami building vulnerability assessment method was proposed by Benchekroun et al. (2015). The study was based on geographic information systems integrated with multi-criteria decision analysis for the assessment of tsunami vulnerability for harbor area of Tangier, Morocco. For the consideration of the worst case, authors selected the Cadiz Wedge source for the rupture mechanism of 1755 Lisbon as the scenario to be able to obtain the highest tsunami impact along the coastal area of Tangier, Morocco. According to the selected scenario, topographic and bathymetric data processed in the tsunami numerical model COMCOT-1x for the calculation of inundation at land. The calculations showed that there is a vertical inundation depth reaching up to 6 meters, while maximum horizontal inundation distances were seen along some canals and their surroundings reaching 2.7 m inland.

For calculation of building vulnerability, authors used a modified version of the BTV method of Omira et al. (2010). They have classified the buildings and protective structures according to the construction types and materials within the study area according to the field survey data, calculated the inundation with numerical modeling and applied the GIS-based BTV equation which is based on main criteria and weighting factors. As a result, they obtained the vulnerability level for each building in the inundated area along the bay of Tangier, Morocco.

Recently, Çankaya et al., (2016) developed a new tsunami vulnerability method, which is called as MeTHuVA (METU Tsunami Human Vulnerability Assessment) and applied it to the Yenikapı region of İstanbul. The developed method is composed of assessments of tsunami hazard and human vulnerability separately. Hazard assessment was carried out by the utilization of tsunami numerical model NAMI DANCE for the estimation of near shore tsunami parameters, especially flow depth on land. To calculate the maximum hazard and the worst case scenario two different tsunami sources in the Sea of İstanbul was used. For human vulnerability assessments GIS-based MCDA methods were used. Among MCDA methods Analytical Hierarchy Process (AHP) was selected. With the available datasets 8 different parameter layers

were produced by using GIS tools. To build the hierarchical structure of AHP, these eight parameters were grouped in two different aspects, vulnerability at location and evacuation resilience. Among the eight parameters, distance to shoreline, geology, elevation and metropolitan use were included in the vulnerability at location, whereas distance to buildings, slope, distance to road networks and distance to flat areas were grouped in the evacuation resilience.

The study of Çankaya et al., (2016), presented a new approach for tsunami risk assessment where, vulnerability at location, evacuation resilience and the results of hazard assessment were associated. Addition to these parameters, the constant n , which represents the awareness and preparedness level of the community was introduced. According to the authors, the awareness factor, n , is the only parameter that can be controlled with increasing the awareness level of the community, within the presented risk equation. They used $n = 3$ for İstanbul according to the comparison of awareness and preparedness between communities.

CHAPTER 3

TSUNAMI HAZARD ASSESSMENT

The researches on geosciences are often relies on numerical models in modern world, since they simulate the processes and help for forecasting the natural hazards. Numerical models are especially useful where the natural hazards are rare to observe in the real world for examinations and also time and size scales of physical experiments remain inadequate compared to the real processes. The results of natural hazard models are used for mitigation strategies, land use planning, evacuation planning, etc. (Courtland et al., 2012).

There are models existing for many natural hazards including tsunami. The natural phenomena that trigger tsunamis and the time that they take place remained unpredictable until now. However, once the tsunami triggered, the time of arrival of the wave, run-up and inundation can be forecasted through numerical models. Besides that, a tsunami numerical model could always calculate the impact of a hypothetical tsunami wave, even there isn't any occurrence of an event in the history. Hence, some mitigation strategies can be developed by responsible agencies, while the awareness and preparedness of the community for the tsunami are increased.

3.1 Tsunami Numerical Modeling

A tsunami model requires topographical and bathymetrical data in appropriate resolution for the area and one or multiple tsunami sources. The verified and validated tsunami numerical model uses these two data as inputs and calculates tsunami generation, propagation and inundation when the waves climb to the land (Özer, 2012 and Aytöre, 2015).

There are many tsunami numerical models developed to predict tsunamis for academic and operational purposes. The most common ones among them are; COMCOT (Liu et al, 1994; 1998), TUNAMI-N2 (Imamura, 1996) and MOST (Titov and Synolakis, 1998). Throughout this thesis, the simulations have been made by using the tsunami numerical model NAMI DANCE, which is developed in collaboration with Ocean Engineering Research Center, Middle East Technical University, Turkey and Institute of Applied Physics, Russian Academy of Science, and Special Research Bureau for Automation of Marine Researches, Far Eastern Branch of Russian Academy of Sciences, Russia by the scientists Andrey Zaytsev, Ahmet Yalçiner, Anton Chernov, Efim Pelinovsky and Andrey Kurkin, particularly for tsunami simulation and visualization (NAMI DANCE, 2016).

3.1.1 Theoretical Background for Tsunamis and the Computational Tool

NAMI DANCE

Tsunamis are giant waves that generated by the occurrence of a displacement on the sea floor or along coastline. Mostly the generation mechanisms are earthquakes and submarine/subaerial landslides, but tsunamis can also be induced by submarine volcanos, volcanic eruptions, glacier calving, meteorite impacts and explosions (Özer, 2012).

The earthquake induced tsunamis occurred in the deep sea initially behave as described in the long wave theory when it began to propagate. This is a wave that has a very large wave length and velocity that reaches up to 800 kilometers per hour, while the wave height in the deep sea is very low and it can be barely noticed by the ships. Approaching the shoreline, the height of the wave increases, while the wave length and the velocity of the wave decrease according to the equation below.

$$C = \sqrt{g * d} \quad \text{(Equation 3.1)}$$

Where C is the velocity of the wave, g is gravitational acceleration and d is the water depth. Therefore, the 800 km/h velocity could be observed when the water depth is about 5 km. In the case of the Sea of Marmara, since the maximum water depth is about 1200 m, the velocity of a tsunami wave can be approximately 390 km/h.

When the tsunami wave approaches to the shore the nonlinear effects and the hydrodynamic parameters become significant. Throughout this thesis for hazard assessments the tsunami numerical tool NAMI DANCE is used and this tool solves Nonlinear Shallow Water Equations (NSWE) in single or nested domains.

The important hydrodynamic parameters when the tsunami hit the land are flow depth, run-up, and inundation distance (Figure 3.1). Among these, inundation distance and flow depth are the most important hydrodynamic parameters for this study. While inundation distance identifies the presence level, flow-depth determines the hazard level at the inundated area. Inundation distance is the horizontal distance between original shoreline and the maximum level that the tsunami wave reach. Correspondingly, the flow depth is height of water surface in inundation zone.

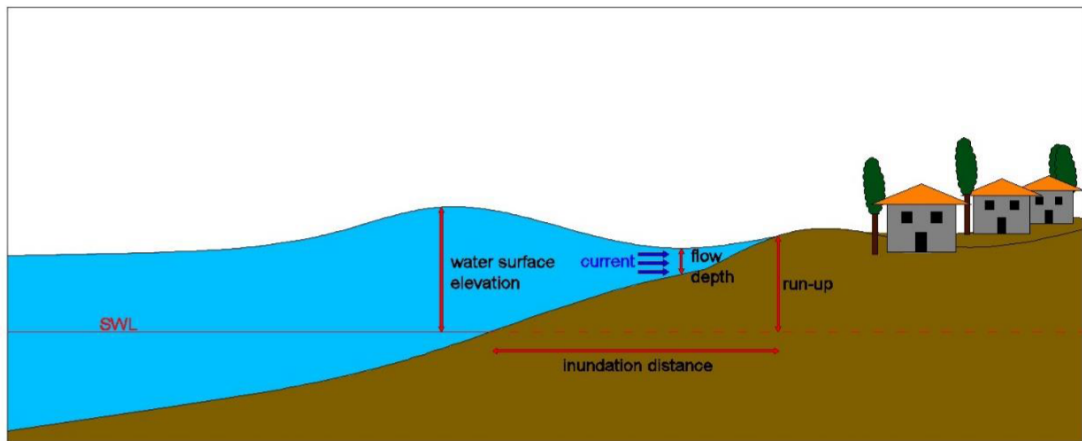


Figure 3.1 A cross sectional view of the tsunami parameters (modified from Yalçiner and Aytöre, 2012)

The initial wave for the simulation is generated using NAMI DANCE by entering the required tsunamigenic source parameters that are, epicenter coordinates, width and length of the fault, strike angle, dip angle, rake, focal depth and vertical displacement of the fault. Besides that, NAMI DANCE allows to create initial water surface disturbance with user defined dimensions and shapes (Aytöre, 2015).

With the determined tsunami source and topographical and bathymetrical data and gauge locations as inputs, NAMI DANCE calculates the principal tsunami

hydrodynamic parameters for the selected domain and the water level changes by time in the gauge locations. While simulation continues it is possible to observe the situation of sea level is possible.

The computational tool is also able to generate 3D plotting of the sea state with the selection choice of light and camera locations, therefore at the end of the simulation it is possible to create 3D animations showing the propagation and inundation within the domain.

NAMI DANCE is a validated and verified numerical tool and applied in numerous studies for different tsunami events (Yalçiner et al., 2010; Yalçiner et al.,2011, Heidarzadeh et al., 2013; Onat and Yalçiner, 2013, Özer and Yalçiner, 2011; Yalçiner et al., 2014; Dilmen et al., 2014; Sözdinler et al., 2014; Zaytsev et al., 2015).

3.2 Application of NAMI DANCE to Study Area

3.2.1 Selection of Tsunami Source Parameters

Tsunamis are caused by abrupt displacement of water body and can be triggered by different phenomena including earthquakes, submarine or subaerial landslides, volcanic eruptions etc. The study area of this thesis is located in an active fault zone, therefore it is prone to undergo earthquakes with different magnitudes. Furthermore, this area is also faced with landslide occurrences including the earthquake induced ones. According to the historical documents the area of the Sea of Marmara suffered from tsunami events both induced by earthquakes and landslides.

Throughout this thesis the generating mechanism for tsunamis are assumed to be the earthquakes, and the fault segments in the Sea of Marmara, that can trigger tsunami were surveyed from the related studies and reports (Yalçiner et al, 2002; Hebert et al, 2005; OYO-IMM Report, 2008; Ayca, 2012). According to these studies, on the northernmost branch of the North Anatolian Fault, there are six faults that can be tsunamigenic (Figure 3.2). These are the Prince's Island fault (PI), Prince's Island Normal fault (PIN), Ganos fault (GA), Yalova Normal fault (YAN), Central Marmara fault (CMN) and the combination of GA and PI. These characteristics of five of these faults are presented in the Table 3.1.

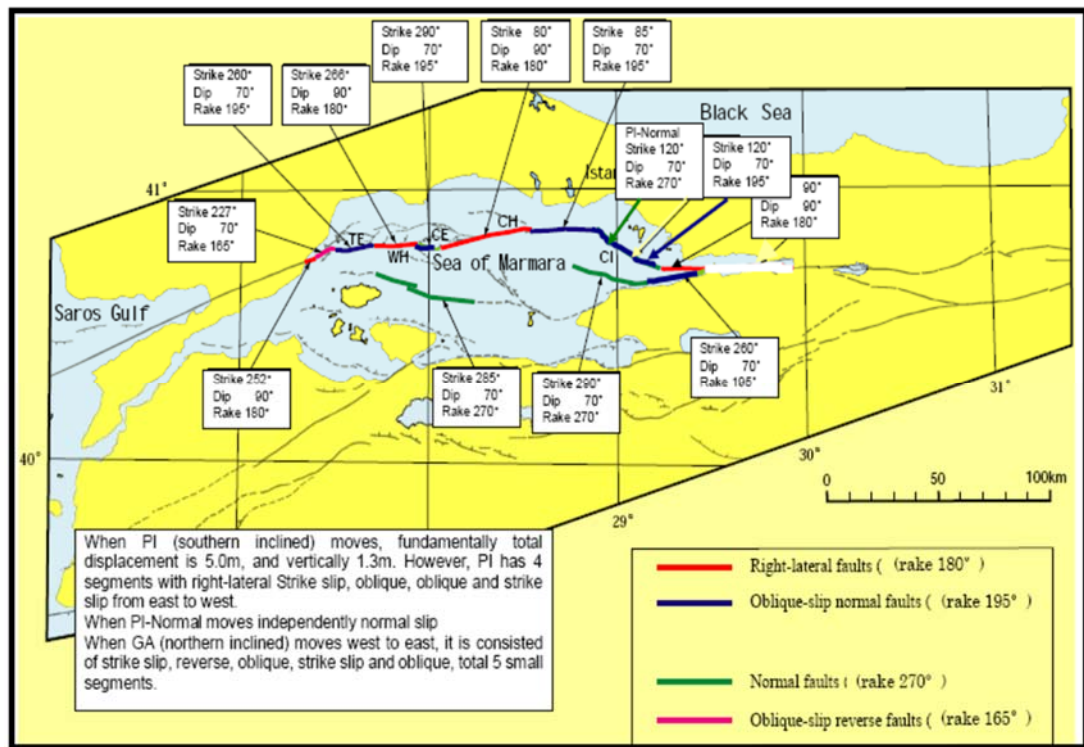


Figure 3.2 Setting distribution and parameters of the faults in the Sea of Marmara (OYO, IMM, 2008)

Table 3.1 List of tsunamigenic faults located in the Sea of Marmara and their characteristics

<i>Fault</i>	<i>Fault Characteristics</i>
Prince's Island fault (PI)	Oblique-Normal
Prince's Island Normal fault (PIN)	Normal
Ganos fault (GA)	Oblique-Normal and Oblique-Reverse
Yalova Normal fault (YAN)	Oblique-Normal and Normal
Central Marmara fault (CMN)	Normal

Since the vertical displacement of the sea floor is one of the main parameters for the tsunami generation, among the five faults in Table 3.1, PIN, YAN and CMN have been selected for the next stage of calculations in the tsunami numerical tool for hazard assessment of Bakırköy district of İstanbul.

As stated in the OYO-IMM Report (2008), a submarine survey with the unmanned submersible vessel performed by MARMARASCARP cruise, in 2002, in order to

observe the fault scarps from 1912 Ganos Earthquake and 1999 İzmit earthquake. Armijo et al., (2005) mentioned the results of the submarine cruise and the displacements caused by the above mentioned earthquakes. According to these results the vertical displacement were changing between 2 and 4 m. Considering these references and in order to stay in the conservative side, in the simulations carried out for this thesis, vertical displacement of selected ruptures is assumed to be 3.7 m.

Tsunami source YAN composed of 8 segments and three of these segments are oblique-normal while the other five are normal. While simulations it is assumed that all segments were ruptured as the worst case scenario. The rupture parameters of those segments and initial minimum and maximum wave amplitudes and the resulting initial wave position can be seen in the Table 3.2 and Figure 3.3, respectively.

Table 3.2 Estimated rupture parameters and initial wave amplitudes for tsunami source YAN (modified from Ayça, 2012)

Fault	Type	Longitude (ED_50)	Latitude (ED_50)	Depth from sea	Strike	Dip	Rake	Length	Width	Vertical Displacement	Initial Wave Amplitude	
		degree	degree	m, GL-	degree	degree	degree	m	m	m	Max (m)	Min (m)
YAN	Oblique-Normal	29.47103	40.72115	1978	257.96	70	195.00	7058	17027	3.7	0.36	-1.15
		29.38946	40.70750	1960	261.14	70	195.00	6873	17027	3.7	0.44	-1.22
		29.30920	40.69751	1823	260.98	70	195.00	10952	17027	3.7	0.68	-1.74
	Normal	29.18143	40.68121	1681	262.35	70	270.00	4448	17027	3.7	0.38	-1.15
		29.12936	40.67550	1557	273.96	70	270.00	4562	17027	3.7	0.76	-1.86
		29.07551	40.67791	1252	283.78	70	270.00	10021	17027	3.7	0.39	-1.32
		28.96007	40.69843	1219	294.84	70	270.00	3154	17027	3.7	0.41	-1.31
		28.92602	40.71005	1178	284.90	70	270.00	14043	17027	3.7	0.58	-1.59

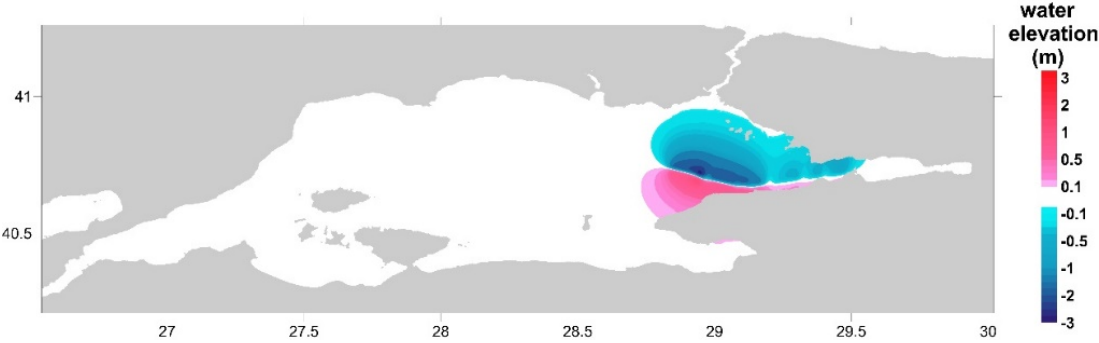


Figure 3.3 Initial wave condition of tsunami source YAN

The other tsunami source CMN has 5 segments and all of them are in normal fault characteristics. For the simulations it is assumed that all the segments are ruptured. The rupture parameters of those segments and initial minimum and maximum wave amplitudes and the resulting initial wave condition are presented in the Table 3.3 and Figure 3.4, respectively.

The tsunami source PIN composed of the first four oblique-normal segments of the source PI. While creating the source in computational tool it is assumed that the 4 segments are ruptured simultaneously. The rupture parameters of the PIN and the initial minimum and maximum wave amplitudes that has been generated and the resulting initial wave position can be seen in Table 3.4 and Figure 3.5, respectively.

Table 3.3 Estimated rupture parameters of initial wave amplitudes for tsunami source CMN (modified from Ayça, 2012)

Fault	Type	Longitude (ED_50)	Latitude (ED_50)	Depth from	Strike	Dip	Rake	Length	Width	Vertical Displacement	Initial Wave Amplitude	
		degree	degree	m, GL-	degree	degree	degree	m	m	m	Max (m)	Min (m)
CMN	Normal	28.19394	40.61261	1924	276.59	70	270.00	9505	17027	3.7	+0.55	-1.49
		28.08215	40.62063	1922	279.18	70	270.00	7069	17027	3.7	+0.47	-1.34
		27.99943	40.62938	1917	299.07	70	270.00	10705	17027	3.7	+0.58	-1.55
		27.88744	40.67421	1598	283.92	70	270.00	7850	17027	3.7	+0.56	-1.51
		27.79683	40.68952	1637	291.38	70	270	7269	17027	3.7	+0.53	-1.46

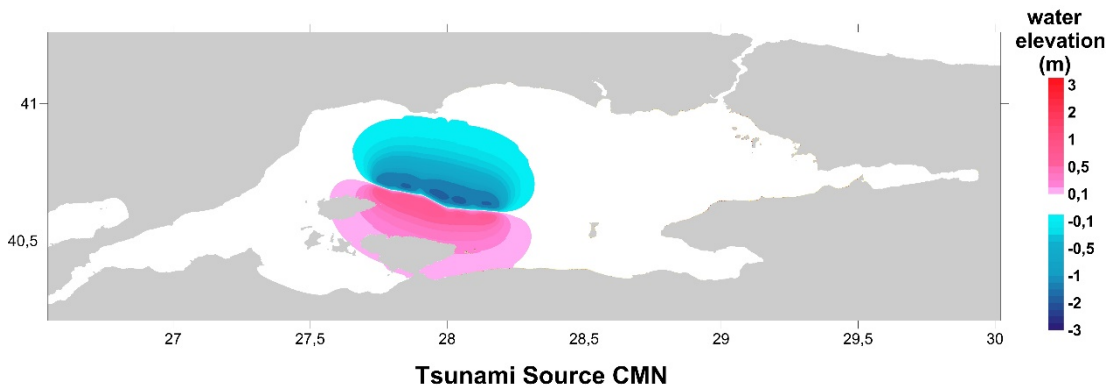


Figure 3.4 Initial wave condition of tsunami source CMN

Table 3.4 Estimated rupture parameters and initial wave amplitudes for tsunami source PIN (modified from Ayça, 2012)

Fault	Type	Longitude (ED_50)	Latitude (ED_50)	Depth from	Strike	Dip	Rake	Length	Width	Vertical Displacement	Initial Wave Amplitude	
		degree	degree	m, GL-	degree	degree	degree	m	m	m	Max (m)	Min (m)
PIN	Normal	29.12942	40.75691	744	108.15	70	270.00	8753	17027	3.7	+0.77	-1.90
		29.06928	40.78610	740	123.15	70	270.00	6024	17027	3.7	+0.70	-1.78
		28.99465	40.81653	779	118.85	70	270.00	7148	17027	3.7	+0.73	-1.83
		28.90432	40.87251	1210	129.90	70	270.00	9834	17027	3.7	+0.68	-1.75

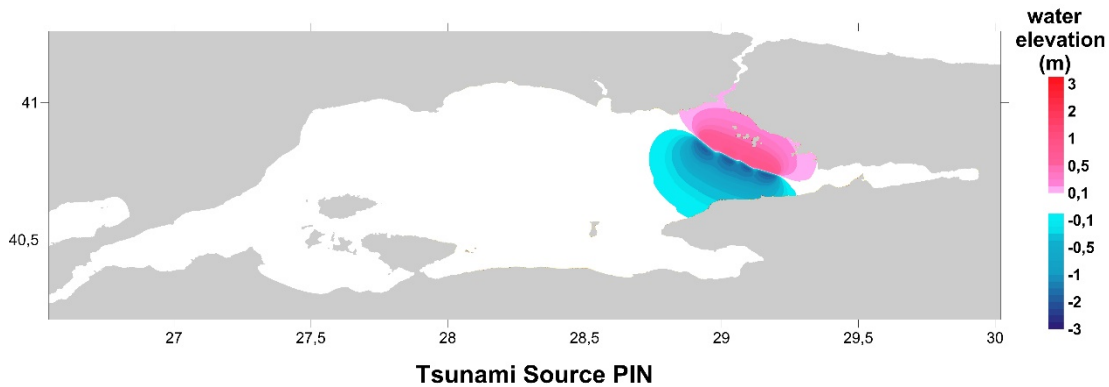


Figure 3.5 Initial wave condition resulted by tsunami source PIN

3.2.2 Domain Selection for Numerical Model

The application of numerical modeling to the study area covers nested domain simulations. Throughout the study it is aimed to calculate the hazard, vulnerability and risk in high resolution. In order to reduce the computational time for calculation of tsunami parameters on land, nested domain simulations were governed for the study.

For nested domain simulations for hazard assessment, four nested domains were used; B, C, D, E domains. These four domains are in different sizes (larger to smaller) and in different resolutions (Table 3.5). The largest domain (domain B) covers the central and eastern parts of Marmara Sea and has 81 m resolution. The following smaller domains covers the region of Bakırköy district and its vicinity including the marine area. Each following domain is smaller and has 3 times higher resolution than the previous domain. Therefore, while the largest domain (domain B) has 81 m resolution, domain C, D and E has resolutions of 27 m, 9 m and 3 m, respectively. The details

about coordinates and resolutions and visuals of the nested domains are presented in Table 3.5 and Figure 3.6.

Table 3.5 Coordinates of Nested Domains

Domain Name	Grid Size	Coordinates	
Domain B	81 m	40.21° - 41.26° N	27.60° - 30.02° E
Domain C	27 m	40.9207° - 41.0069° N	28.7716° - 28.8962° E
Domain D	9 m	40.9210° - 41.0066° N	28.7719° - 28.8958° E
Domain E	3 m	40.9212° - 41.0065° N	28.7721° - 28.8956° E

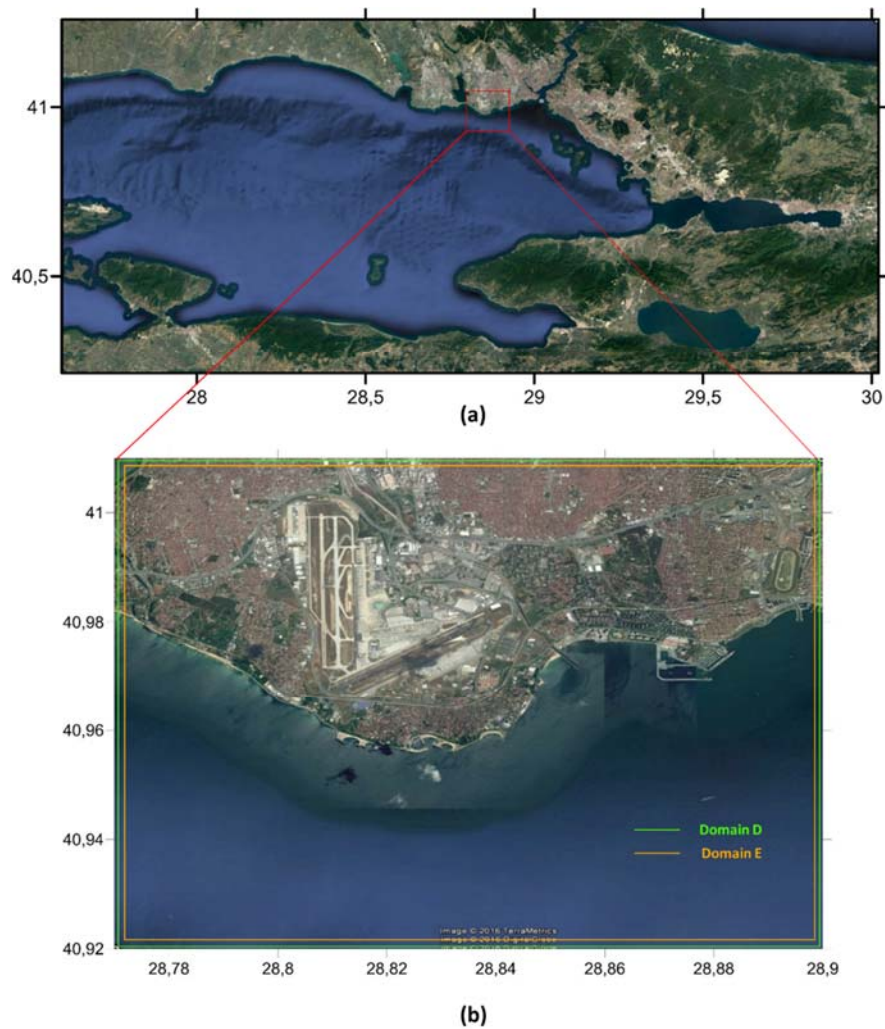


Figure 3.6 Selected domains for the simulations in NAMI DANCE. (a) Domain B, (b) Domain C, including Domain D with green and Domain E with orange

3.2.3 Development of High Resolution Topographic and Bathymetric Data for Tsunami Simulations

Development of the high resolution topographic data were performed by using the 5 m resolution DEM created by aerial photogrammetric methods and the vector dataset including all structures and infrastructures with adequate attributes obtained from IMM.

In order to develop a high resolution digital elevation model from the 5m resolution DEM obtained from IMM has been used at the first step. Since a raster data basically includes the geographic coordinates (XY), and elevation values (Z) of the center of each cell, the 5 m resolution DEM has these data of each 5 m spaced point. With the appropriate interpolation method, the raster dataset of the Bakırköy area has been up-sampled to 1 m cell size. This step was applied only for the proper integration of the 5 m DEM to the improved high resolution DEM, hereinafter called ‘metropolitan topography’.

For development of metropolitan topography after the resampling of 5 m resolution DEM, the vector dataset acquired from IMM has been used. This vector dataset includes all the structures and infrastructures of the region in polygon, line and point data format including, different types of buildings, utilities, roads, railways, underpasses and overpasses etc.

For the development of the high resolution metropolitan topography, the polygon dataset has been used from this database. All the features of the polygon dataset have many attributes in the attribute table, including elevation values of each corner point of the individual building polygons. Final development of the metropolitan topography required the elevation of all the buildings joined within one dataset. For the successful integration of the building polygons to the resampled 1 m DEM, all the polygons were converted to raster with 1 m cell size, having the highest elevation value of the corners, to which polygon it belongs.

The largest river that passes through Bakırköy district is the Ayamama Stream, as stated earlier and the 5 m resolution DEM obtained by aerial photogrammetric methods contains the water surface elevation of that river. For the further development of the

metropolitan topography at the area where Ayamama Stream is located, an additional vector database that stores the bottom elevation of the Ayamama river was obtained from İstanbul Metropolitan Municipality. This database was used to generate a bottom elevation topography of the river in 1 m resolution.

The three produced raster data, (i) the resampled 1m resolution DEM of the area and, (ii) building polygons converted to raster with the appropriate elevation values, (iii) the bottom elevation topography of Ayamama Stream have been integrated for the final generation of the ‘metropolitan topography’ by writing a script.

Bathymetric data obtained from GEBCO were improved by using the nautical charts acquired from Turkish Naval Forces and a final bathymetric map with 1 m resolution were produced. The data has been modified as having negative values for land and positive values for sea since the tsunami numerical model requires the dataset like that.

In order to join topographic and bathymetric data properly, the most recent shoreline was digitized from Google Earth images. According to that shoreline high resolution metropolitan topographic data and bathymetric data were integrated by using overlay operations (Figure 3.7).

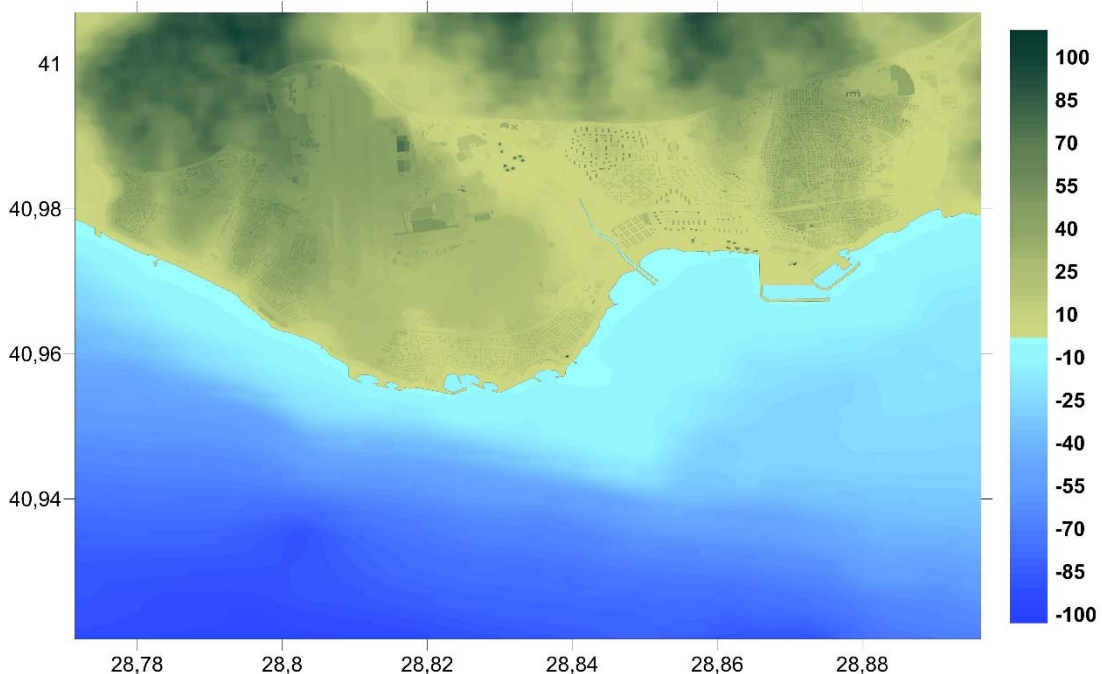


Figure 3.7 Integrated elevation dataset

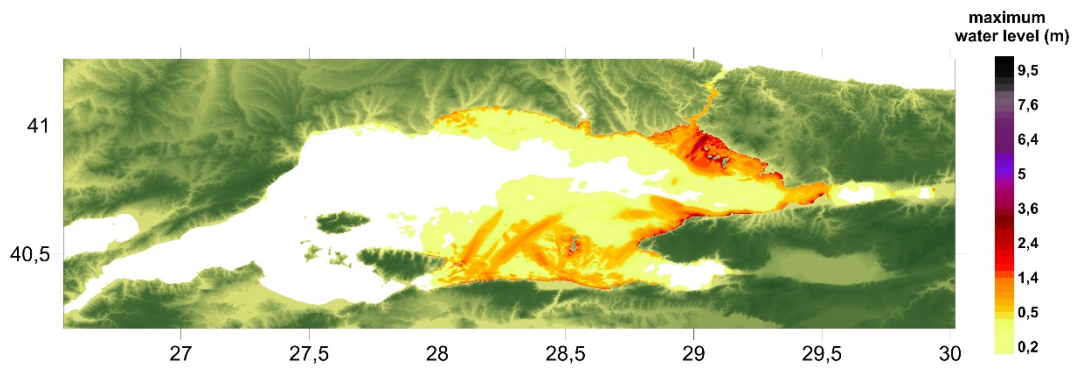
3.2.4 Tsunami Simulations for Hazard Assessment for Bakırköy District

3.2.4.1 Single Domain Simulations for Worst Case Scenario Selection

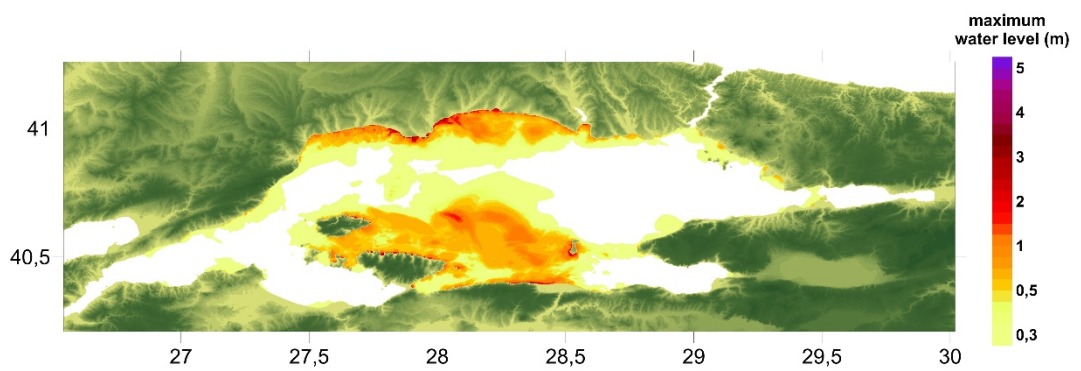
For selection of the most destructive tsunami source among the three sources that was explained earlier (PIN, CMN and YAN) a single domain simulation was performed with 42 m resolution data of whole Marmara Sea and the land surrounding. The bathymetric data obtained from GEBCO (General Bathymetric Chart of the Oceans) and the topographic data obtained from ASTER Global DEM have been combined together and arranged to have the resolution of 42 m. This data has been used as the input for the tsunami computational tool NAMI DANCE.

In order to select the worst case scenario among the three tsunami sources, three different 60 minute simulations have been performed for the tsunami sources CMN, PIN and YAN. The wave propagation using each source were calculated. The distributions of maximum water elevations in this domain can be seen in the Figure 3.8.

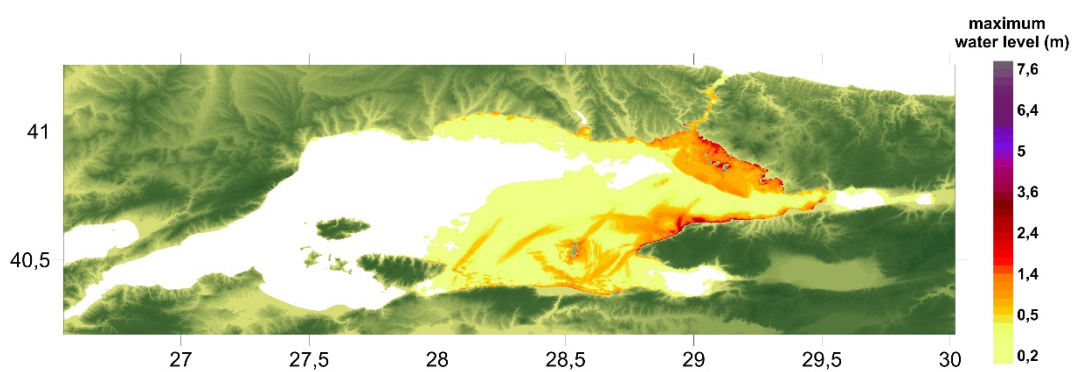
Comparing the result from three different tsunami sources and the distribution of maximum water elevation it can be seen that the most effective tsunami source for the Bakırköy district is YAN. Tsunami source CMN is located in the central Marmara near Marmara Island and for effecting the Bakırköy district it seems to have the appropriate location and direction. However, since the rupture of the CMN source is located at the west of Bakırköy district and almost parallel to the shoreline the most affected areas from that source are located to the west of the study area. The other tsunami sources considered in this study are PIN and YAN. These two sources are located in the east of Marmara Sea. Comparing these too, it can be said that the tsunami source YAN has more impact on Bakırköy district than PIN. The reason of this can be explained by the depression plate of the sources. The leading depression wave of YAN is on the north where the Bakırköy district is located, while the leading depression wave of PIN is towards the south of Marmara. The leading-depression waves causes higher amplification and run-up when compared to the elevation waves of similar amplitude (Tadepalli and Synolakis, 1996).



Tsunami source YAN
(a)



Tsunami source CMN
(b)



Tsunami source PIN
(c)

Figure 3.8 The tsunami sources and maximum water elevation distributions according to the single domain 60 minute simulations that has been performed in NAMI DANCE. (a) Tsunami source YAN, (b) Tsunami source CMN and (c) Tsunami source PIN

Additionally, according to the simulations for three sources, the water elevation by time at the southern border of the Domain E was measured (Figure 3.9). As seen in the figure; tsunami source CMN is arriving after more than 10 minutes and the oscillation caused by that source is very low at the southern border of Domain E. As discussed earlier among the other two tsunami sources, YAN causes more water oscillation than PIN with minimum wave amplitude lower than -0,8 m and maximum wave amplitude over 0.4 m of at the southern border of Domain E.

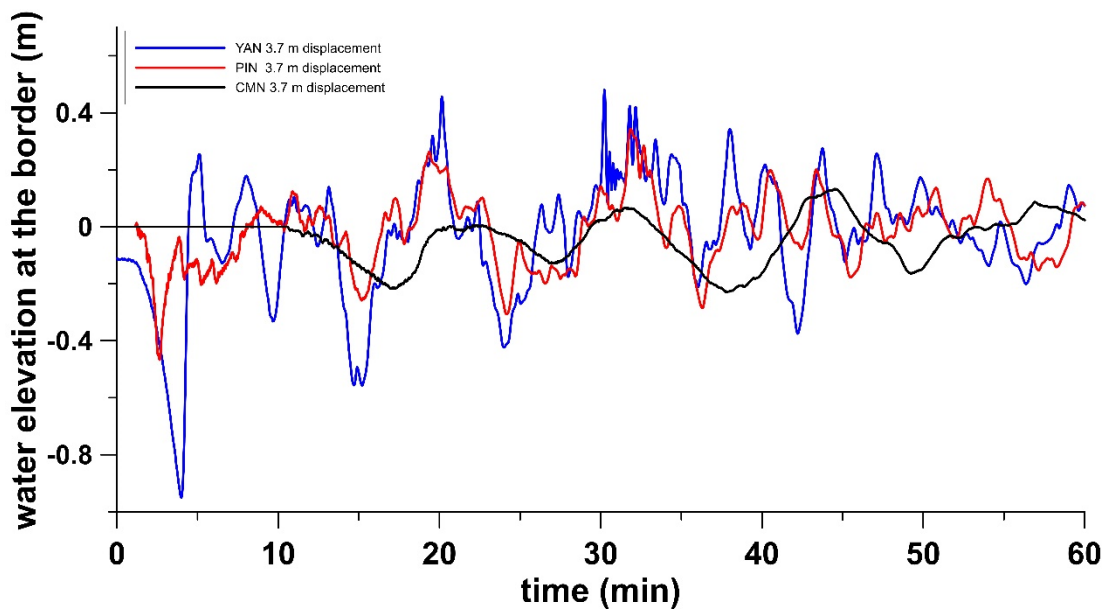


Figure 3.9 Time history of water level changes at the southern border of domain C resulting simulations of tsunami sources PIN, YAN and CMN.

3.2.4.2 Nested Domain Simulations for the Tsunami Source YAN

The comparison of the results obtained from nested domain simulations revealed that the tsunami source YAN is the most effective tsunami source. Hence, tsunami source YAN has been selected as the worst case scenario for Bakırköy district and the following parts of the study the analysis has been carried on accordingly.

After the selection of worst case scenario, a nested domain simulation has been performed in the tsunami computational tool NAMI DANCE. Using the tsunami source YAN, a 60 minute simulation was realized by using the domains B, C and D.

The 3 m resolution Domain E was not included to the nested domain simulations due to excess amount of computational time. The simulation for Domain E was realized by using the results of nested domain simulation. The water level changes at the southern border of the Domain E was obtained from the nested domain simulation and used as initial condition for 3 m resolution Domain E simulations.

The near shore tsunami parameters mentioned earlier have been calculated for Bakırköy district for the smallest domain (Domain E). For the hazard assessments of Bakırköy district the most important near shore tsunami parameter was flow depth. Therefore, flow depth for every location of the Bakırköy district was obtained from the simulations and plotted to show the hazard level (Figure 3.10). According to the results of the simulation, the maximum flow depth on land reaches up to 5.7 m and the horizontal inundation distance exceeds 350 m. Moreover, water penetrates almost 1700 m along Ayamama Stream.

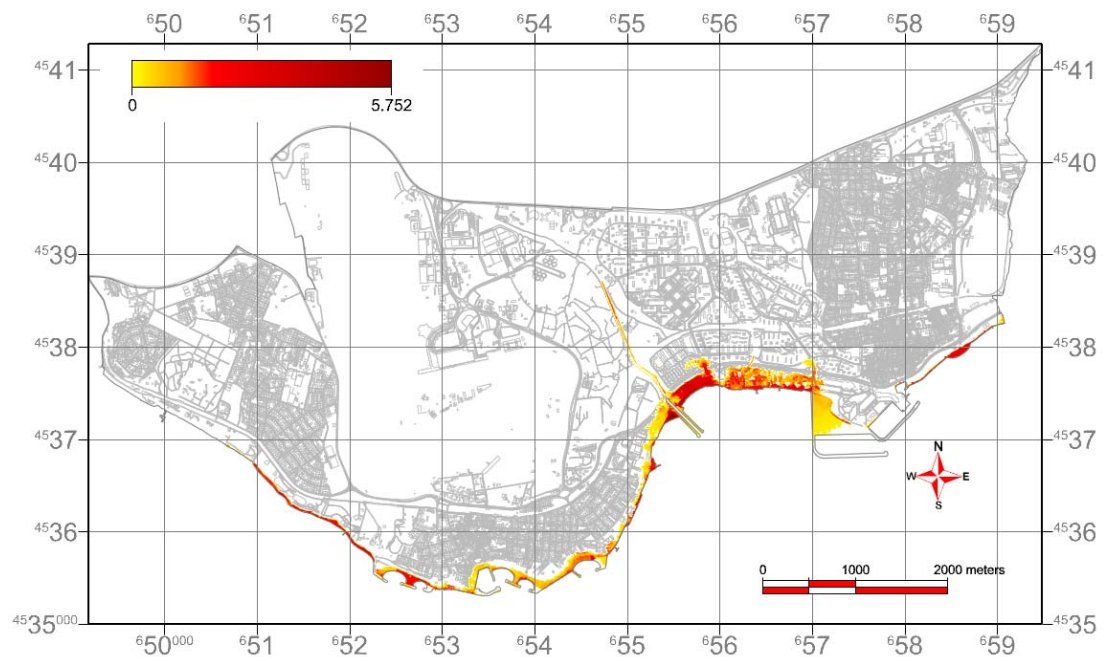


Figure 3.10 The flow depth (hazard) map of the simulated tsunami event according to the tsunami source YAN

CHAPTER 4

METROPOLITAN TSUNAMI HUMAN VULNERABILITY ASSESSMENT (MeTHuVA) WITH GIS BASED MCDA

The recent devastating tsunami events, 2004 Indian Ocean Tsunami and 2011 Tohoku Tsunami, raised the awareness of both governments and communities worldwide that paved the way for developments about mitigation strategies.

Since the major modern tsunamis took place, tsunami numerical models, early warning systems, hazard, risk and vulnerability assessment studies were increased drastically. Tsunami vulnerability assessment studies form a considerable part of this development. However, a great part of them remain only to assess the building vulnerabilities. While there are studies indicating the need of tsunami human vulnerability assessments (Dominey-Howes et al., 2010), there are a few studies which involve the building based human vulnerability (Papathoma and Dominey-Howes, 2003) to their studies.

To cover the need of tsunami human vulnerability assessment methods, Çankaya et al., (2016) developed a new methodology; METU Tsunami Human Vulnerability Assessment (MeTHuVA). In this study, the method MeTHuVA has been further developed and modified by introducing new parameters. Since the introduced parameters represent a metropolitan area the name of MeTHuVA has been changed as Metropolitan Tsunami Human Vulnerability Assessment.

As offered by Çankaya et al., (2016), in this study, two issues have been used to evaluate tsunami human vulnerability for Bakırköy district of İstanbul; Vulnerability at Location (VL) and Evacuation Resilience (RE)

In this chapter, firstly a general information is given about the GIS based MCDA, then the use of MCDA for this study is discussed by explaining the method and its

application. Later, the parameters under the ‘vulnerability at location’ and ‘evacuation resilience’ are introduced and their detailed production steps are explained in separate sections. At the last stages of each section, the generation of the final vulnerability at location and evacuation resilience maps with GIS based MCDA are described.

4.1 GIS-based MCDA

The time when the fundamental concept of MCDA first appearing goes back to the second half of nineteenth century. At that time this concept was established by F.Y. Edgeworth and V. Pareto in order to propose an approach for combining conflicting criteria into a single evaluation index (Malczewski and Rinner 2015).

The roots of today’s GIS-MCDA lean on two main research traditions: Operations Research and Management Sciences (OR/MS) and landscape architecture/planning (Malczewski and Rinner 2015). The landscape architecture and spatial planning stem of GIS-MCDA concept has the first applications in late nineteenth and early twentieth century with the overlay of hand-drawn maps by the American landscape architects (Steinitz et al. 1976; Collins et al. 2001). In 1969, McHarg and Mumford improved the overlaying techniques, by producing individual transparent maps using light to dark shading and superimposing these maps to build overall suitability maps. The overlay method that has been used by the above mentioned researchers is probably the most important precursor of the future complex forms of GIS-MCDA (Malczewski and Rinner 2015).

During the 1990’s increasing use of personal computer based GIS and decision support software lead the considerable progress of the GIS-MCDA. In various application domains, many different methods of MCDA has been applied in the GIS environment and a significant amount of studies has been published. The application areas can be listed as; environmental, transportation and urban planning/management, waste management, hydrology and water resource management, agriculture, forestry and natural hazards. The most popular MCDA methods within these studies include: the weighted linear combination and related procedures (e.g., Carver 1991; Eastman et al.

1995; Malczewski 2000), ideal/reference point methods (e.g., Pereira and Duckstein 1993; Malczewski 1996), the analytical hierarchy/network process (e.g., Banai 1993; Zhu and Dale 2001; Marinoni 2004), and outranking methods (e.g., Carver 1991; Joerin et al. 2001; Martin et al. 1999).

Considering all methods Analytical Hierarchy Process (AHP) is applied for the GIS-based MCDA sections of this study. The fundamentals of the method will be discussed in following section.

4.1.1 Analytical Hierarchy Process – AHP

The Analytical Hierarchy Process method is developed by Saaty in 1980. AHP is one of the most comprehensive methods of multi criteria decision analysis (Malczewski and Rinner 2015). The method is based on three principles: decomposition, comparative judgement and synthesis of priorities. Decomposition principle requires the decision problem to decompose into different levels of hierarchy. Comparative judgement requires the pairwise comparison of the elements at the same level of the hierarchy. Lastly the synthesis principle accounts each of the resulting ratio-scale priorities of the various levels of hierarchy to construct a composite set of priorities for the elements at the lowest level of hierarchy (Malczewski, 1999).

Following these principles AHP covers three fundamental steps;

- i. Developing the hierarchical structure; as the first principle requires the decomposition of decision problem to more simple decision problems, a hierarchical structure is constructed at the first step. The higher level of this hierarchy is the ultimate goal of the decision. Then the hierarchy descends to more specific levels until the level of decision alternatives (Figure 4.1). In the case of raster data models, a decision alternative is often defined as a single raster of specified size or a combination of rasters (Malczewski and Rinner 2015).

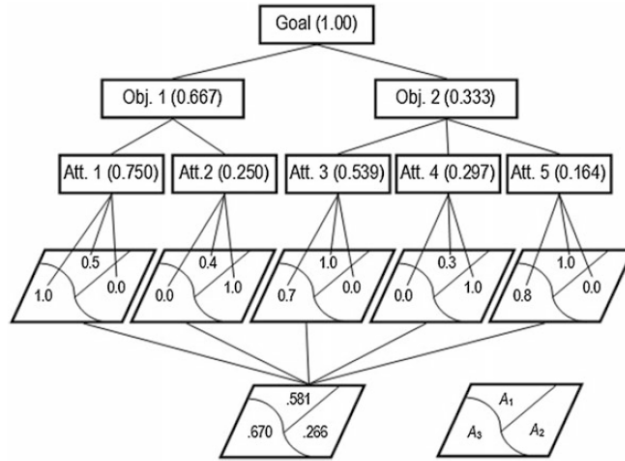


Figure 4.1 An example of hierarchical structure of GIS-based AHP model. A_1 , A_2 and A_3 are decision alternatives, $Obj.$ is objectives, $Att.$ is attributes and the numbers are showing standardized attributes values for each level of hierarchy (Malczewski and Rinner 2015).

- ii. Pairwise comparison and weight assignment: Pairwise comparison is the basic measurement mode employed in the AHP procedure (Malczewski, 1999). The pairwise comparison method decreases the complexity of comparing action as only two elements are taken account each time.

Pairwise comparison method

Pairwise comparison method creates a ratio matrix and generates relative weights. While making the comparison it employs the Saaty’s scale of relative importance (Table 4.1) that has values from 1 to 9 to compare each two elements in the same level of the hierarchy. Method involves three steps:

Table 4.1 Saaty’s scale of relative importance

Weight/Rank	Intensities
1	Equal
3	Moderately dominant
5	Strongly dominant
7	Very strongly dominant
9	Extremely dominant
2, 4, 6, 8	Intermediate values
Reciprocals	For inverse judgements

- Construction of comparison matrix by using the scale of relative importance for each level of hierarchy
 - Computation of weights for each element requires few steps. First the values in each column of the matrix are summed, and then each element in the matrix is divided by the column total it belongs. These two steps generate the normalized matrix. As the last step the average of the elements in each row of the normalized matrix is computed. This step generates the relative weights for each criteria of the hierarchy level which the pairwise comparison is applied.
 - Estimation of consistency ratio (CR) is performed. CR measures the admissible level of consistency in the pairwise comparison. To have reasonable consistency the CR value should be less than 0.10. If the CR value is equal or higher than 0.10 pairwise comparison should be revised.
- iii. Construction of overall priority rating; this final step is for aggregation of relative weights obtained in the second step to produce composite weights. This is achieved by the sequence of multiplications of the relative weight matrices at each level of hierarchy. These composite weights represent the ratings of alternatives regarding the overall goal.

Although there can be different hierarchical structures where the elements of the hierarchy could differ, the structure of a AHP hierarchy is generally composed of four levels; goal, objectives, attributes and alternatives. In this general case, the calculation of the overall evaluation score is calculated by the following equation:

$$V(A_i) = \sum_{k=1}^n w_l w_{k(l)} v(a_{ik}) \quad (\text{Equation 4.1})$$

Where $v(a_{ik})$ is the value function; w_l is the weight associated with the l^{th} objective ($l = 1, 2, \dots, p$) and $w_{k(l)}$ is the weight assigned to the k^{th} attribute associated with the l^{th} objective (Malczewski and Rinner 2015).

The applications of AHP to GIS environment can be categorized in two groups. First is the implication of hierarchy and combining the priority for each level, including the alternative level. This application can be done when there is a small amount of alternatives to realize the pairwise comparison. The second implication type of AHP integration with GIS is basically used for the estimation of criterion weights. After calculation of weights, they are combined with the map layers by using a WLC (weighted linear combination) rules. This method is mostly used when the number of alternatives are too many to achieve pairwise comparison.

4.2 Production of Parameter Maps and Datasets

The database of the available dataset mentioned in the section 1.3.1 was used to produce the thematic parameter maps for Vulnerability at Location and Evacuation Resilience. These are, vector dataset, 5m resolution raw DEM and geological map of the region which were obtained from Istanbul Metropolitan Municipality (IMM) with a production date of 2006. Both datasets are clipped according to the borders of study area before modifications.

The vector dataset was composed of many different layers of point (tree types, billboards, bus stops etc.), line (roads, railways, borders of streams, shoreline etc.) and polygon (all types of constructions) feature types. The suitable layers have been selected from this feature types and used for the following production of parameter maps. The geological formations and landslide scarps were digitized from the geological map of the region and added to vector database.

Since İstanbul is a great metropolitan city with population of almost 15 million and is still growing, the metropolitan structure of the city considering buildings and infrastructures are prone to change rapidly. For this reason, since the year 2006 a lot of changes has been observed in the metropolitan structure of İstanbul. These changes can be listed as below;

- Old residential buildings were replaced with new buildings with the urban transformation, also there are still buildings under construction
- New shopping malls have been constructed
- New hotels have been constructed
- The road network was renewed
- New coastal structures were constructed

The changes have been observed from Google Earth Images and accordingly the related datasets have been modified. New building constructions resulted changes in the vector dataset and the changes of the coastal structures lead the changes of final shoreline. The modified versions of the datasets have been used for the production of parameter maps.

Vector dataset has been used to produce seven of the nine parameter maps. The other two maps were produced with DEM of the region. The parameter maps are produced as raster maps with 1m cell size. This level of resolution leads the study to continue to be compatible with the high resolution metropolitan topography map which was generated for tsunami simulation and hazard assessment.

4.3 Assumptions for Vulnerability analysis of Bakırköy District

For the vulnerability assessment part of this thesis, there are a number of assumptions made as listed below;

- As clarified in the Chapter 3, the tsunami is assumed to induced by an earthquake caused by the rupture of Yalova Normal Fault. Therefore, this earthquake assumed as a warning that a tsunami wave is coming and would give time to people for evacuation.
- Tsunami arrival time to the land could differ in real case, but it is assumed that the wave arrived at the same time to whole inundated area.
- It is assumed that the tsunami inducing earthquake is occurred at a time when neither the high tide nor a storm event is present. All analyses were made on the mean sea level.

- All the buildings of the Bakırköy region are thought to be reinforced concrete buildings and assumed to remain undamaged after the earthquake and during tsunami. Hence the vertical evacuation to all the buildings of Bakırköy is assumed to be suitable.
- It is assumed that the day and night population density is constant.
- A large area of Bakırköy district is occupied by the İstanbul Atatürk Airport. Airport area is excluded from the vulnerability analysis. Because it is not possible to evacuate over the borders of this area since it is forbidden to enter other than the entrance of the airport. Moreover, including this area to the vulnerability analysis of the study would affect the result of the study and would be unnecessary.

4.4 Application of Analytical Hierarchy Process for MeTHuVA

The MCDA method Analytical Hierarchy Process (AHP) has been applied to assess the tsunami human vulnerability for Bakırköy district of İstanbul. As the first task of the AHP, the ultimate goal has been decomposed to smaller parts and the hierarchy has been constructed.

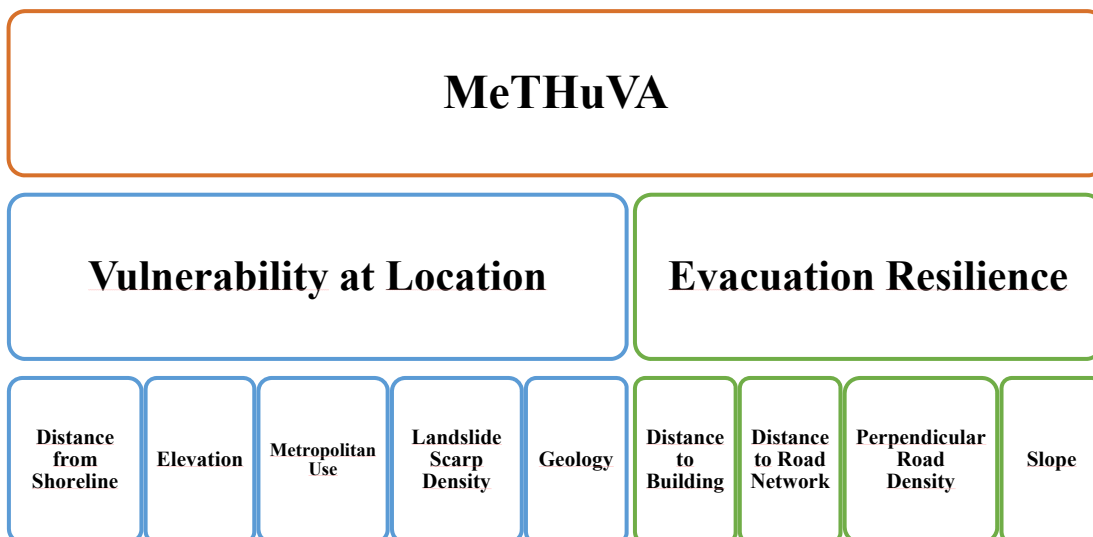


Figure 4.2 The hierarchical structure used in the vulnerability analysis

Figure 4.2 shows the hierarchy levels. ‘Metropolitan Tsunami Human Vulnerability Assessment (MeTHuVA)’ is the top level of the hierarchy and the ultimate goal. ‘Vulnerability at Location’ and ‘Evacuation Resilience’ are the objectives. The lower level of the objectives are the attributes. Lastly the lowest level of the hierarchy is the alternatives which are individual 1m size pixel of Bakırköy district of İstanbul.

Bakırköy district covers an area of 32.42 km² and extends approximately 10 km in E-W and 5 km in N-S direction. Therefore, a raster of Bakırköy district with 1m cell size creates a matrix composed of 10294 x 5970 cells. As stated earlier in this chapter, in the application of AHP to GIS environment with raster data, the lowest element of the hierarchy, which are decision alternatives, can be defined as every single cell of the raster. Since there is a great amount of cells within our data for Bakırköy district, making pairwise comparison for this level of hierarchy is almost impossible.

According to assess the vulnerability level of each pixel of our raster data, AHP has been used for the estimation of the criterion weights, which is the second implication type of AHP to GIS. Considering these, the weight estimations for criteria has been made;

- for distance from shoreline, elevation, metropolitan use, landslide scarp density and geology in order to generate ‘Vulnerability at Location’ object,
- for distance to buildings, distance to road network, perpendicular road density and slope in order to generate ‘Evacuation Resilience’ object.

The details about application of AHP will be explained in following sections. It should be noted that the criteria have been selected considering the tsunami event and the vulnerability for every part of the district have been calculated regardless the hazard level at that location.

4.4.1 Vulnerability at Location

Since this study deals with the tsunami human vulnerability, one of the important factor is to assess the locational vulnerability for every part of the Bakırköy district. For that purpose, 5 criteria have been generated for assessment of locational vulnerability and the available data have been processed to generate the raster maps related to those criteria, which are called as parameter maps. Then each of the

parameter maps has been ranked and classified according to the vulnerability level and class maps has been generated.

4.4.1.1 Parameter Maps of Vulnerability at Location

4.4.1.1.1 Metropolitan Use Layer

Generation of this layer has been done by using the vector database obtained from Istanbul Metropolitan Municipality (IMM). The polygon and line layers which contain the buildings and infrastructures located in Bakırköy district has been examined. According to their utilization type, features has been classified into 21 subgroups (Table 4.2).

Table 4.2 Classification of the buildings of Bakırköy according to their utilization type

Classes of Metropolitan Use	Structure and Building Type
Important Places	Governmental Buildings
	Underpasses
	Religious Facilities
	Schools
	Barns of Horses
Infrastructure / Utility	Gas Stations
	Electricity Transformers
	Pump House of İstanbul Water and Sewerage Administration
Assembly Areas	Sports Facilities
	Shopping Malls
Flat Areas	Suburban Railways
	Asphalt Roads
	Parking Places
	Others (green fields etc.)
Buildings	Small-scaled Production Centers
	Factories
	Residential Buildings
	Under Construction Buildings
	Commercial Building
	Parking Buildings
	Weight Control Stations

Considering the vulnerability level those 21 subgroups were gathered into 5 main groups (Table 4.2) which are, important places (governmental buildings, underpasses, religious facilities, schools, barns of race horses), infrastructure/utility (gas stations,

electricity transformers, pump houses), assembly areas (sports facilities, shopping malls), flat areas (suburban railways, asphalt roads, parking places and other flat areas), and buildings (small scaled production centers, factories, residential buildings, under construction buildings, commercial buildings, parking buildings, weight control stations). The map prepared according to these 5 groups is presented in Figure 4.3.

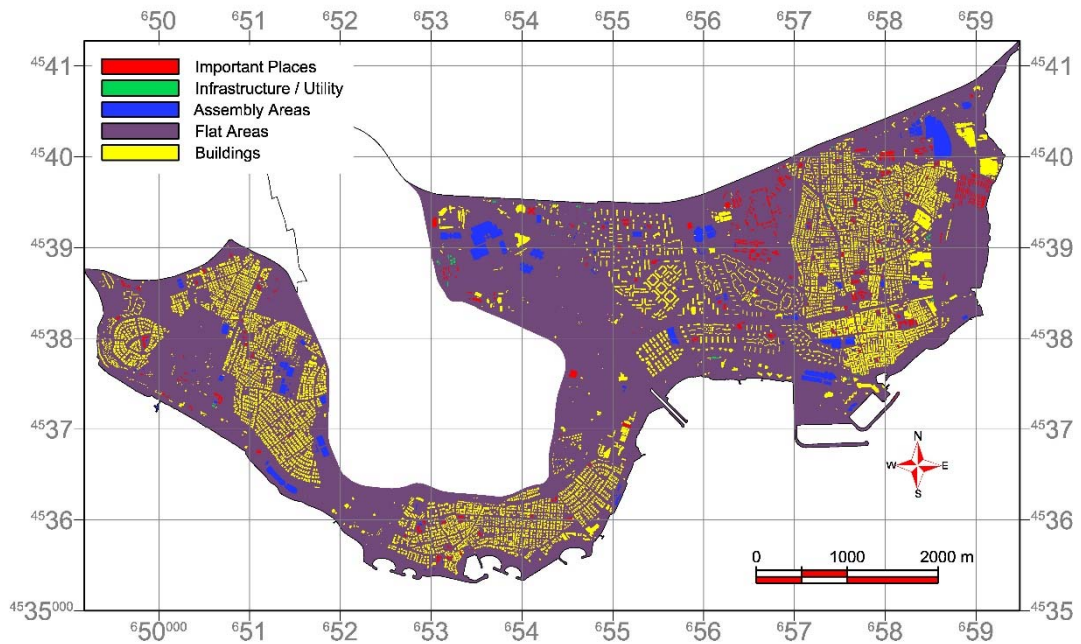


Figure 4.3 The parameter map of the metropolitan use layer

After the generation of parameter map of ‘metropolitan use’, 5 classes within that layer have been ranked between 1 and 10 according to their vulnerability level (Table 4.3), where the value 10 shows the most vulnerable features. From most vulnerable to least vulnerable the classes can be listed as; important places, infrastructure/utility, assembly areas, flat areas and buildings and the rank values for this layers are 10, 9, 8, 7 and 1, respectively. The rank value between buildings and the other classes has a steep difference, because they are the structures where the people density is constant. because all other classes have a potential of congregation whereas the building class is mainly composed of residential elements, the population density is not changing frequently.

Table 4.3 Classification and ranking of the metropolitan use layer

Metropolitan Use		
Class	Rank	Standardized Rank
Buildings	1	0.1
Flat Areas	7	0.7
Assembly	8	0.8
Infrastructure / Utility	9	0.9
Important	10	1

After ranking of the classes in the ‘metropolitan use’ layer, the ranks have been standardized (Table 4.3). When standardization was done, ranked map of metropolitan use has been produced (Figure 4.4) to use in the AHP application for the generation of ‘Vulnerability at Location’ map.

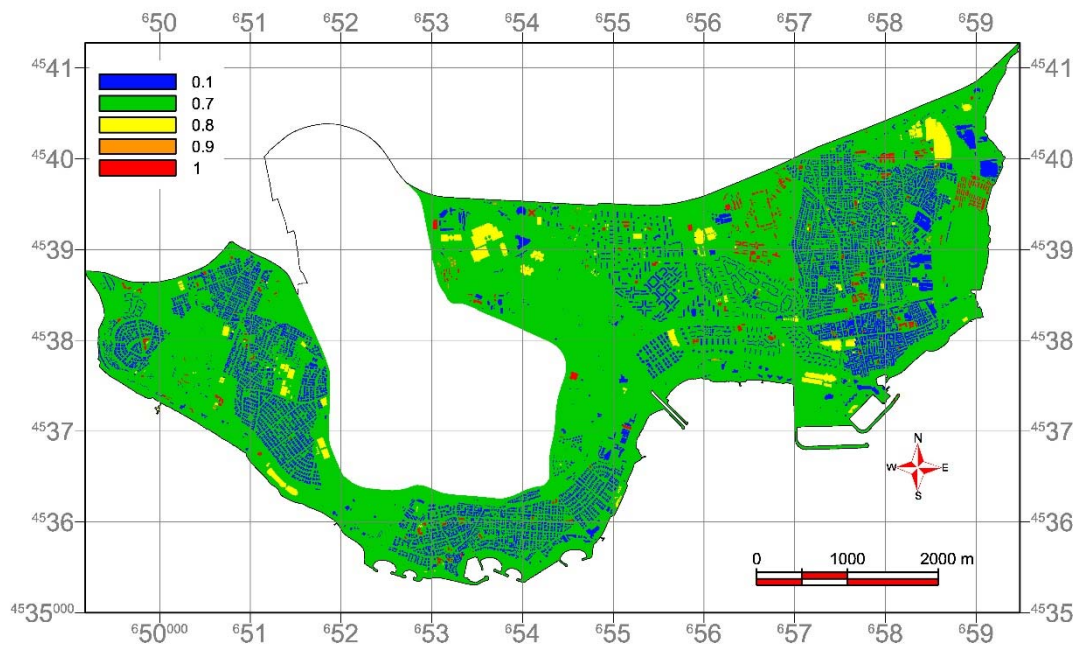


Figure 4.4 Ranked map of metropolitan use layer

4.4.1.1.2 Geology

One of the prominent and the well-known generation mechanism of tsunamis are the earthquakes. While assessing the tsunami vulnerability, the condition of land after the ground shake caused by the earthquake should be considered. Therefore, for this study resistivity of the geological formations in Bakırköy district has been taken into account and geology layer has been produced.

Istanbul Metropolitan Municipality has carried out a project for generation of microzonation maps for southern European side of İstanbul, which ended in 2007. Within the scope of this project several maps were produced; geological, hydrogeological, structural geology, ground shaking, liquefaction hazard, flooding and inundation, average shear wave velocity, fundamental period, resonant frequency, site amplification and land suitability maps. Among these maps, geological map (Figure 4.5) has been used for the generation of geology layer for ‘vulnerability at location’ map.

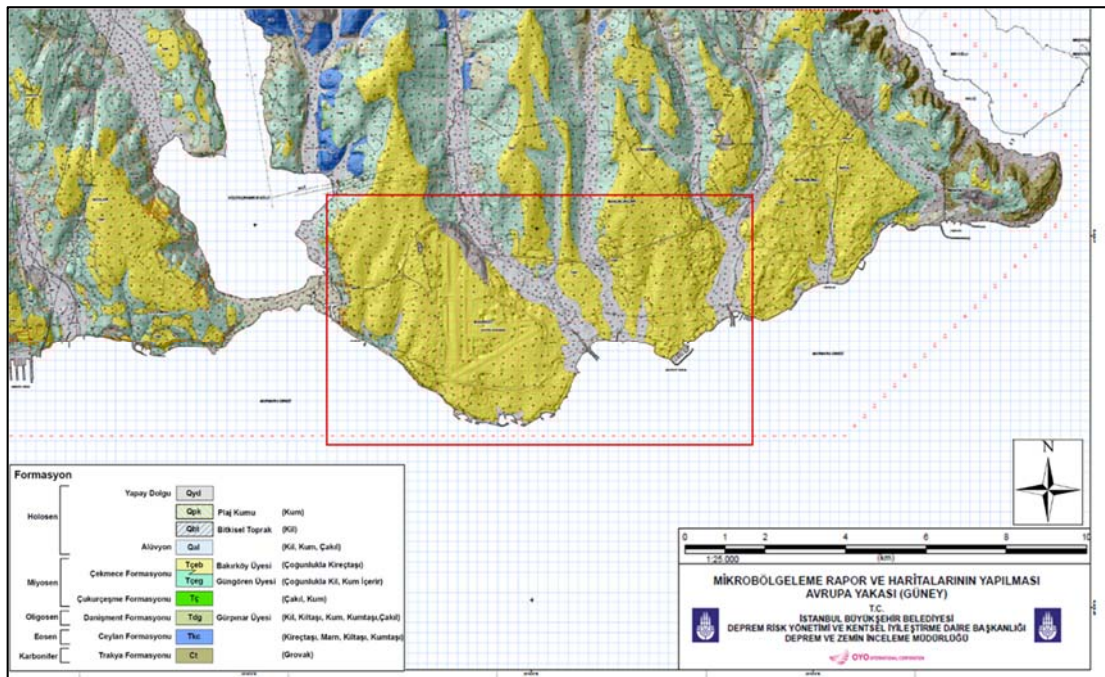


Figure 4.5 Geological map of southern European side of Istanbul (IMM, 2007). Study area, Bakırköy district, is shown with the red rectangle.

The geology map produced by IMM (2007) was georeferenced according to the projection system used in generation of the map, then reprojected to the projection system that has been used throughout the study. The geology map has been clipped covering the study area and digitized (Figure 4.6).

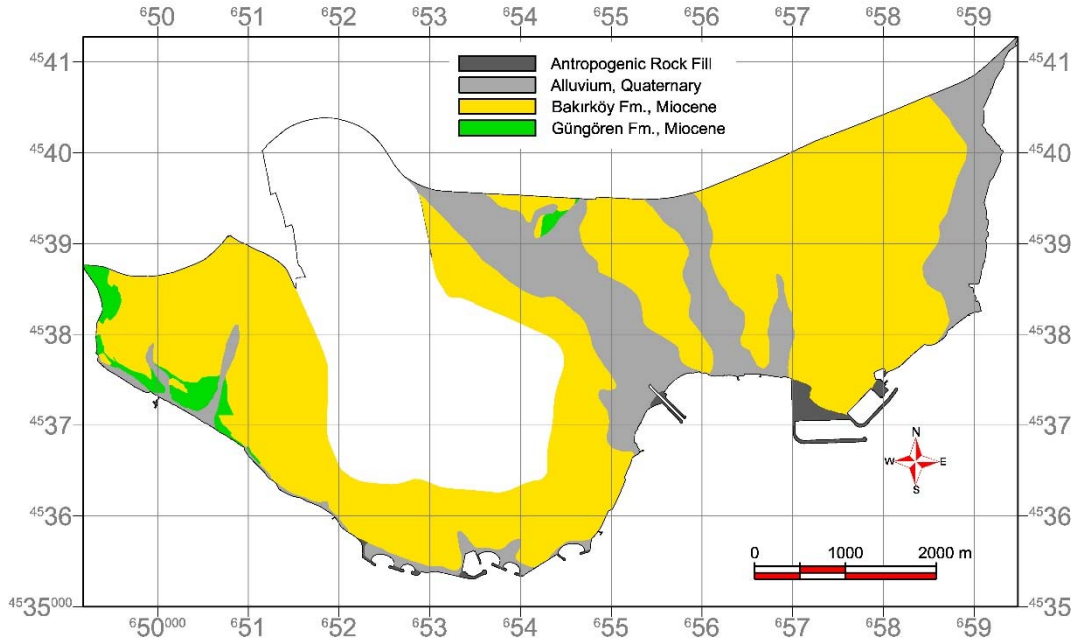


Figure 4.6 Digitized geological map of Bakırköy district

In Bakırköy district, there are 4 different geological units; Miocene Güngören Formation at the west and northern sides of area, Miocene Bakırköy Formation covering a great part of the area, Quaternary alluvium and anthropogenic fill. These units have been evaluated according to their behavior in general and as well as their behavior after an earthquake and has been ranked considering the vulnerability level (Table 4.4). Considering vulnerability, the Quaternary Alluvium is accepted as the most vulnerable with the highest vulnerability score. The second most vulnerable formation after unconsolidated Quaternary Alluvium is Güngören formation with swelling problem. Bakırköy formation is relatively more resilient then former two even though it contains karstic voids. The most resilient unit is considered as the Anthropogenic fill since it is an artificial rock fill. After standardization of the rank values, ranked map of the geology parameter layer has been produced (Figure 4.7).

Table 4.4 Classification and ranking the geology layer

Geology		
Class	Rank	Standardized Rank
Quaternary	10	1
Güngören Formation	7	0.7
Bakırköy Formation	5	0.5
Anthropogenic Rock Fill	1	0.1

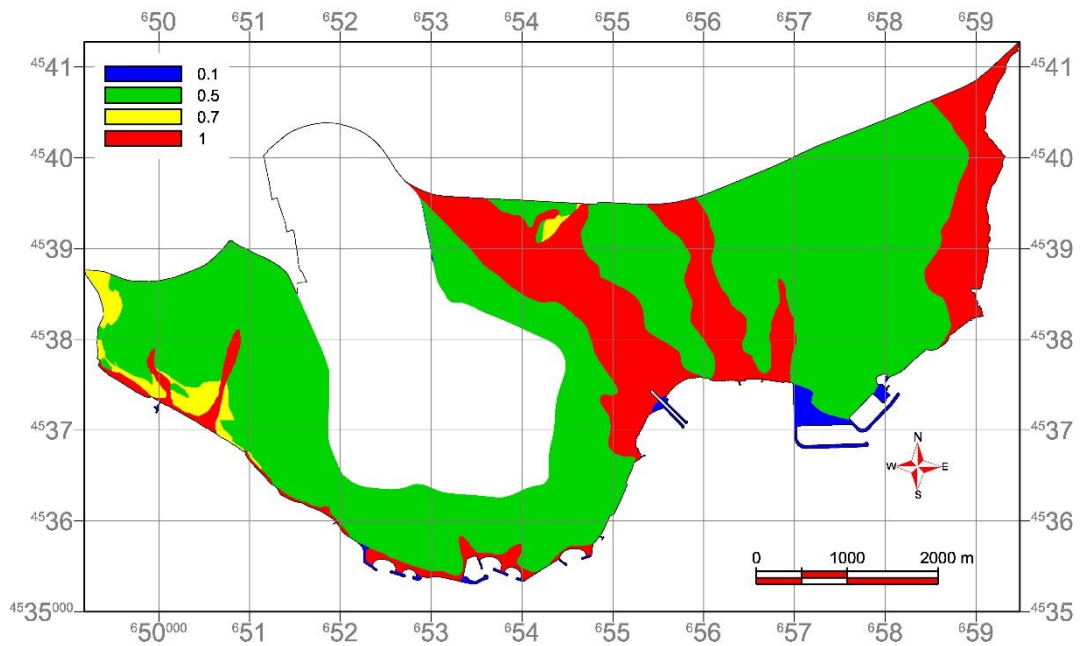


Figure 4.7 Ranked map of geology layer

4.4.1.1.3 Landslide Scarp Density

Besides the geological formations, the geological map obtained from IMM (2007) contains landslide scarps. Since the landslides were not considered in the geology layer it has been generated as a separate parameter layer.

The landslide scarps have been digitized from the geological map (Figure 4.8). Digitization was performed as lines then those lines have been converted to 5m spaced points. The ‘landslide scarp density’ layer has been generated by calculating the density of these points within a circle area with 500 m radius and the obtained raster

map had values changing from 0 to 411 (Figure 4.9). The generated raster map was then classified according to vulnerability level and ranked (Table 4.5). After the standardization of rank values, the final ‘landslide scarp density’ map has been generated (Figure 4.10) in order to use in the further steps of AHP.

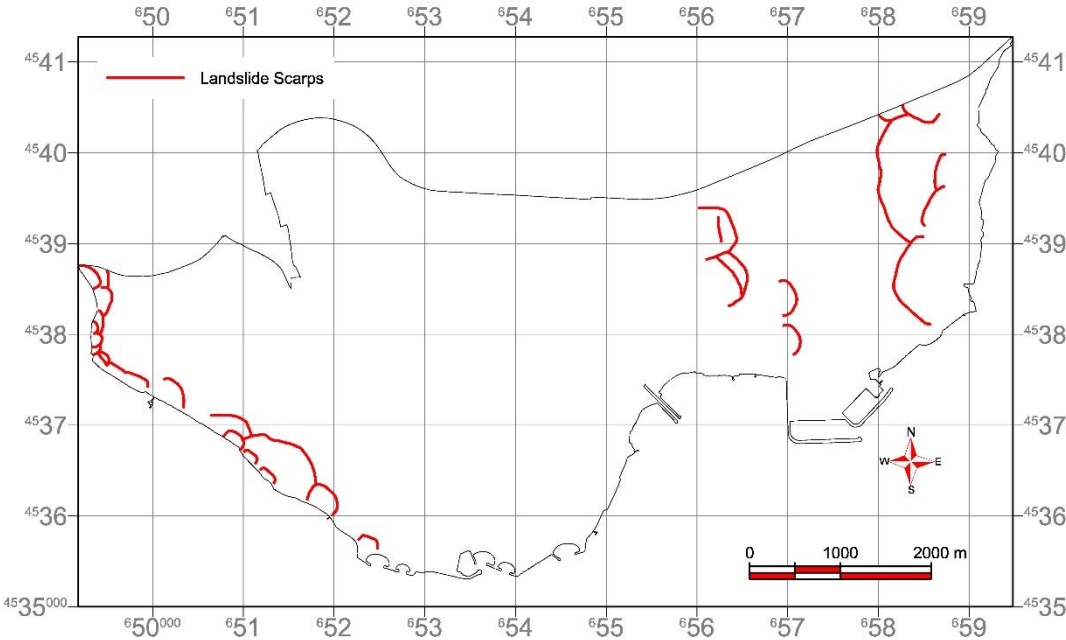


Figure 4.8 Digitized landslide scarp map

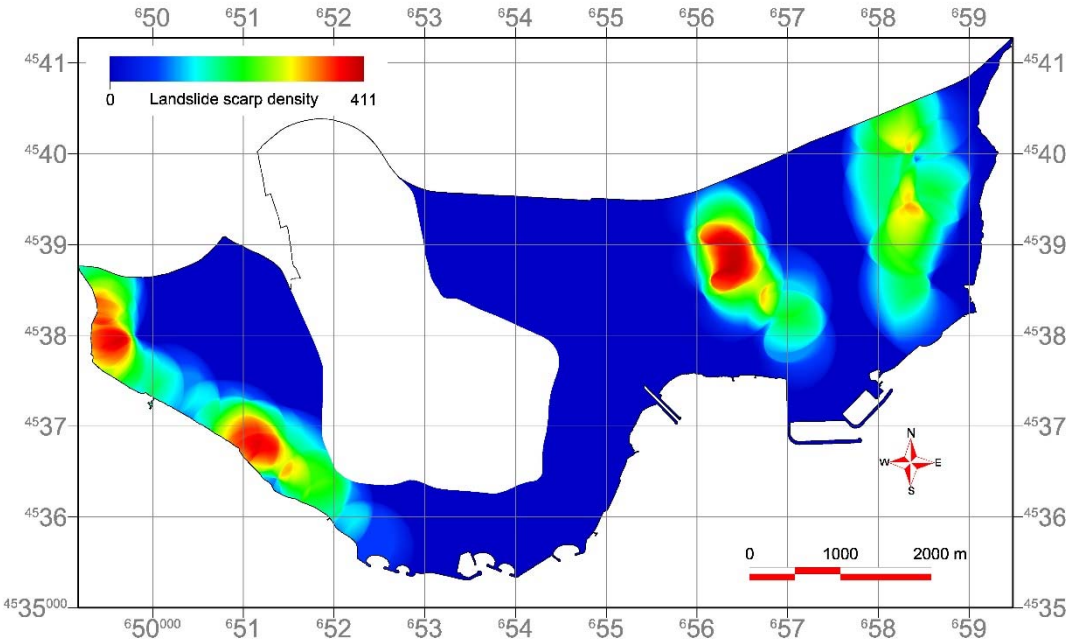


Figure 4.9 Parameter map of landslide scarp density layer

Table 4.5 Classification and ranking of the landslide density layer

Landslide Scarp Density		
Class	Rank	Standardized Rank
<70	10	1
70 - 164	8	0.8
164 - 246	6	0.6
246 - 328	4	0.4
>328	1	0.1

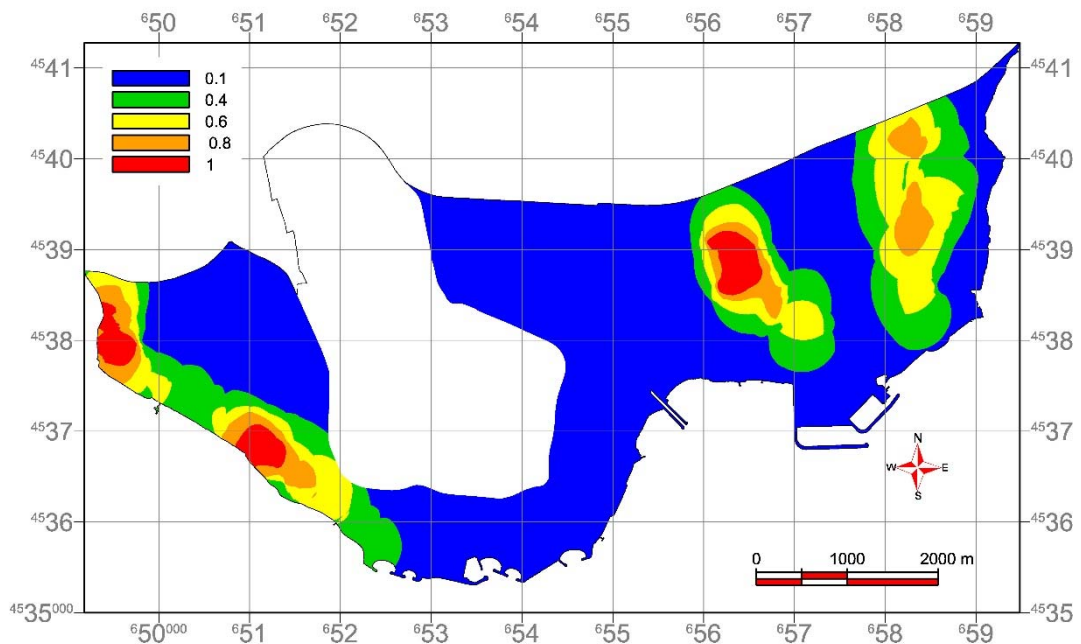


Figure 4.10 Ranked map of landslide density layer

4.4.1.1.4 Distance from Shoreline

In a probable tsunami event the places spatially closer to the sea would be affected more. People who are farther from shoreline will be safer since there will be more time to run away from incoming tsunami wave. When considering the buildings regardless of their construction type or usage, if they are closer to the shore, the vertical interaction with water will be higher. And also the time span that will pass with inundation will be more. Consequently, the damage to people or buildings will be higher closer to the shoreline.

The raster map of 'distance from shoreline' has been produced by using the digitized shoreline vector data. From this vector data the distance raster has been calculated for

each location in Bakırköy district, to eventually produce the ‘distance from shoreline’ parameter map (Figure 4.11). The produced map is composed of raster cells with 1 m size and values changing between 0 and 3469 m.

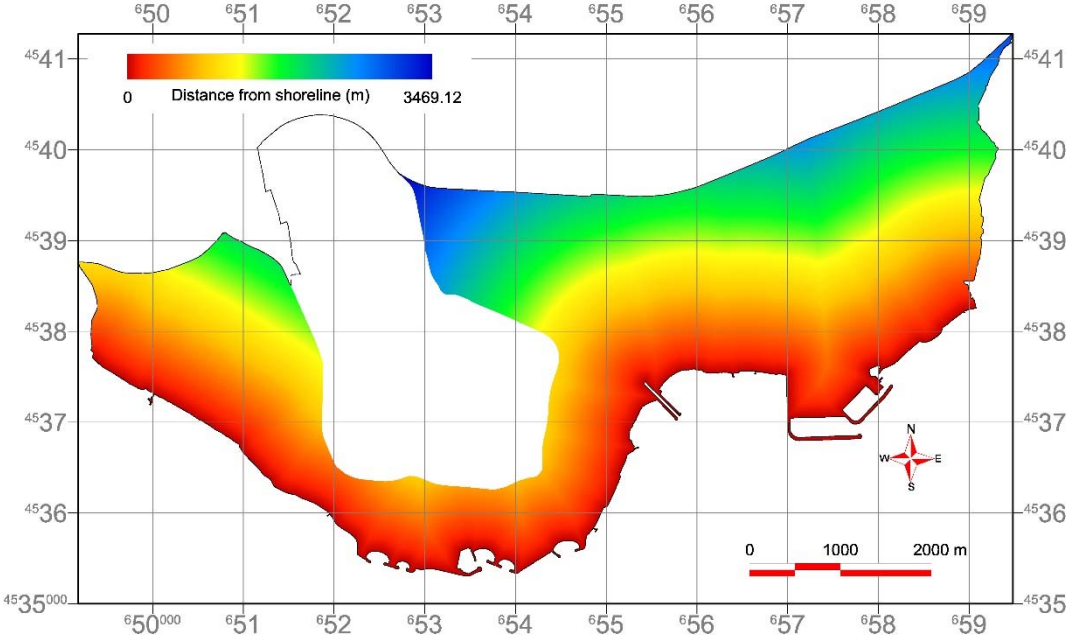


Figure 4.11 Parameter map of distance from shoreline layer

After generation of parameter map, the values of this map have been divided into classes considering the vulnerability level and ranked and standardization of ranks values realized (Table 4.6). Using the standardized values, ranked ‘distance from shoreline’ map (Figure 4.12) has been produced in order to use in the application of AHP for generation of ‘Vulnerability at Location’ map.

Table 4.6 Classification and ranking of distance from shoreline layer

Distance from Shoreline		
Class	Rank	Standardized Rank
<50	10	1
50 - 100	9	0.9
100 - 250	7	0.7
250 - 400	3	0.3
>400	1	0.1

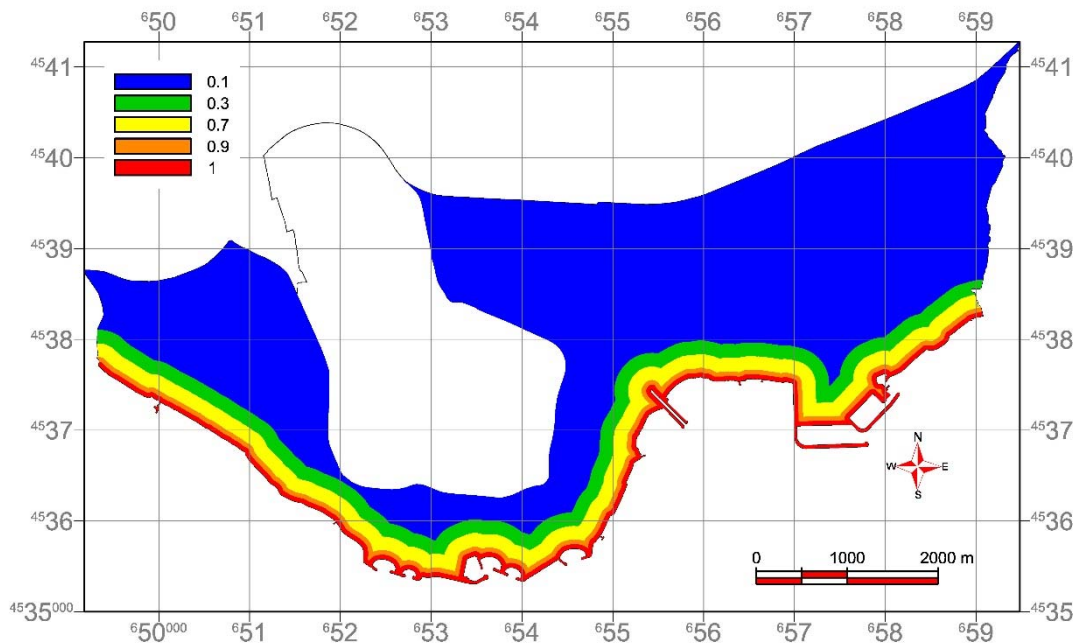


Figure 4.12 Ranked map of distance from shoreline layer

4.4.1.1.5 Elevation

While measuring locational vulnerability, the elevation from sea level has a great importance when a tsunami wave is the threat. Since the tsunami parameters on land, which are inundation distance and run-up, are identified by the characteristics of tsunami source and the bathymetry, these parameters can differ in different events. But still in any case, both the people or buildings and structures located in higher elevations will be safer. The destructive effects of incoming tsunami wave will reduce or even cease in the higher elevation levels. Therefore, for this study, elevation have been included in the generation of ‘vulnerability at location’ map.

The 5 m resolution DEM has been used for the generation of elevation map. In order to keep the compatibility of the map with the other maps and the hazard map, DEM has been resampled to 1 m cell size (Figure 4.13).

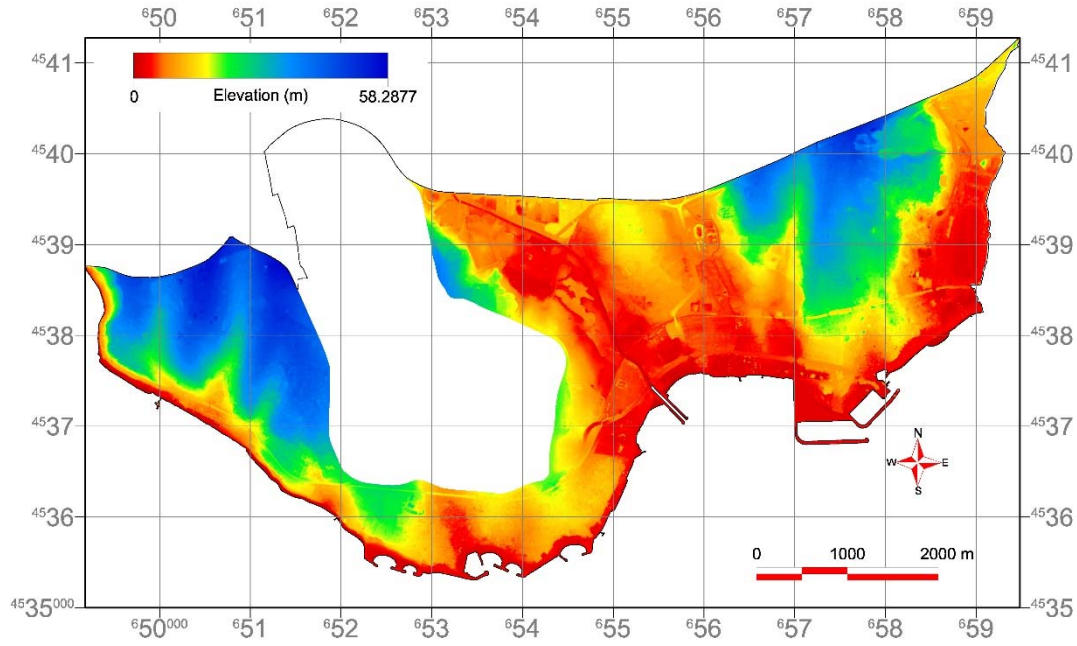


Figure 4.13 Parameter map of elevation layer

The elevation values in Bakırköy region was changing between 0 and 58 meters. The values of parameter map have been classified and ranked according to the vulnerability level considering the elevation (Table 4.7). After the standardization of rank values, ranked map of ‘elevation’ was produced to use in the further steps of vulnerability assessment (Figure 4.14).

Table 4.7 Classification and ranking of elevation layer

Elevation		
Class	Rank	Standardized Rank
<2	10	1
2 – 4	8	0.8
4 – 6	6	0.6
6 – 8	3	0.3
>8	1	0.1

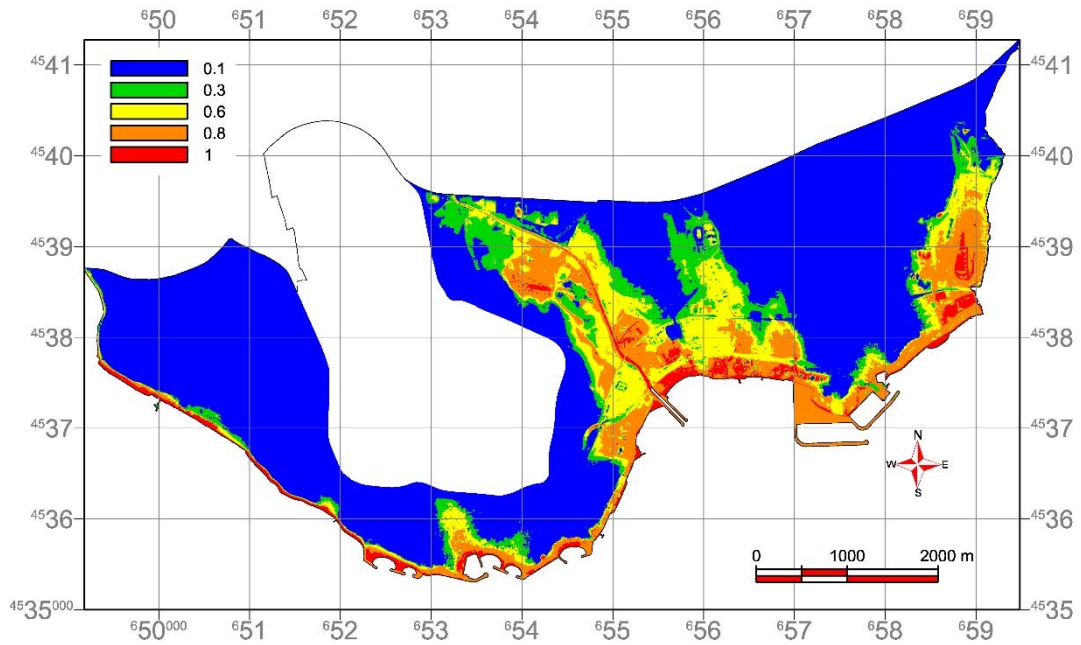


Figure 4.14 Ranked map of elevation layer

4.4.1.2 Final Map of Vulnerability at Location Produced by Application of AHP

The parameters and the ranked maps was generated in the previous sections with the aim of providing the base for final ‘Vulnerability at Location’ map. In this step of the study, the pairwise comparison for the locational vulnerability map has been performed (Table 4.8) and weights for five parameters was determined. While performing the pairwise comparison, Saaty’s scale of relative importance table was used (Table 4.1).

Table 4.8 Pairwise comparison matrix for Vulnerability at Location map

Vulnerability at Location	Geology	Metropolitan Use	Distance from Shoreline	Elevation	Landslide Scarp Density
Geology	1	4	1/2	2	1
Metropolitan Use	1/4	1	1/4	1/2	1/2
Distance from Shoreline	2	4	1	4	3
Elevation	1/2	2	1/4	1	2
Landslide Scarp Density	1	2	1/3	1/2	1

The explanations related to the pairwise comparison are as follows;

- The metropolitan use layer is the only layer without any superiority on the other layers. Elevation and landslide scarp density layers are equal to moderately dominant, and geology and distance from shoreline layers are moderately to strongly dominant against metropolitan use layer.
- Geology layer is considered as in an equal importance with the landslide scarp density. While it has an equal to moderate dominance over the elevation layer and moderate to strong dominance over metropolitan use layer, the distance from shoreline layer is equally to moderately dominant than geology layer.
- Landslide scarp density layer has the equal importance with the geology layer. It is equal to moderately dominant than metropolitan use. However, elevation and distance from shoreline layers are equal to moderately and moderately dominant against landslide scarp density layer, respectively.
- Distance from shoreline layer has equal to moderate, moderate to strong, moderate to strong and moderate prevalence against the geology, metropolitan use, elevation and landslide scarp density layers, respectively.
- Elevation layer is equal to moderately strong dominant than metropolitan use and landslide scarp density layers. But the geology layer has equal to moderate dominance and the distance from shoreline layer has moderate to strong dominance against elevation layer.

The comparisons made by the help of experts and by using a AHP software and the weights were calculated (Table 4.9). While calculating the weights accordingly the given ranks within the pairwise comparison, AHP also calculates the consistency of given ranks. This process is called as the estimation of the consistency ratio. In a performed pairwise comparison, if the consistency ratio (CR) is lower than 0.10, the ranks and weights determined are consistent. The CR value for the estimation of ‘Vulnerability at Location’ in this study was 0.047. Therefore, the weight assigned weight values for the parameters were consistent.

Table 4.9 Computed weights of parameters of vulnerability at location

Vulnerability at Location parameters by weight order	
Distance from Shoreline	0.416
Geology	0.223
Elevation	0.151
Landslide Scarp Density	0.138
Metropolitan Use	0.072
Consistency Ratio	0,0468 (Acceptable)

According to the calculated weights by pairwise comparison, all five ranked parameter maps have been integrated for the calculation of ‘Vulnerability at Location’ map in GIS environment by writing scripts. The final map of ‘Vulnerability at Location’ has been obtained as in the Figure 4.15. Every 1 m size cell of the resulting raster have values changing between 0 and 1, where the value 0 represents the least vulnerable and 1 represents the most vulnerable locations in Bakırköy district.

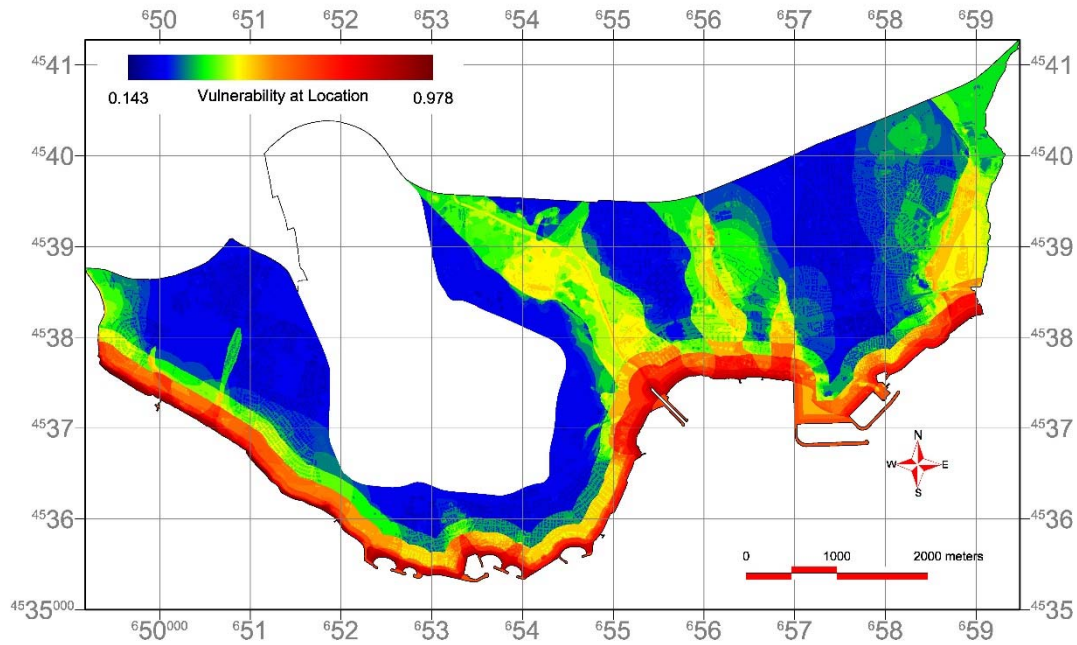


Figure 4.15 The final map of vulnerability at location

4.4.2 Evacuation Resilience

In the scope of this study, the second important factor for tsunami human vulnerability was specified as evacuation resilience. Resilient evacuation is one of the most vital factors when the tsunami event is considered since there is a wave approaching to the land. For the assessment of evacuation resilience for every location in Bakırköy district, 4 different parameter maps were produced by using the available vector and raster data. Compatible raster maps have been generated for each parameter map and these maps were classified and ranked according to the resilience for evacuation.

4.4.2.1 Parameter Maps of Evacuation Resilience

4.4.2.1.1 Distance to Buildings

The presence of building nearby is the best option for vertical evacuation without covering long distances, in the case of a tsunami event. Even the buildings located in the max inundation zone might save lives or decrease injuries by providing vertical evacuation possibility. When considering the vertical evacuation supplied by the buildings, the number of stories of those buildings becomes an important factor. The

low-lying or single story buildings may not offer any vertical evacuation (Dominey-Howes and Papatoma, 2007).

Furthermore, to provide a vertical evacuation route, a building should be non-damaged either from the earthquake or the waves of tsunami. In some studies, the shutter openings in the base floors of the buildings was considered as providing an easier passing of water with causing less damage to building itself (Dall’Osso et al., 2010).

Neither the number of the floors nor the shutter openings at the base floor of the buildings were considered in this study due to insufficient data of the study area. However, since İstanbul is a metropolitan city which regularly faces with the ground shaking events and the Bakırköy is one of the important coastal district of İstanbul, it is assumed that all the buildings are reinforced concrete and the vertical evacuation is possible for every building in that district.

For generation of ‘distance to buildings’ layer the vector data has been used and distance calculation for each location of Bakırköy was performed in the form of raster data (Figure 4.16).

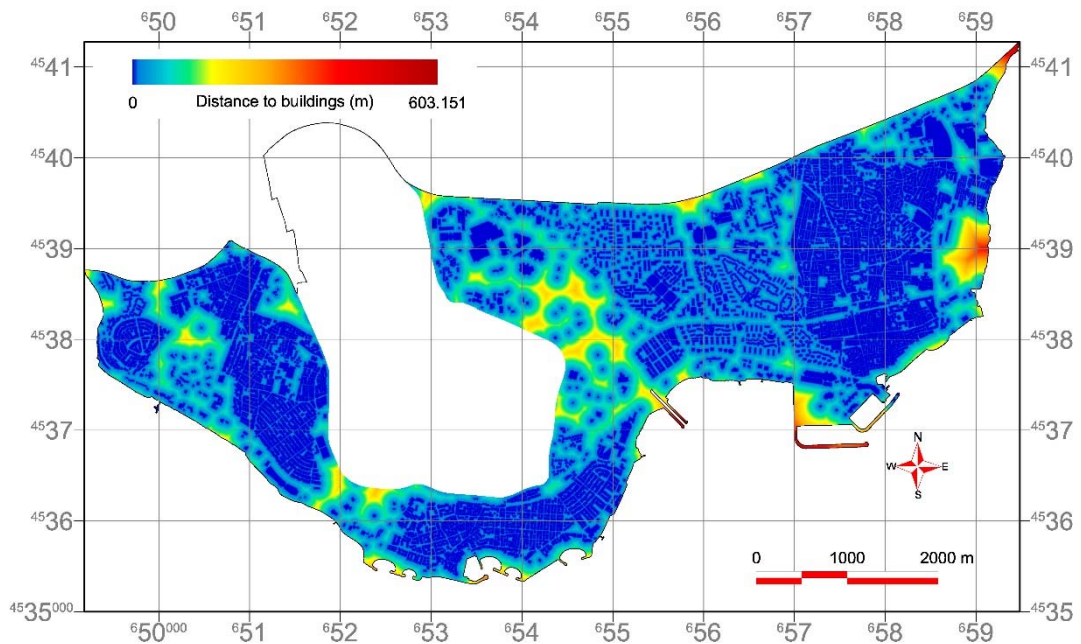


Figure 4.16 Parameter map of distance to buildings layer

The resulting raster map reveals that the max distance to the buildings reach up to 603 m at some locations of Bakırköy. Considering the evacuation easiness, the values of the parameter map has been classified and ranked (Table 4.10). According to the standardized rank values, a ranked parameter map has been produced to use in the final generation of ‘Evacuation Resilience’ map (Figure 4.17).

Table 4.10 Classification and ranking of distance to buildings layer

Distance to Buildings		
Class	Rank	Standardized Rank
<10	10	1
10 – 50	9	0.9
50 – 100	3	0.3
100 – 250	2	0.2
>250	1	0.1

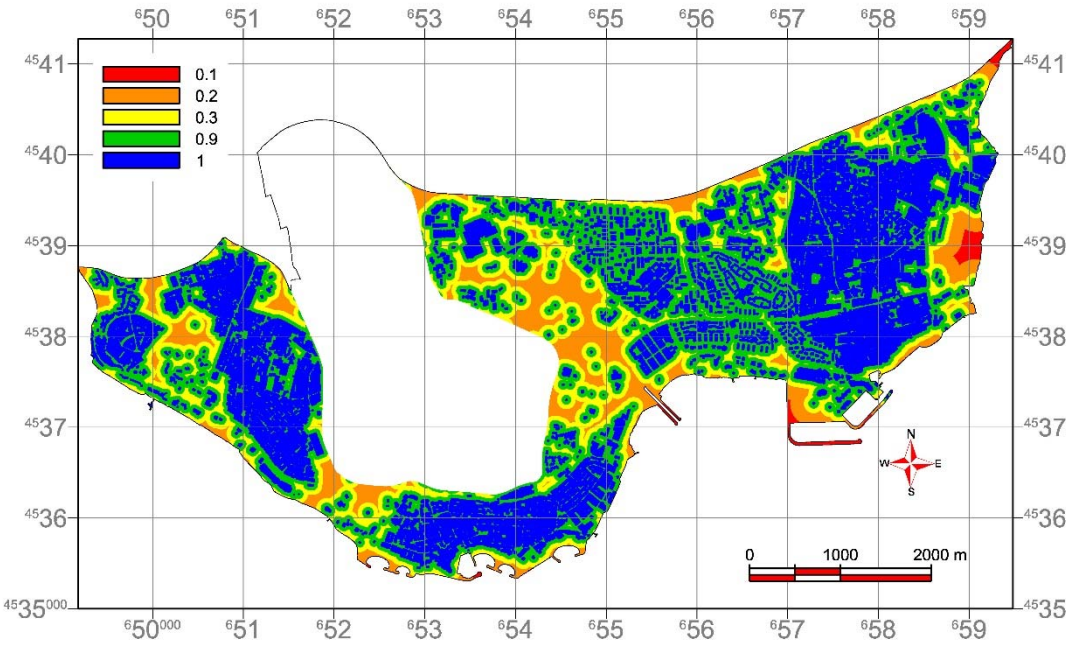


Figure 4.17 Ranked map of distance to buildings layer

4.4.2.1.2 Distance to Road Network

Roads are the main elements of the evacuation routes in a tsunami event, since they offer the easiest way to reach the safe places. Therefore, being on the roads or near to the road network is considered as a parameter for the calculating the evacuation resilience for Bakırköy district.

The closeness to roads was calculated for single story buildings in the study of Papathoma and Dominey-Howes (2003), since those buildings were not suitable for vertical evacuation. In this thesis, the proximity to roads of every location of Bakırköy district has been calculated by using the vector data as input to eventually obtain a distance raster map. The values of this distance raster was changing between 0 and 503 m (Figure 4.18).

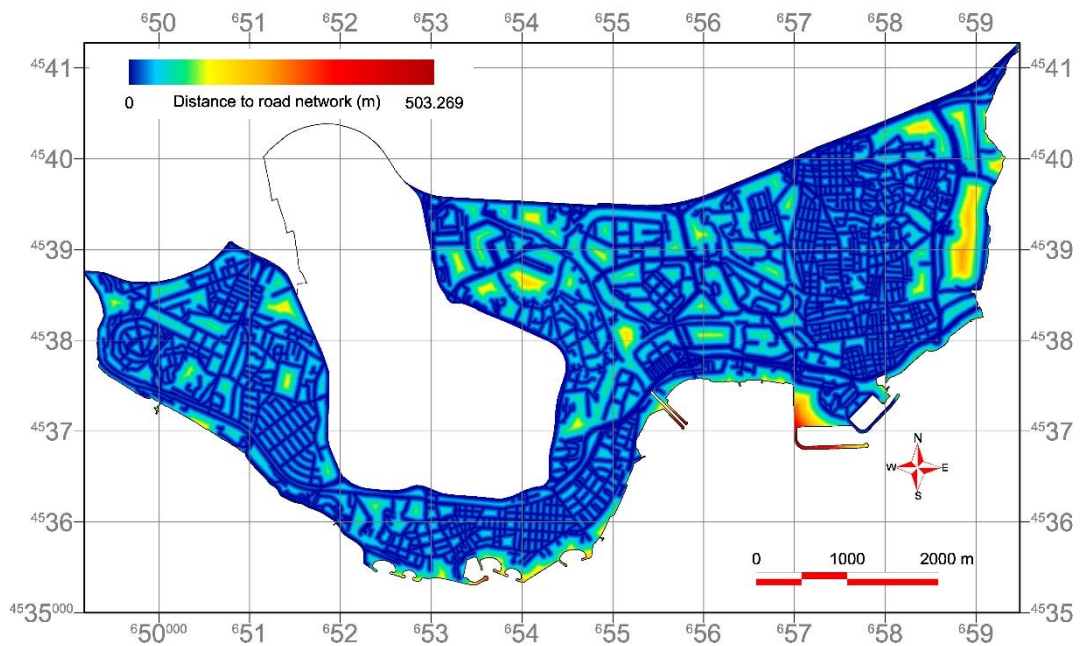


Figure 4.18 Parameter map of distance to road network layer

In order to use in the final calculation of ‘Evacuation Resilience’ map, the values of parameter map have been classified and ranked according to the resilience level (Table 4.11). According to the standardized rank values, a ranked parameter map has been produced for ‘distance to road network’ layer (Figure 4.19).

Table 4.11 Classification and ranking of distance to road network layer

Distance to Road Network		
Class	Rank	Standardized Rank
<10	10	1
10 – 30	8	0.8
30 – 50	5	0.5
50 – 100	3	0.3
>100	1	0.1

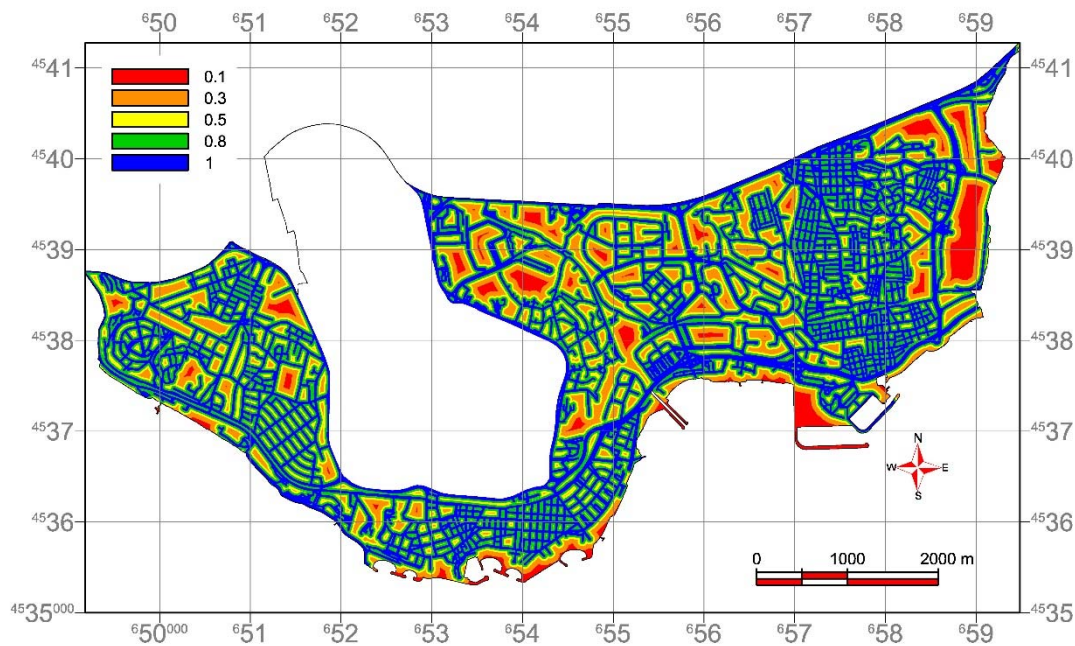


Figure 4.19 Ranked map of distance to road network layer

4.4.2.1.3 Perpendicular Road Density

In the coastal areas near oceans, especially the ones that have suffered from tsunami event earlier have evacuation route signs on the road which lead the people to the safer places. When this is not the case and there are no evacuation routes that has been defined by the responsible organizations, the roads that can lead the way directly away from shoreline become more important.

Being on the road will ease the evacuation as considered while generating the distance to road network layer. But the roads which are parallel to the shoreline would not provide a direct evacuation routes away from the shoreline. Therefore, as one of the

parameter for evacuation resilience, a perpendicular road density map was thought to be required. In order to determine the roads that are perpendicular to the shoreline 5 different baselines with different directions were generated (Figure 4.20). These baselines were needed since the shoreline of the Bakırköy district is sinuous. The roads of Bakırköy has been divided according to these 5 baselines.

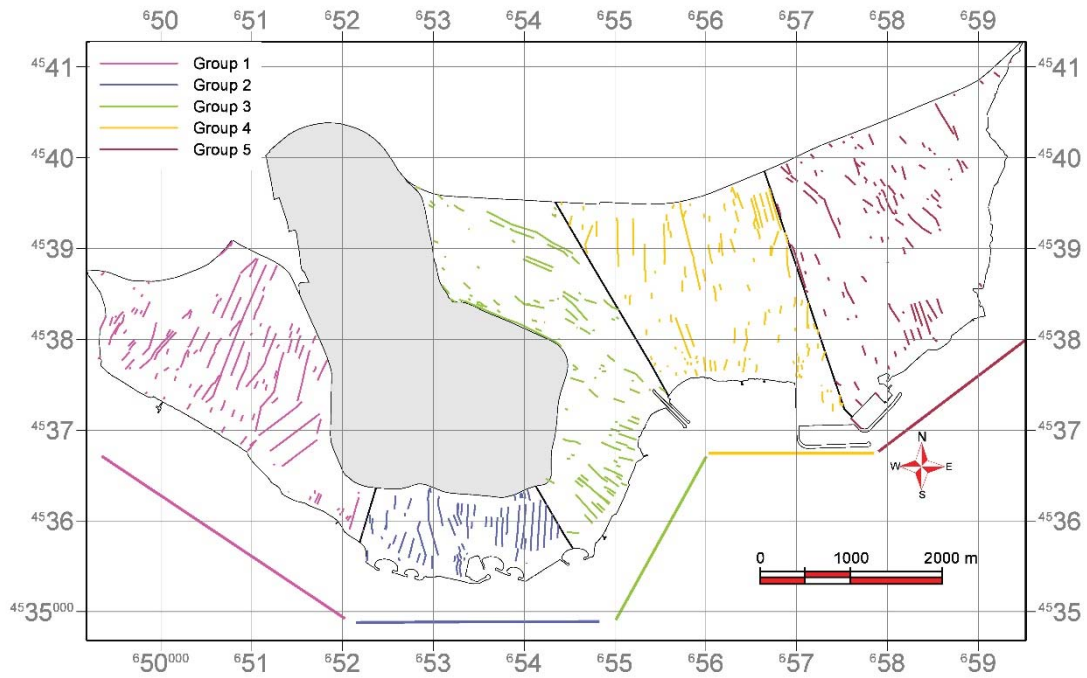


Figure 4.20 Baselines for the selection of perpendicular roads

For the generation of this density map, the road network vector data was processed and road segments that are perpendicular to the shoreline was determined according to these 5 baselines. The determined road segments have been converted to 5 m spaced points. The parameter map of perpendicular road density has been produced by calculating the density of the 5 m spaced point data within a circle area with 250 m radius. The obtained density map has value changing between 0 and 654 (Figure 4.21). The values of this raster map was classified and ranked considering evacuation (Table 4.12). A final ranked parameter map has been produced with the standardized rank values (Figure 4.22).

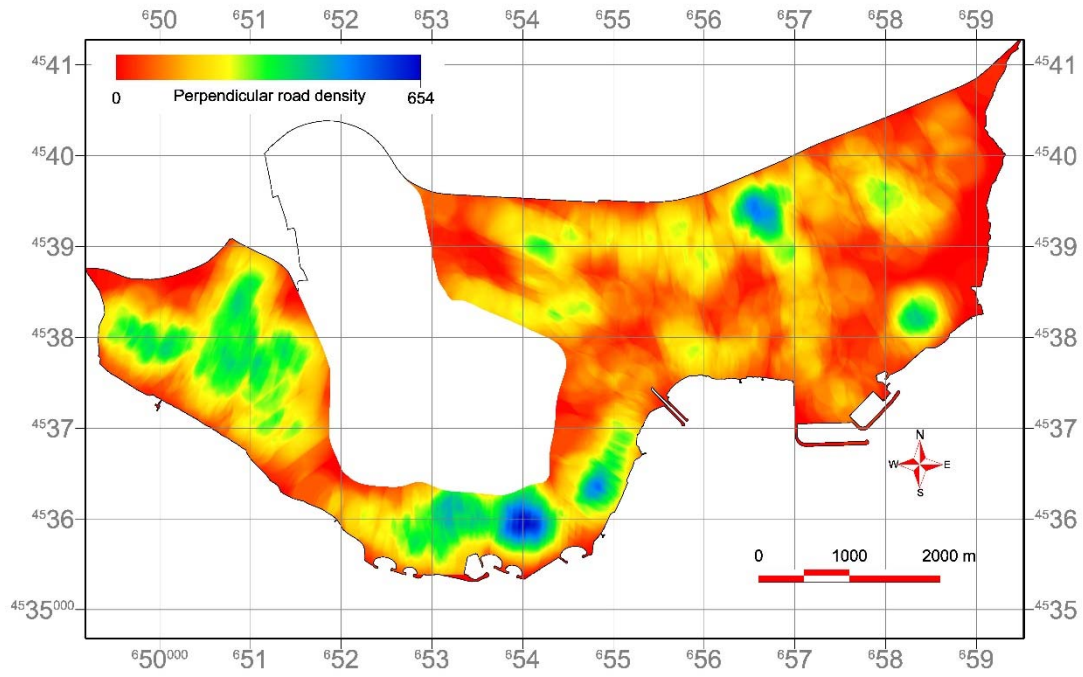


Figure 4.21 Parameter map of perpendicular road density layer

Table 4.12 Classification and ranking of perpendicular road density layer

Perpendicular Road Density		
Class	Rank	Standardized Rank
>520	10	1
390 – 520	7	0.7
260 – 390	5	0.5
130 – 260	3	0.3
<130	1	0.1

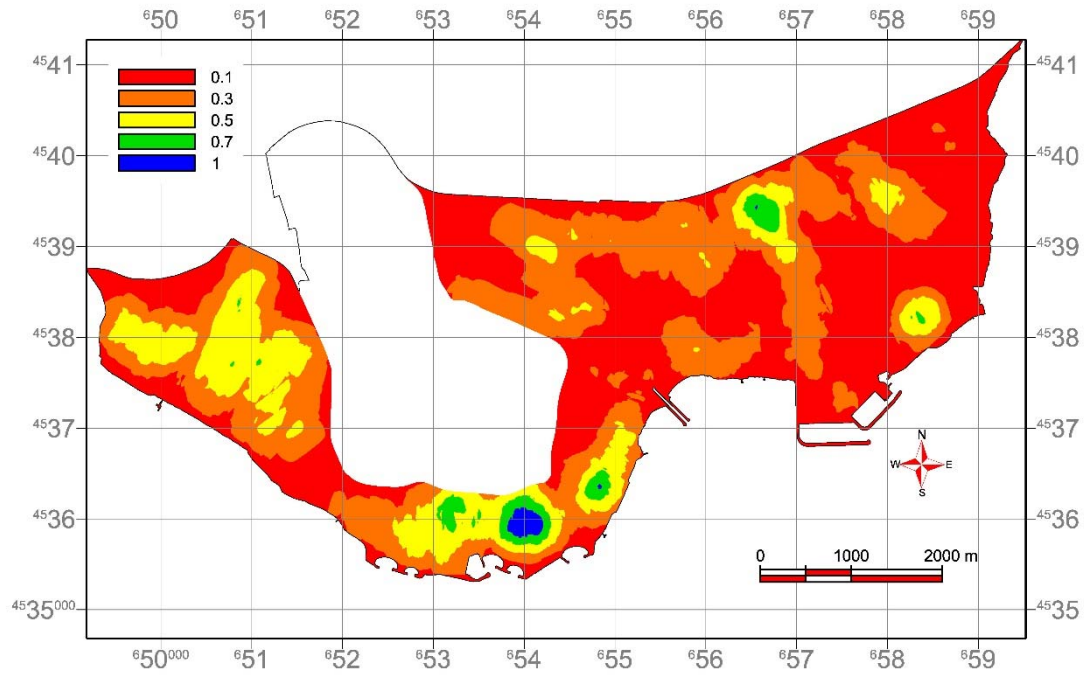


Figure 4.22 Ranked map of perpendicular road density layer

4.4.2.1.4 Slope

When it is the case of the evacuation resilience of pedestrians, the importance of slope increases. The degree of slope has a direct impact on the velocity of movement of a human. Excluding the influence of slope on elevation, where the slope is gentle, people would more easily evacuate while a tsunami wave is approaching. Hence, a slope layer was produced for 'Evacuation Resilience' map. The 1m DEM was used to calculate the slope layer in degrees (Figure 4.23).

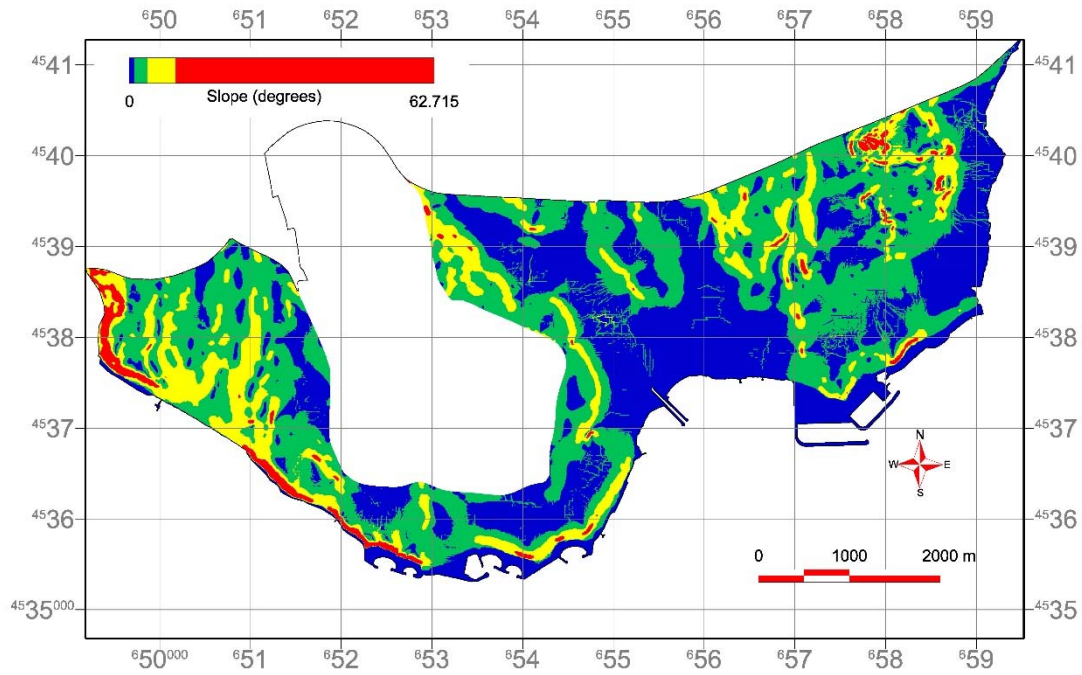


Figure 4.23 Parameter map of slope layer

The values of the slope map have been classified and ranked considering the evacuation easiness (Table 4.13). The resulted ranked parameter map was prepared in order to use in the next stages of AHP (Figure 4.24).

Table 4.13 Classification and ranking of slope layer

Slope			
Class	Rank	Standardized Rank	
<2	10	1	
2 - 4	7	0.7	
4 - 6	4	0.4	
6 - 10	2	0.2	
>10	1	0.1	

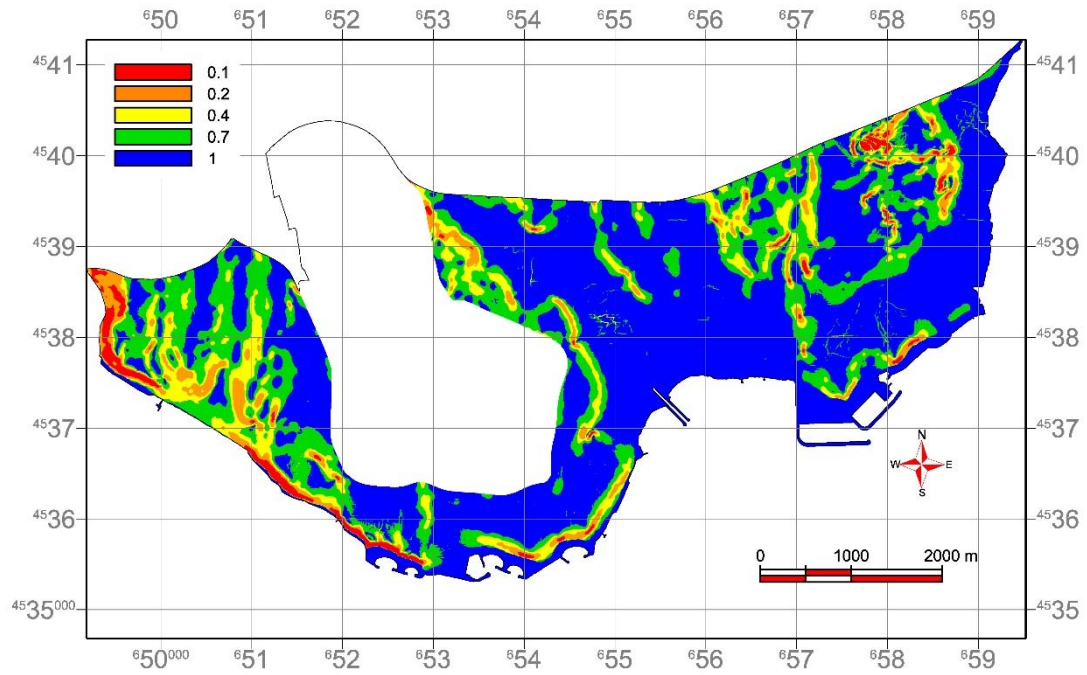


Figure 4.24 Ranked map of slope layer

4.4.2.2 Final Map of Evacuation Resilience Produced by Application of AHP

The four parameters which was defined while creating the hierarchy for the ‘Evacuation Resilience’ map were subjected to pairwise comparison. Pairwise comparison made by the use of Saaty’s relative importance scale (Table 4.1) and the parameters were compared according to each other. Performing pairwise comparison helped to assess the weights for each parameter (Table 4.14).

Table 4.14 Pairwise comparison matrix for Evacuation Resilience map

Evacuation Resilience	Distance to Road Network	Distance to Buildings	Slope	Perpendicular Road Density
Distance to Road Network	1	1/3	2	1/2
Distance to Buildings	3	1	6	2
Slope	1/2	1/6	1	1/4
Perpendicular Road Density	2	1/2	4	1

The explanations related to the pairwise comparison are as follows;

- Distance to buildings layer is the most powerful layer among each layer within the evacuation resilience parameters. It is moderately dominant, strongly to very strongly dominant and equal to moderately dominant against distance to road network, slope and perpendicular road density, respectively.
- Distance to road network layer is equally-moderately prevalence against slope layer. However, distance to building and perpendicular road density layer has equal to moderate dominance and distance to buildings layer has moderate dominance over distance to road network layer.
- Perpendicular road density layer equal to moderately dominant and moderately to strongly dominant than distance to road network and slope layers, respectively. But the distance to buildings layer has equal-moderate dominance against perpendicular road density layer.
- Slope layer is the least dominant layer and it doesn't have any dominance over any layer according to the pairwise comparison. The layers of distance to buildings, distance to road network and perpendicular road density have strong to very strong, equal to moderate and moderate to strong dominance against slope layer.

According to the pairwise comparison made by expert opinions the weights for each parameter of 'Evacuation Resilience' were calculated by using a AHP software (Table 4.15). Besides leading the pairwise comparison, AHP also calculates the consistency of the pairwise comparison. The calculates consistency ratio for the pairwise comparisons made for evacuation resilience was 0.004, which is lower than 0.10. Hence the pairwise comparisons and calculated weights were acceptable for the rest of the study.

Table 4.15 Computed weights of parameters of evacuation resilience

Evacuation Resilience	
Distance to Buildings	0.490
Perpendicular Road Density	0.283
Distance to Road Network	0.152
Slope	0.076
Consistency Ratio	0.004 (Acceptable)

With the assigned weights for each parameter map, a final ‘Evacuation Resilience’ map was produced in GIS environment (Figure 4.25). The resulting raster map reveals the evacuation resilience for each location with 1 m cell size considering each parameter and their weights. The evacuation resilience scores of the map were changing between the values of 0 and 1, where 0 shows least resilient places and 1 shows the most resilient places of the Bakırköy district of İstanbul.

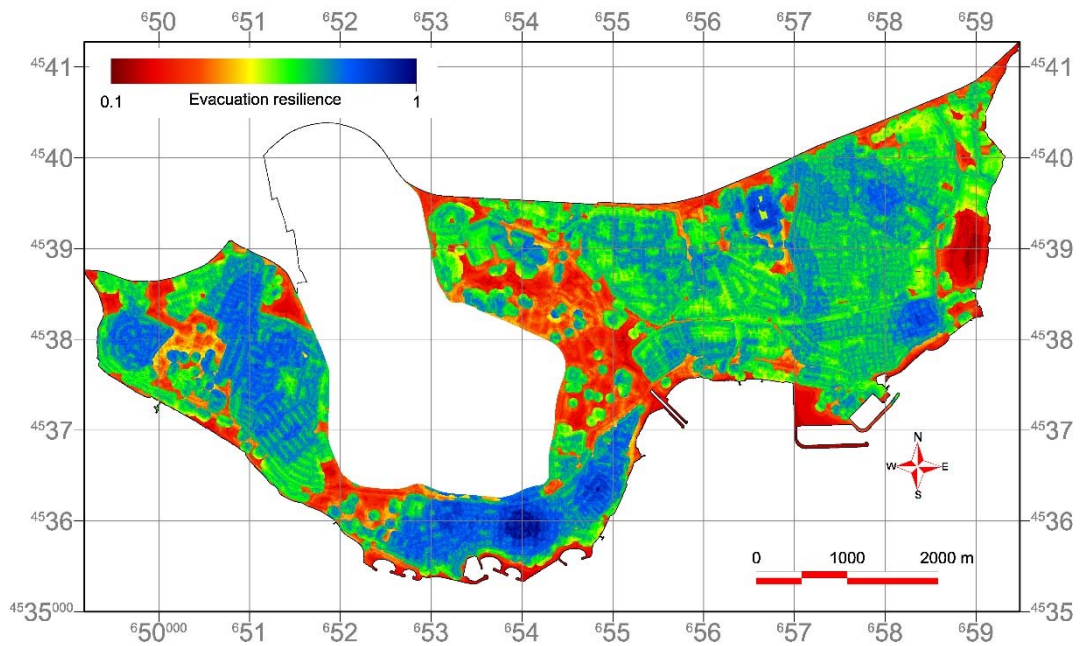


Figure 4.25 The final map of evacuation resilience

4.5 Vulnerability at Location and Evacuation Resilience Ratio: MeTHuVA

MeTHuVA represents the overall tsunami human vulnerability and produced by the integration of the VL and RE maps. Basically it is the ratio of final vulnerability at location and evacuation resilience maps. The resulted map of the ratio can be observed in Figure 4.26.

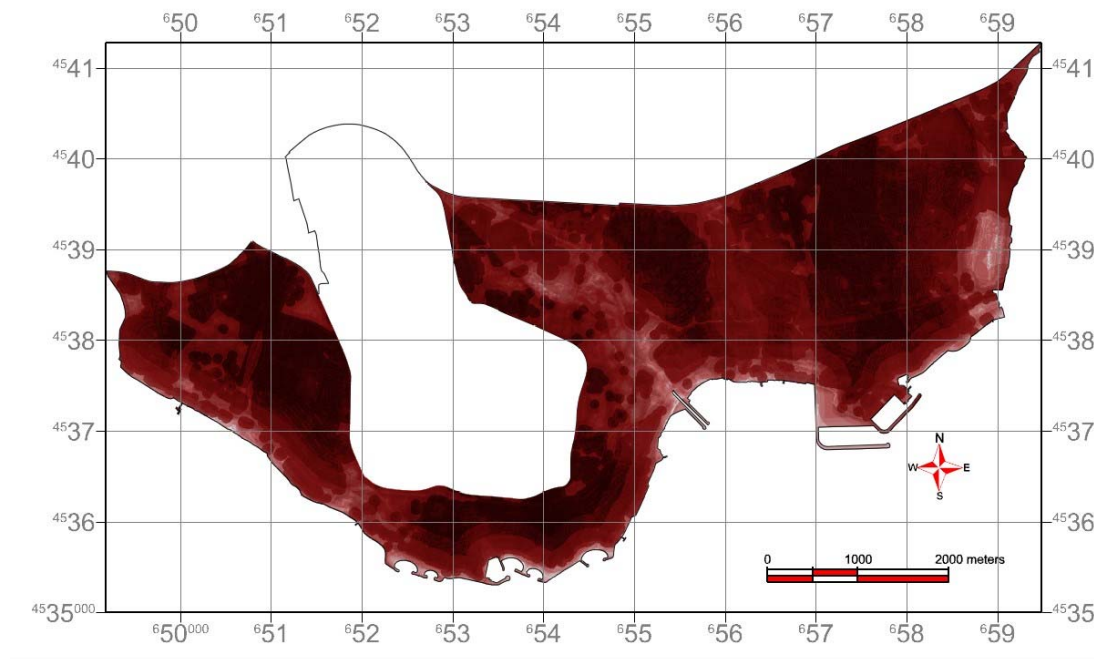


Figure 4.26 VL/RE (MeTHuVA) distribution of Bakırköy district. Lighter colors showing higher vulnerability scores.

Figure 4.26 represents VL/RE ratio for each location of Bakırköy district of İstanbul in a color scale where a relative evaluation can be performed. In the figure, lighter colored parts show the places where the overall tsunami human vulnerability is higher, while the dark colored places is relatively less vulnerable. It can be seen from the figure that the places where the human vulnerability is higher are located, along shoreline, along the three stream beds and at the locations where the building and road density is lower.

CHAPTER 5

TSUNAMI RISK ASSESSMENT

5.1 Tsunami Risk Analysis

The relationship that proposed by Çankaya et al. (2016) has been used for the risk assessment of the Bakırköy district. The relation aims to calculate the risk at each location of the study area.

$$Risk = (H) * \left(\frac{VL}{n*RE} \right) \quad (\text{Equation 5.1})$$

In the equation, H represents the hazard, which was the flow depth value in the inundation zone calculated with tsunami numerical modeling. Where $H = 0$, the tsunami risk at that location would be zero since that location is not inundated. VL and RE represent vulnerability at location and evacuation resilience, respectively. Both are created considering human vulnerability. VL and RE are inversely proportional and are in the range of 0 and 1. Increase of the value within the range shows the increase of vulnerability for VL and increase of resilience (therefore decrease of vulnerability) for RE . Hence, an increase in RE or a decrease in VL , would reduce the overall vulnerability. The overall vulnerability is multiplied with the factor of awareness and preparedness level of the community, which is represented by n .

5.2 The Parameter of Awareness and Preparedness of the Community

As stated earlier the parameter n , represents the awareness and preparedness of the community of an area to a tsunami disaster. In other words, it represents the coping level of a community in the case of a tsunami threat.

The tsunami phenomenon is a rare occurring event, yet it is one of the most destructive natural hazards. When the risk of probable tsunami event is taken account considering the above mentioned equation, the tsunami hazard cannot be ceased or reduced since it is controlled by the nature. Even it can be increased as a result of sea level rise related with climate change (Suppasri et al., 2015). Since this study deals with the human vulnerability both the VL and RE are the parameters that are delimited for changes. Therefore, the only controllable parameter in the risk equation proposed by Çankaya et al. (2016) is the awareness parameter, n .

In the study of Çankaya et al. (2016), the value of the parameter n was in the range of 1 and 10, where the value 10 represents a well-prepared and hazard aware community, while the value 1 representing reverse. According to the study of Çankaya et al. (2016), the awareness level of İstanbul was used as $n = 3$, and the overall risk calculations were made by using the hazard results obtained from two different tsunami sources.

5.3 Tsunami Risk at Bakırköy District

In the previous chapters of this study it is explained the obtainment procedure of hazard (using tsunami source YAN) and vulnerability parameters (VL and RE) and their related maps. The tsunami risk equation is presented in the Section 5.1.

As mentioned before the only controllable parameter of the risk equation is the awareness parameter, n . Although it is assumed to be $n = 3$ in the study of Çankaya et al. (2016) for whole İstanbul, in this study it is considered appropriate to evaluate the risk level by giving different values of the parameter n . According to that, relative risk maps have been produced in GIS environment for the Bakırköy district of İstanbul by using the relation explained in the Section 5.1.

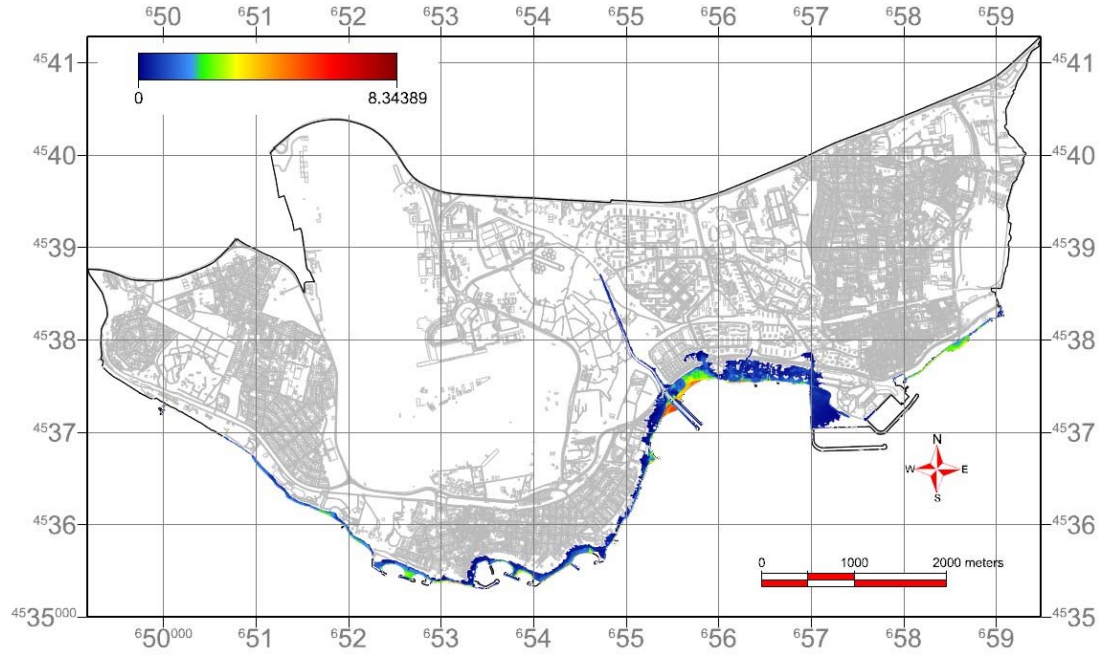


Figure 5.1 The risk map of Bakırköy district calculated with proposed equation with inputs of Hazard (H), awareness level of community (n) Vulnerability at Location (VL) and Evacuation Resilience (RE)

5.4 Neighborhood Based Evaluation of Hazard, Vulnerability and Risk

Bakırköy district consists of 15 neighborhoods. The vector data of the borders of these neighborhoods and the population data has been obtained from Turkish Statistical Institute. The map of the neighborhoods is presented in Figure 5.2. The extracted area of the İstanbul Atatürk airport is also considered during the neighborhood based evaluation. İstanbul Atatürk Airport is located in the Yeşilköy neighborhood and covers a great amount of that area. Since there are no residential buildings thus no population in that area, it was appropriate to exclude that area for this part of the study either. After extracting the area of the airport, Yeşilköy neighborhood was divided into two parts and these parts were considered as Yeşilköy South and Yeşilköy North. It should be noted that at Yeşilköy North, there are no residential buildings. Therefore, throughout the neighborhood based analyses, it is assumed that all the population of Yeşilköy neighborhood is dwelled in the Yeşilköy South part. In the evaluations that are not related with the population data, these two parts of Yeşilköy neighborhood are considered as different areas.

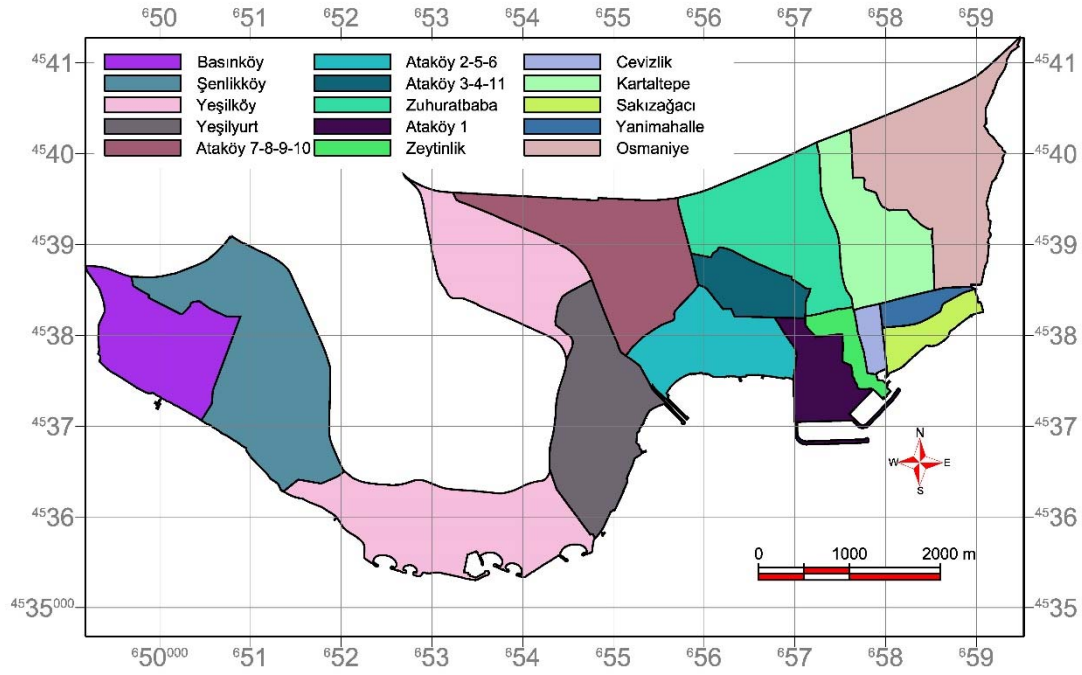


Figure 5.2 Neighborhoods of Bakırköy District

The neighborhoods of Bakırköy district were evaluated considering different parts of the study and to make the comparison among them, charts have been prepared. At the first step the mean values of vulnerability at location, evacuation resilience and VL/RE ratio scores was evaluated for each neighborhood regardless the hazard presence (Figure 5.3 and Figure 5.4)

Comparison of the mean locational vulnerability values of the neighborhoods shows that the highest score belongs to the Sakızağacı neighborhood with a very well noticeable difference. This neighborhood is small and has an elongated structure parallel to the shoreline. Hence, all the locations on that neighborhood has higher score being close to the shoreline. Although Cevizlik, Zeytinlik and Yenimahalle are small and elongated neighborhoods, Cevizlik and Zeytinlik are perpendicular to the shoreline and the area that are close to shoreline is less, whereas Yenimahalle does not have a coastal section. According to the comparison Kartaltepe is the least vulnerable neighborhood of Bakırköy district. Besides being away from the shoreline, it is located in a higher elevation area with less landslide scarp presence (Figure 5.3.a and Figure 5.4.a).

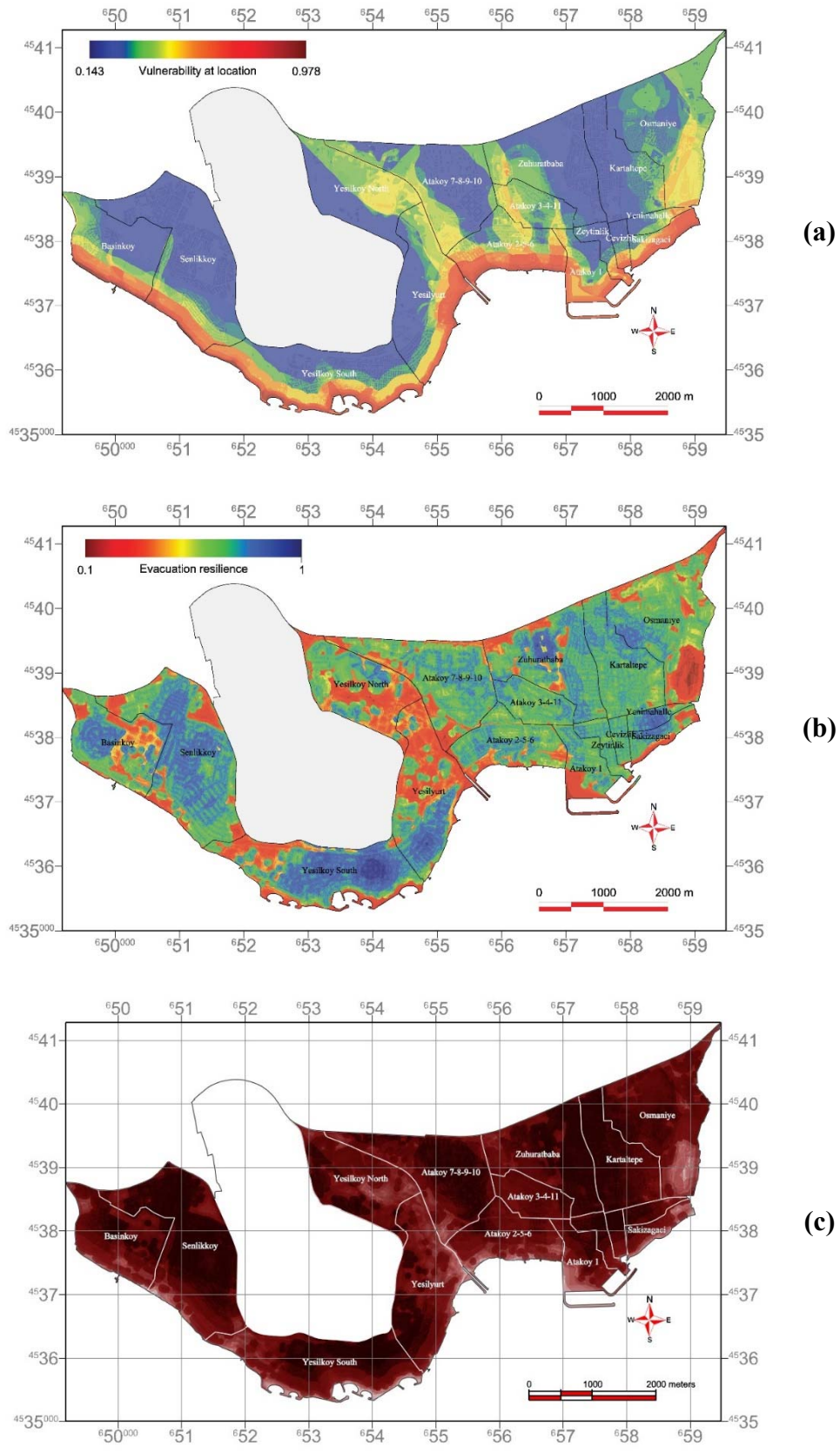
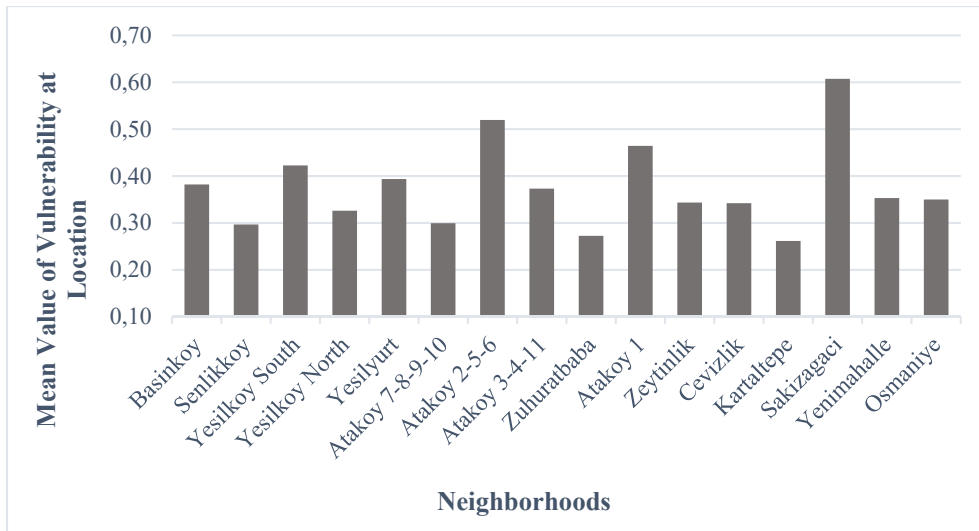
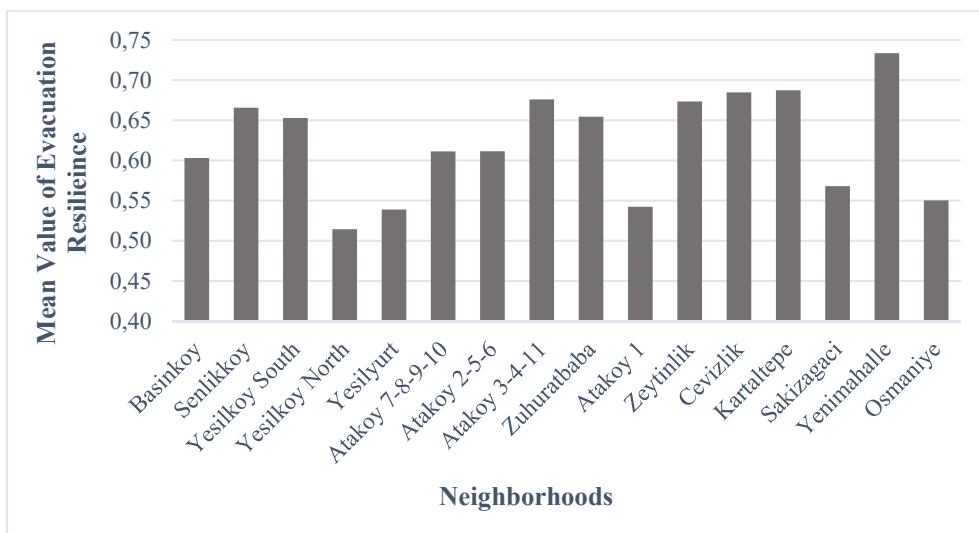


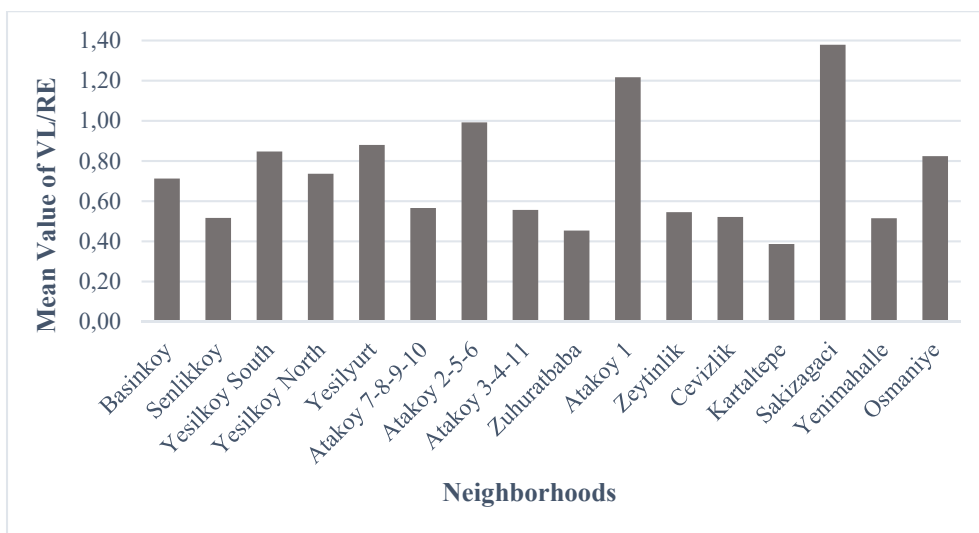
Figure 5.3 (a) Locational vulnerability (VL) map, (b) Evacuation resilience (RE) map, (c) VL/RE map, lighter colors represent more vulnerable locations.



(a)



(b)



(c)

Figure 5.4 (a) Neighborhood based comparison of locational vulnerability, (b) Neighborhood based comparison of evacuation resilience, (c) Neighborhood based comparison of VL/RE

Comparison of the mean evacuation resilience scores revealed that the most of the neighborhoods have similar scores (Figure 5.3.b and Figure 5.4.b). Still the lowest evacuation resilience score belongs to Yeşilköy North and it is followed by Yeşilyurt, Ataköy 1 and Osmaniye. The main reasons behind that are the absence of buildings and also the roads that are perpendicular to the shoreline. Yenimahalle neighborhood has the highest score since it has many buildings and perpendicular roads.

Additionally, without considering the tsunami hazard level, a map of VL/RE ratio map (MeTHuVA) was produced for the neighborhood based evaluations for the observation of overall vulnerability levels for each neighborhood (Figure 5.3.c). The comparison of the neighborhoods shows that the most overall vulnerability score is belongs to Sakızağacı and it is followed by Ataköy 1, ataköy 2-5-6, Yeşilyurt, Yeşilköy South and Osmaniye neighborhoods.

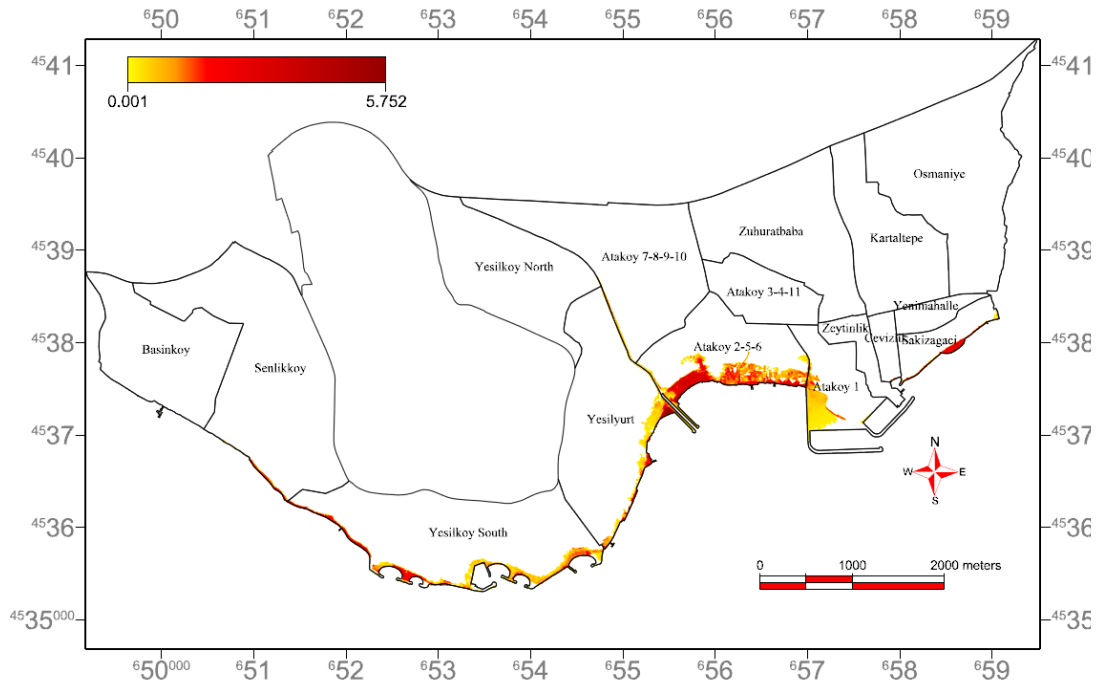
Secondly, the hazard scores were evaluated for the neighborhoods of Bakırköy district. The evaluation scores were obtained by the summation of flow depth values of each inundated pixel for every neighborhood. Naturally, the area that are not inundated were with zero score. These scores than normalized by the area of the neighborhood that it belongs (Figure 5.5). The most hazardous neighborhood is obtained as Ataköy 2-5-6 with a very distinct difference. It is followed by Sakızağacı, Yeşilköy South, Yeşilyurt, Ataköy 1, Senlikköy, Cevizlik. Ataköy 7-8-9-10 and Yeşilköy North are not coastal neighborhoods. However, since it is next to the Ayamama Stream, it is inundated by the overflow caused by the tsunami wave. The inundation seen in Basıncıköy and Zeytinlik is almost negligible, even if these are coastal neighborhoods.

Eleven neighborhoods of Bakırköy district have inundated areas. The amount of the inundated areas is determined and represented in Table 5.1. The largest inundated area is seen in Ataköy 2-5-6 with 30 hectares which equals to 25.15 % of the neighborhood, and it is followed by Yeşilköy South, Yeşilyurt and Ataköy 1 with areas of 23.3, 15.3 and 13.3 hectares, respectively. The inundated area of whole Bakırköy is 90 hectares which equals to 4.18 % of the district.

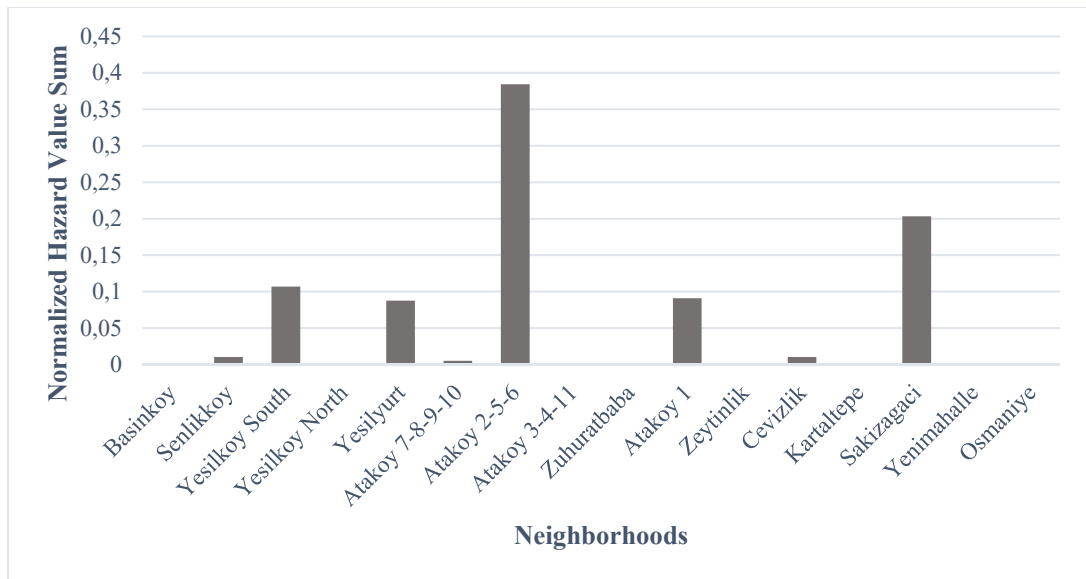
Table 5.1 Amount of inundated area of each neighborhood and whole Bakırköy district

Neighborhood	Inundated area (hectare)	Percent
Ataköy 2-5-6	30,943	25,15
Yeşilköy South	23,324	9,96
Yeşilyurt	15,265	7,71
Ataköy 1	13,263	18,39
Sakızağacı	4,132	10,87
Şenlikköy	2,412	0,81
Ataköy 7-8-9-10	1,386	0,68
Cevizlik	0,178	0,95
Yeşilköy North	0,124	0,07
Basıncöy	0,097	0,06
Zeytinlik	0,024	0,08
Bakırköy	91,147	4,18

The comparison of the neighborhoods was made also for the calculated risk. Risk equation consists of the locational vulnerability, evacuation resilience, hazard and awareness factor. Naturally, risk is not present where the hazard is absent. The normalized risk value sum chart is presented in Figure 5.6, where the summation of risk values of each pixel was normalized by the area of the neighborhood. According to that chart considering the size of the neighborhoods, the most affected area is visibly Ataköy 2-5-6, where the one of the highest horizontal distance of inundation seen (except Ayamama Stream). This is a neighborhood where the inundated buildings are present greatly. Sakızağacı, Yeşilköy South, Yeşilyurt and Ataköy 1 follows it with considerable risk values. Besides that, Şenlikköy, Cevizlik, Ataköy 7-8-9-10 has lower values for the risk evaluations. The values for Basıncöy, Yeşilköy North and Zeytinlik are negligible.

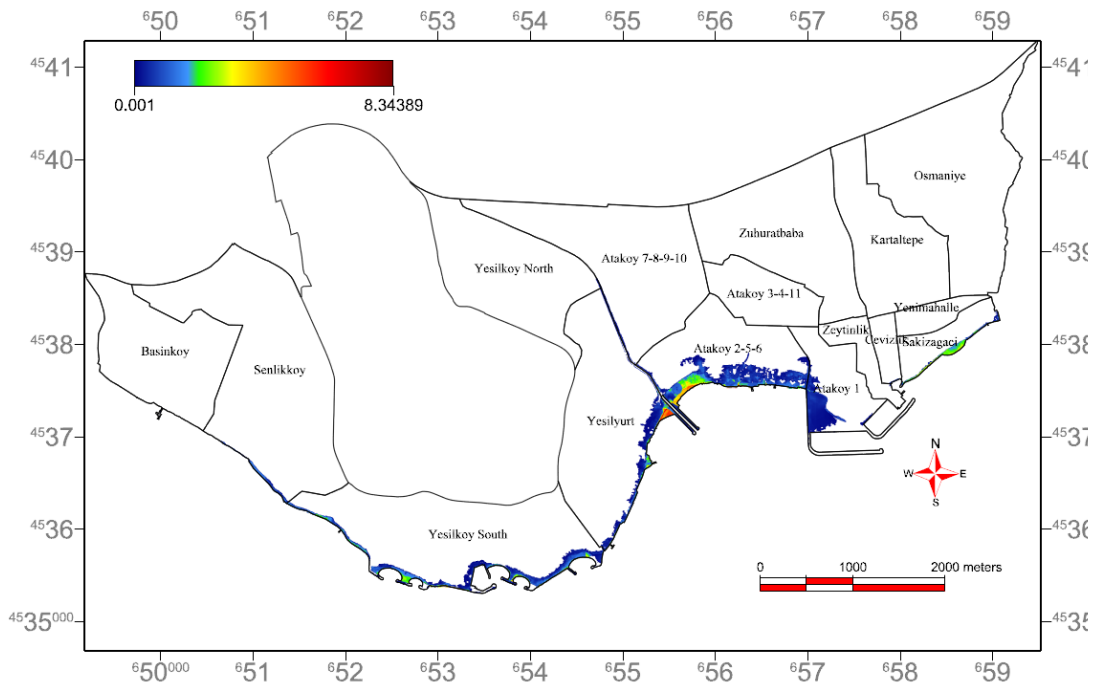


(a)

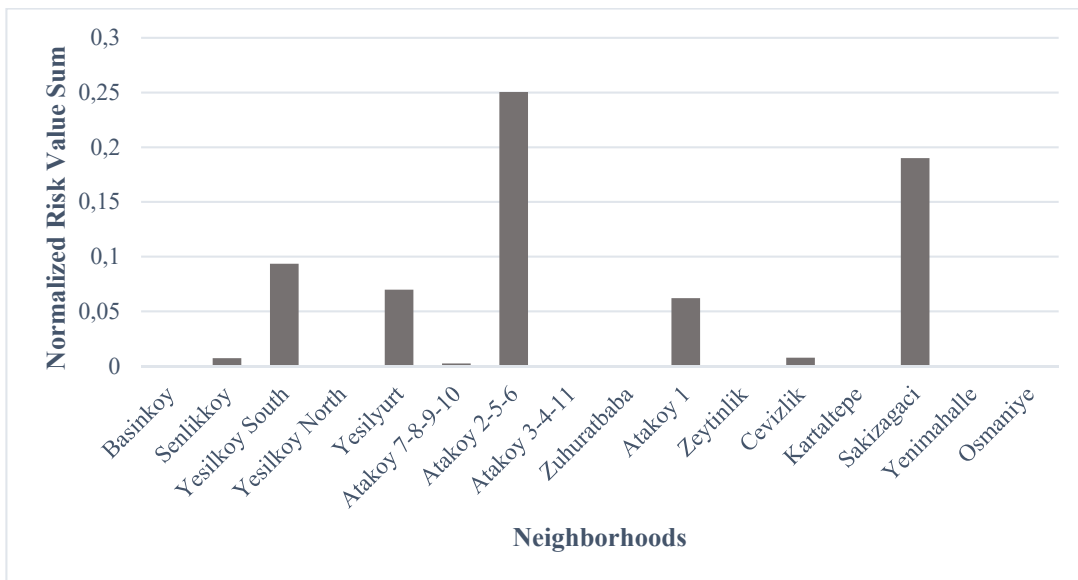


(b)

Figure 5.5 (a) Hazard map with neighborhoods, (b) Sum of hazard scores of the neighborhoods normalized by the area



(a)



(b)

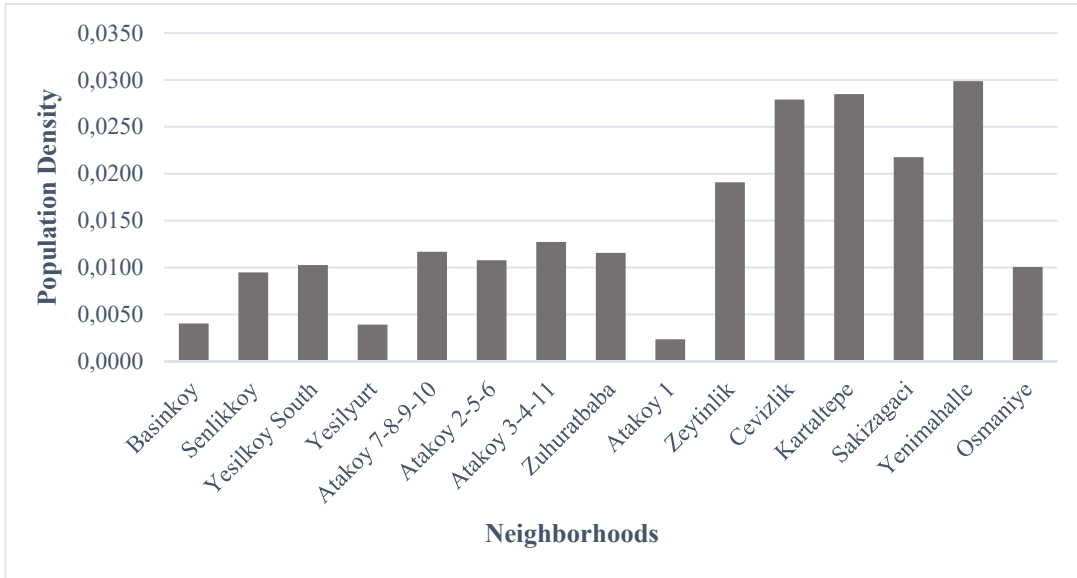
Figure 5.6 (a) Risk map with neighborhoods, (b) Sum of risk scores of the neighborhoods normalized by the area

The population data of the neighborhoods was available. Therefore, a population based analysis has performed. The population density was calculated for each neighborhood. For Yeşilköy neighborhood a special case was defined. The northern part of the neighborhood and the area of the airport was excluded from the analysis, since there are no residential buildings at that parts. To evaluate the population, taking into account the hazard levels of the neighborhoods, population density was multiplied with the summation of the hazard values of each neighborhood normalized with their area. The resulting charts can be seen in Figure 5.7. According to these charts the most densely populated areas are Yenimahalle, Kartaltepe and Cevizlik. However, and when considered with the hazard level, Yenimahalle and Kartaltepe are not located in the inundated area and the residents of Cevizlik is one of the least exposed community. Among the inundated neighborhoods the most exposed population is located in Ataköy 2-5-6 and Yeşilköy South with a clear difference, Sakızağacı and Yeşilyurt are also showing noticeable amount of exposed population.

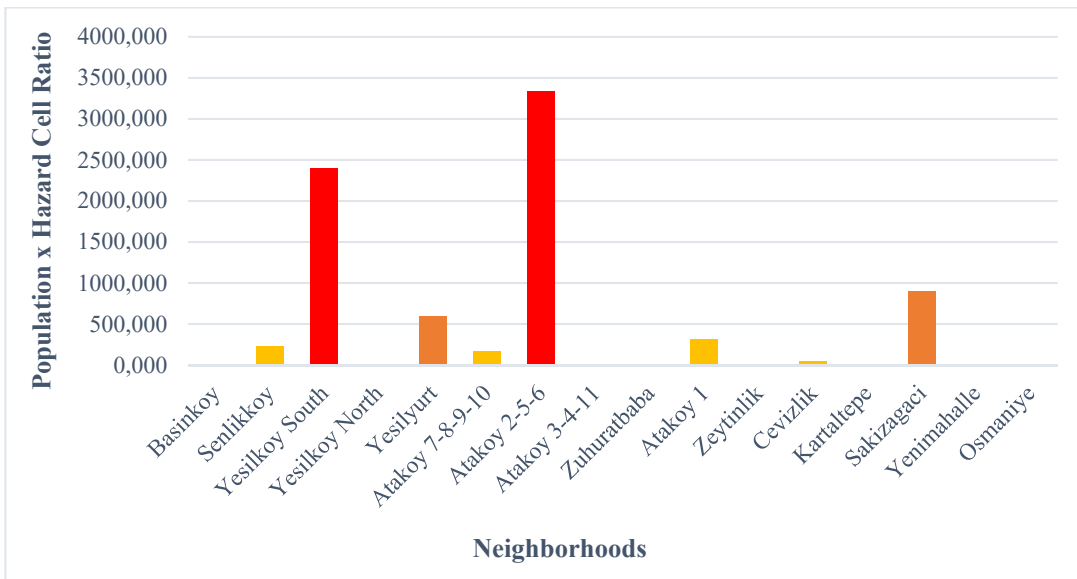
Lastly the building exposure is evaluated for each neighborhood of Bakırköy district. The number of the buildings in the inundation zone has been calculated first. There are 61 buildings that are inundated by tsunami waves in Bakırköy district. However, in some of the neighborhoods there are not any exposed buildings, even there is inundation occurs in those neighborhoods. After the discovery of exposed buildings, the percentage of exposed buildings among total buildings of the neighborhoods were calculated (Figure 5.8).

According to these evaluations the number of exposed buildings are very high in Ataköy 2-5-6, over 30. Also great number of buildings were inundated in Yeşilyurt and Yeşilköy South. When the percentage is taken account, Ataköy 2-5-6 is still has highest percentage over 10 %. The exposed building percentage is almost 4% in Yeşilyurt, while it is under 1% in Yeşilköy South even the inundated building number is not negligible. However, in Ataköy 1 the exposed building percentage is almost 2%, even if the inundated building number is only two.

Although the building damage and economic effect of that would not considered in the risk calculation of this study, in the further studies this damage could be involved to the tsunami risk assessments.

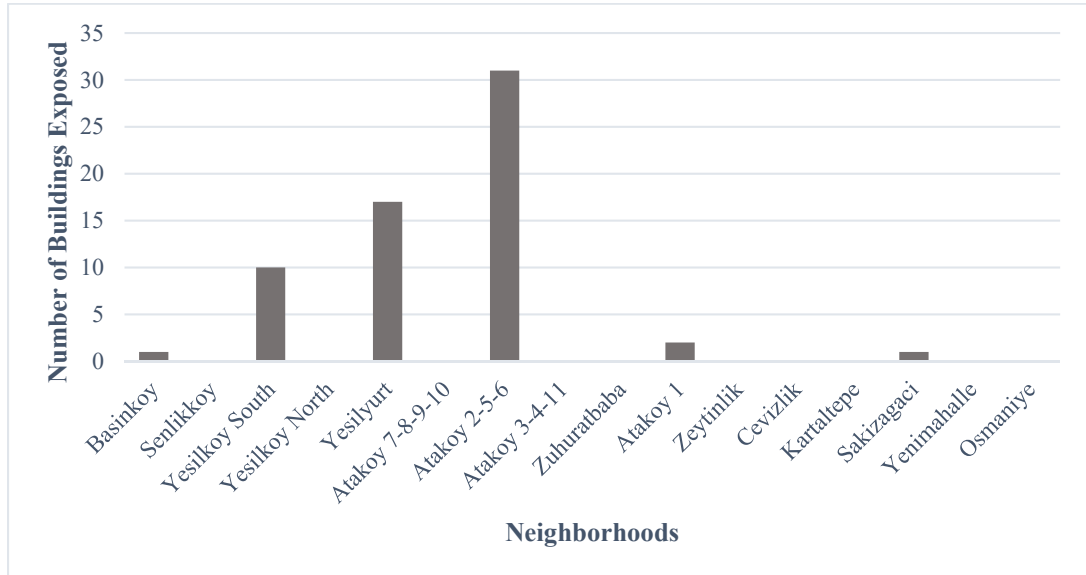


(a)

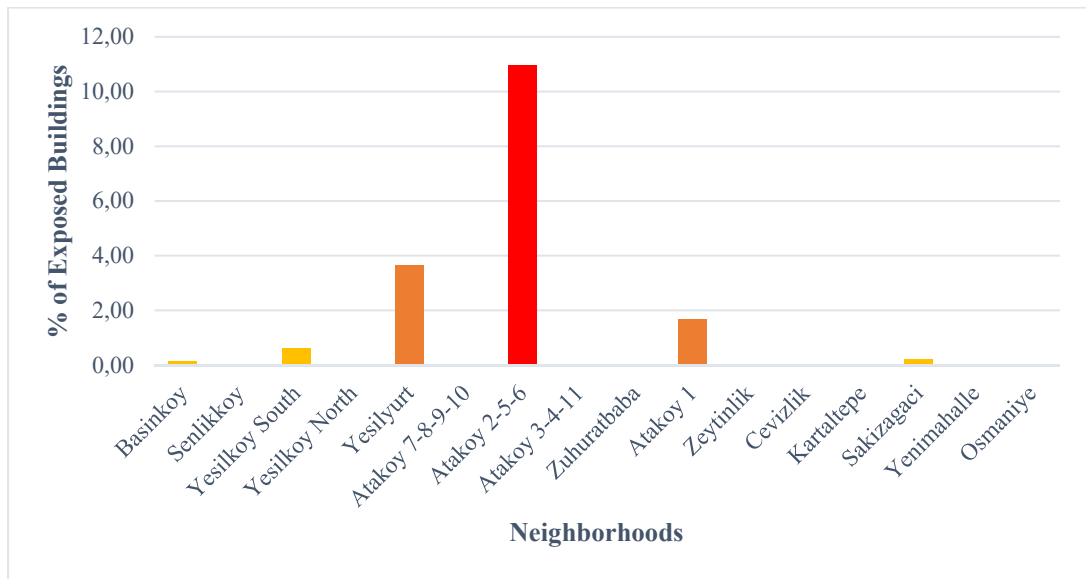


(b)

Figure 5.7 (a) Chart of population density by neighborhood, (b) Chart of hazard related population density



(a)



(b)

Figure 5.8 (a) Chart of exposed buildings by neighborhoods, (b) Percentage of exposed building for each neighborhood

CHAPTER 6

DISCUSSION

Vulnerability assessments are necessary for developing mitigation strategies and emergency plans. There are many vulnerability assessment studies in the literature that has been applied considering different natural hazards, including tsunamis. However, in the area of tsunami vulnerability assessment, many of these studies are based on building vulnerability and dealing mostly with economic losses, not human vulnerability.

Considering the need of tsunami human vulnerability assessments, in this thesis, the tsunami human vulnerability assessment method MeTHuVA, generated by Çankaya et al., (2016) is improved and further developed and applied to the Bakırköy district of İstanbul. Besides the vulnerability of human, the hazard level of the study area was calculated with tsunami numerical model NAMI DANCE. Eventually the tsunami risk assessment of the area is performed.

Since İstanbul is a megacity and growing every day, the available data (dates back to 2006) was processed according to the changes that are observed from the satellite images. These changes can be listed as changes of shorelines due to the construction of new coastal facilities like marinas, construction of new shopping malls, renewed buildings, constructions of new buildings and roads. The changes are mostly observed from the Google Earth images. The extents of the structures are digitized from the satellite images and heights of the buildings were estimated according to the number of floors as seen from the Google Street photographs. These changes were the most time consuming parts of the study. With more recent data the time required for the study would be less.

In order to use in the steps of the study, a high resolution spatial data was produced by integrating the available datasets from different sources. This data consists of elevation values of each 1 m pixel of the Bakırköy district and the marine area of its vicinity. The terrestrial part of this data named as metropolitan topography, since it is composed of the elevation values of all the structures and infrastructures. This data was produced by generating a 1 m cell sized raster data from the vector data of the structures using the top elevation value of that structure and joining it with raw DEM obtained from IMM. For the marine part of the data, the bathymetric data from GEBCO is upsampled to have the same pixel size of terrestrial data. In order to enhance this data, Nautical Charts taken from Turkish Navy were digitized. These two datasets have been joined to have improved bathymetric data. Eventually the topographic and bathymetric data was aggregated to have a final dataset to use in the tsunami numerical model NAMI DANCE.

The hazard assessment of this study was performed by the application of Tsunami Numerical Modelling. The available spatial data to use in this process was in 1 m resolution. However, the raster data of Bakırköy in that high resolution was composed of 10525x9600 matrix. The process of a data with a huge size like this requires a great amount of time in the computers used in this study. For reducing the computational time, the 1 m resolution data was downsampled to 3 m (and also to 9 m, 27 m resolution for nested domain simulations) resolution and the hazard assessment simulations were made using this dataset. Since the scope of this study is the whole Bakırköy district the 3 m simulation was adequate to assess the hazard. Furthermore, it can be said that, one the of the highest resolution tsunami hazard assessment (also vulnerability and risk assessments) in the literature is carried out in this study. However, a 1 m resolution simulation could be realized to the most hazardous parts of the area (with lower amount of data) if needed.

The selection of tsunami source for the study is made by literature review and three possible sources were selected. The selection made by the evaluation of the possible tsunami sources considering the location of the study area. For each of these sources 60 minute simulations were made with accepting the vertical displacement caused by ruptures as 3.7 m according to the observations of MARMARASCARP cruise revealed by Armijo et al., (2005) and OYO-IMM reports. These simulations were

made with a 42 m resolution data to keep the preliminary computational time acceptable. According to the results of these simulations, the maximum inundated area and the maximum flow depth was observed in the YAN source. Additionally, the leading wave of the tsunami source YAN was a depression wave, and leading depression waves causes higher amplification and run up at coastal areas. Therefore, the tsunami source YAN has been selected as the worst case scenario.

Evaluation of the vulnerability assessments are carried out with GIS-based MCDA. Among MCDA methods AHP was selected. In AHP method the decision problem is divided into simpler problems in a hierarchical structure, to make the decision making process easier to handle. Furthermore, AHP is a method that restricts the subjectivity of the decision maker to a level. It provides a comparison method that one can compare only two criteria each time (pairwise comparison), instead of directly weighting the decision criteria. This comparison method also provides calculation of consistency of the weights assigned after the pairwise comparison (Consistency Ratio). The judgements for the pairwise comparisons of this study is made by experts. Therefore, they are reliable and consistent.

Assessment of the tsunami vulnerability of Bakırköy district taken account as the ultimate decision problem and divided into two subjects; vulnerability at location and evacuation resilience. These subjects are further divided into decision criteria for the ease of evaluation. Vulnerability at location subject has five criteria, while the evacuation resilience has four. Before weight estimation, a classification and ranking process within each of those nine criteria was performed considering the level of vulnerability or evacuation resilience. This process of classification and ranking was performed with expert judgements, considering the tsunami event that might threat Bakırköy district. This classification process was needed for the proper and clearer evaluation of the vulnerability of each location. Any change of the classification or ranking would change the final vulnerability or resilience result of a specific location regardless the weight of the criteria.

According to the weight estimations resulting the pairwise comparison, the distance from shoreline criteria was the most effective criteria in the vulnerability of location evaluations with the weight of 0.416145. Hence, the most remarkable differences

observed in the final map of locational vulnerability is produced by that layer. Geology layer is the second important layer and caused significant effects on the final map.

In the evacuation resilience evaluations, distance from buildings criteria is found to be the most effective one with the calculated weight 0.489916, showing that being close to the buildings is the most effective way of evacuation since it provides a vertical evacuation route. Consequently, buildings and their vicinity are the most resilient areas of the Bakırköy district regardless of the type of the building. The second most effective criterion is the presence of the density of the roads that are perpendicular to the shoreline. Perpendicular road density has a dominancy over the distance to road layer since the perpendicular roads allow the direct secession from where the wave is coming from.

In the application of AHP to decision problems, it is possible to apply the pairwise comparison to all levels of the hierarchy. However, in this study the only application level was the criteria level. The application of the pairwise comparison was not possible to the decision alternatives level, since the decision alternatives of this study was the 1 m sized pixels of the study area, and comparing this amount of alternatives was not possible. On the other hand, the pairwise comparison of the subject level (VL and RE) was not performed either. They are assumed to be at the same importance and inversely proportional. The integration of these two to obtain the ultimate vulnerability score is performed in the risk assessment part of the study.

The risk assessment of the Bakırköy district of İstanbul is made by governing the risk equation of Çankaya et al. (2016). For calculating the risk, the hazard analysis from TNM, vulnerability analysis from GIS-based MCDA was used. The value of the parameter n in the risk equation was selected to be 3 for Bakırköy district of İstanbul. The reason of the selection of that value is the community of İstanbul is aware of natural disasters since the region is in a tectonically active zone and also flood events are not very rare for the region. Therefore, the community is barely aware of natural disasters even they are not very well prepared yet. In addition, tsunami event is not very well known by the community, since there are not any destructive tsunami events in the near history, and the smaller events are overshadowed by the devastating earthquakes.

However, the parameter n should be studied in detail to evaluate the sensitivity of the value on the risk equation. Also the scope of the values should be discussed broadly characteristics should be determined.

Application of the model requires some assumptions. The causing earthquake event is assumed to be a precursor for the incoming tsunami wave. Therefore, people would be warned and will have time to move safer places. In addition, the inundation on land assumed to be happened at the same time, but in reality the wave could hit the different parts of the shoreline at different times. Moreover, after first hitting the land occupation of whole inundation zone would not be at the same time. Another assumption is about the buildings. After earthquake or during tsunami, the buildings are assumed to remained rigid and undamaged. Hence the building damages were not considered during the study and all the buildings are assumed to be available for providing vertical evacuation.

As known from the general behavior of tsunamis that tsunamis are more effective in the harbors and river mouths and propagate further inland along rivers. Therefore, Ayamama stream becomes one of the most critical regions in Bakırköy district in terms of tsunami inundation and penetration towards land. The regions which has similar morphology, have to be considered as critical regions under tsunami attack.

The methodology that was presented in this study is applicable to other coastal areas. However, application of the methodology would require few modifications which might change when the application location is different. These changes might involve; (i) excluding some of the criteria if it is not possible or meaningless to evaluate for the area, (ii) introducing new criteria when it is vital to evaluate or where new datasets are available, (iii) changing the classification within each criteria and the rank values for the classes. Moreover, since the pairwise comparison needed to be performed in an area-specific, drastic changes of the weight values might be observed.

CHAPTER 7

CONCLUSION

The aim of this study was bringing new insights to the tsunami vulnerability and risk analysis by developing the present methods. The main difference of the methodology was the evaluation of human exposure to the tsunami event using high resolution spatial data and the use of GIS-based MCDA.

The highlights and the results that was acquired throughout the analysis of the study can be summarized as below.

Historical records reveal the possibility of tsunami occurrence in the Sea of Marmara. Therefore, it is a need to develop hazard, vulnerability and risk assessments to strengthen the mitigation strategies. This study proposes a developed methodology of tsunami risk assessment, applicable to all coastal areas. In this thesis, this methodology is tested on the Bakırköy district of İstanbul.

High resolution spatial data in the application of the methodology results a detailed and more accurate hazard, vulnerability and risk evaluation.

According to the results obtained using tsunami numerical model NAMI DANCE, among the tsunamigenic rupture in the Sea of Marmara, Yalova Normal Fault (YAN) generates the worst case scenario for Bakırköy district with more extreme tsunami parameters near shore and on land. YAN generates over -0.8 m maximum negative amplitude and over +0.4 m maximum positive amplitude at the southern border of Domain E. The maximum flow depth exceeds 5.7 m at some critical places of Bakırköy. While the maximum flow depth is seen west of the mouth of Ayamama Stream in the Yeşilyurt neighborhood, high flow depth values are present in Yeşilköy, Ataköy 2-5-6 and Sakızağacı neighborhoods. The maximum inundation distance in

Bakırköy is over 350 m and seen in the neighborhood Ataköy 2-5-6. The inundated area is 91.1 hectares which equals to 4.2% of whole Bakırköy district. Among the neighborhoods, the largest inundated area is seen in Ataköy 2-5-6 with 30 hectares which equals to 25.15 % of the neighborhood and it is followed by Yeşilköy South, Yeşilyurt and Ataköy 1 with areas of 23.3, 15.3 and 13.3 hectares, respectively

It is clear that the underpasses lead the way for water to inundate inland. In addition to that, the incoming tsunami wave penetrates almost 1700 m along the Ayamama stream, but no overflowing was observed. Moreover, the newly constructed Ataköy Marina located in the neighborhood Ataköy 1 is almost completely inundated by the tsunami wave resulted by the rupture of YAN. According to the result of the hazard assessment, totally 62 buildings were exposed to the tsunami wave interaction in whole Bakırköy district and a 31 of them are located in the neighborhood Ataköy 2-5-6, that equals to 10% of the total buildings in that neighborhood.

Vulnerability assessments that was performed by the application of AHP and pairwise comparisons revealed that, among the criteria of vulnerability at location, distance from shoreline criteria was the most dominant one with weight value of 0.416 and the less dominant criteria was metropolitan use with a weight of 0.072. The most powerful criterion of the evacuation resilience evaluation was distance to building with a weight value of 0.489916 and the least powerful criterion was slope with weight value of 0.076.

According to the neighborhood based evaluations, Sakızağacı and Ataköy 2-5-6 are the locationally most vulnerable neighborhoods while Yenimahalle neighborhood is the one where the evacuation is the most resilient.

The tsunami risk assessment of Bakırköy district of İstanbul was calculated with Equation 5.1. Besides results of hazard and vulnerability assessments, the awareness parameter has a great importance. In this thesis the value of this parameter selected as 3 and the risk results according to the calculations were changing between values of 0.1 and 8.3. However, a greater value of awareness factor, would give reduced values for risk. Since within the relation of risk, the awareness factor is the only parameter that can be controlled, an education that will be provided to the community in order to

increase the awareness and preparedness will decrease the risk that the Bakırköy district will be faced under a possibility of tsunami attack.

The recommendations for future studies which can be considered for application and further development of methodology are listed below:

- For human vulnerability analysis, different MCDA methods can be used. The results of those different MCDA methods can be compared for the final evaluation of human vulnerability analysis.
- New parameters can be introduced with the available datasets or new datasets, to be used in the evaluation of vulnerability at location or evacuation resilience.
- Sensitivity analysis of the classification and ranking process of each criterion might be performed.
- Sensitivity analysis for determination of class boundary limits and ranking processes can be performed.
- With a building inventory that includes the durability conditions of each building a more detailed and proper metropolitan use layer can be produced. With that inventory, it would also be possible to estimate the conditions of the buildings after the earthquake to evaluate their suitability for vertical evacuation.
- The sensitivity analysis for the n , the parameter of awareness and preparedness of the community can be performed. Moreover, the content of the parameter n can be defined more properly, by describing the level. Description of the levels can be performed with application of a worldwide public awareness survey.

REFERENCES

- Alexander, D., 2000. *Confronting catastrophe. New perspectives on natural disasters*. Terra Publishing, New York, p 282
- Alpar, B. and Yaltirak, C., 2002. Tectonic setting of the eastern Marmara Sea. In *Integration of Earth Science Research on the Turkish and Greek 1999 Earthquakes* (pp. 35-46). Springer Netherlands.
- Altinok, Y. and Ersoy, Ş., 2000. Tsunamis observed on and near the Turkish coast. *Natural Hazards*, 21(2-3), pp.185-205.
- Altinok, Y., 2006. *Türkiye ve Cevresinde Tarihsel Tsunamiler*. *Türkiye Mühendislik Haberleri*, pp.25-32
- Altinok, Y., Alpar, B., Ersoy, Ş., and Yalçiner, A. C., 1999. Tsunami generation of the Kocaeli Earthquake (August 17th 1999) in İzmit Bay: coastal observations, bathymetry and seismic data, *Turkish J. Mar. Sci.* 5, 131–148.
- Altinok, Y., Alpar, B., Özer, N. and Aykurt, H., 2011. Revision of the tsunami catalogue affecting Turkish coasts and surrounding regions. *Natural Hazards and Earth System Sciences*, 11(2), pp.273-291.
- Altinok, Y., Tinti, S., Alpar, B., Yalçiner, A.C., Ersoy, Ş., Bortolucci, E., Armigliato, A., 2001. The tsunami of August 17, 1999 in İzmit Bay. *Nat. Hazards* 24, 133-146.
- Ambraseys, N.N. and Finkel, C.F., 1987. The Saros–Marmara earthquake of 9 August 1912. *Earthquake engineering & structural dynamics*, 15(2), pp.189-211.
- Ambraseys, N.N. and Finkel, C.F., 1991. Long-term seismicity of Istanbul and of the Marmara Sea region. *Terra Nova*, 3(5), pp.527-539.
- Ambraseys, N.N., 1962. Data for the investigation of the seismic sea-waves in the Eastern Mediterranean. *Bulletin of the Seismological Society of America*, 52(4), pp.895-913.
- Ambraseys, N.N., 2002. Seismic sea-waves in the Marmara Sea region during the last 20 centuries. *Journal of Seismology*, 6(4), pp.571-578.
- Armijo, R., Pondard, N., Meyer, B., Uçarkus, G., de Lépinay, B.M., Malavieille, J., Dominguez, S., Gustcher, M.A., Schmidt, S., Beck, C. and Cagatay, N., 2005. Submarine fault scarps in the Sea of Marmara pull-apart (North Anatolian fault):

Implications for seismic hazard in Istanbul. *Geochemistry, Geophysics, Geosystems*, 6(6).

Atillah, A., El Hadani, D., Moudni, H., Lesne, O., Renou, C., Mangin, A. and Rouffi, F., 2011. Tsunami vulnerability and damage assessment in the coastal area of Rabat and Salé, Morocco. *Nat. Hazards Earth Syst. Sci*, 11, pp.3397-3414.

Ayca, A., 2012. Development of A Web GIS-Based Tsunami Inundation Mapping Service; A Case Study For Marmara Sea Region. M.S. Thesis METU, Ankara, Turkey

Aytöre, B., 2015. Assessment Of Tsunami Resilience Of Ports By High Resolution Numerical Modeling: A Case Study For Haydarpasa Port In The Sea Of Marmara (MSc Dissertation, Middle East Technical University).

Banai, R., 1993. Fuzziness in Geographical Information Systems: contributions from the analytic hierarchy process. *International Journal of Geographical Information Science*, 7(4), pp.315-329.

Barka, A.A. and Kadinsky-Cade, K., 1988. Strike-slip fault geometry in Turkey and its influence on earthquake activity. *Tectonics*, 7(3), pp.663-684.

Barros, J.L., Emídio, A., Santos, A. and Tavares, A.O., 2015. Composite methodology for tsunami vulnerability assessment based on the numerical simulation of 1755 Lisbon tsunami—application on two Portuguese coastal areas. *Safety and Reliability: Methodology and Applications*, pp.1581-1588.

Bencheqroun, S., Omira, R., Baptista, M.A., El Mouraouah, A., Brahim, A.I. and Toto, E.A., 2015. Tsunami impact and vulnerability in the harbour area of Tangier, Morocco. *Geomatics, Natural Hazards and Risk*, 6(8), pp.718-740.

Birkmann, J., 2006. *Measuring Vulnerability to Natural Hazards – Towards Disaster Resilient Societies*. United Nations University Press, Tokyo, Japan, 450 pp

Bozkurt, E., 2001. Neotectonics of Turkey—a synthesis. *Geodinamica acta*, 14(1-3), pp.3-30.

Çankaya, Z.C., 2015. High Resolution Tsunami Vulnerability Assessment By Gis-Based Multi-Criteria Decision Making Analysis At Yenikapi, İstanbul (MSc Dissertation, Middle East Technical University).

Cankaya, Z.C., Suzen, M.L., Yalçınler, A.C., Kolat, C., Zaytsev, A. and Aytore, B., 2016. A new GIS-based tsunami risk evaluation: MeTHuVA (METU tsunami human vulnerability assessment) at Yenikapi, Istanbul. *Earth, Planets and Space*, 68(1), p.133.

Cardona, O.D., M.K. van Aalst, J. Birkmann, M. Fordham, G. McGregor, R. Perez, R.S. Pulwarty, E.L.F. Schipper, and B.T. Sinh, 2012. Determinants of risk: exposure and vulnerability. In: *Managing the Risks of Extreme Events and*

Disasters to Advance Climate Change Adaptation [Field, C.B., V. Barros, T.F. Stocker, D. Qin, D.J. Dokken, K.L. Ebi, M.D. Mastrandrea, K.J. Mach, G.-K. Plattner, S.K. Allen, M. Tignor, and P.M. Midgley (eds.)]. A Special Report of Working Groups I and II of the Intergovernmental Panel on Climate Change (IPCC). Cambridge University Press, Cambridge, UK, and New York, NY, USA, pp. 65-108.

Carver, S.J., 1991. Integrating multi-criteria evaluation with geographical information systems. *International Journal of Geographical Information System*, 5(3), pp.321-339.

Cheung, K.F., Phadke, A.C., Wei, Y., Rojas, R., Douyere, Y.M., Martino, C.D., Houston, S.H., Liu, P.F., Lynett, P.J., Dodd, N. and Liao, S., 2003. Modeling of storm-induced coastal flooding for emergency management. *Ocean Engineering*, 30(11), pp.1353-1386.

Collins, M.G., Steiner, F.R. and Rushman, M.J., 2001. Land-use suitability analysis in the United States: historical development and promising technological achievements. *Environmental management*, 28(5), pp.611-621.

Courtland, L., Connor, C., Connor, L. and Bonadonna, C., 2012. Introducing Geoscience Students to Numerical Modeling of Volcanic Hazards: The example of Tephra2 on VHub. *org. Numeracy*, 5(2).

Dalgıç S., Turgut M., Kuşku İ., Coşkun İ., Coşgun T., 2009. İstanbul'un Avrupa Yakasındaki Zemin ve Kaya Koşullarının Bina Temellerine Etkisi, *Uygulamalı Yer Bilimleri* (2), 47-70.

Dall'Osso, F., Maramai, A., Graziani, L., Brizuela, B., Cavalletti, A., Gonella, M. and Tinti, S., 2010. Applying and validating the PTVA-3 Model at the Aeolian Islands, Italy: assessment of the vulnerability of buildings to tsunamis. *Nat. Hazards Earth Syst. Sci.*, 10(7), 1547–1562.

Dall'Osso, F., Gonella, M., Gabbianelli, G., Withycombe, G. and Dominey-Howes, D., 2009a. Assessing the vulnerability of buildings to tsunami in Sydney. *Natural Hazards and Earth System Sciences*, 9(6), pp.2015-2026.

Dall'Osso, F., Gonella, M., Gabbianelli, G., Withycombe, G. and Dominey-Howes, D., 2009b. A revised (PTVA) model for assessing the vulnerability of buildings to tsunami damage. *Natural Hazards and Earth System Sciences*, 9(5), pp.1557-1565.

Dilmen, D.I., Kemec, S., Yalçın, A.C., Düzgün, S. and Zaytsev, A., 2015. Development of a Tsunami Inundation Map in Detecting Tsunami Risk in Gulf of Fethiye, Turkey. *Pure and Applied Geophysics*, 172(3-4), pp.921-929.

Dominey-Howes, D. and Papathoma, M., 2007. Validating a tsunami vulnerability assessment model (the PTVA Model) using field data from the 2004 Indian Ocean tsunami. *Natural Hazards*, 40(1), pp.113-136.

Dominey-Howes, D., Dunbar, P., Varner, J. and Papathoma-Köhle, M., 2010. Estimating probable maximum loss from a Cascadia tsunami. *Natural hazards*, 53(1), pp.43-61.

Eastman, J.R., 1995. *GIS and decision making*. Unitar.

Eckert, S., Jelinek, R., Zeug, G. and Krausmann, E., 2012. Remote sensing-based assessment of tsunami vulnerability and risk in Alexandria, Egypt. *Applied Geography*, 32(2), pp.714-723.

Fischer, T., Alvarez, M., De la Llera, J.C. and Riddell, R., 2002. An integrated model for earthquake risk assessment of buildings. *Engineering Structures*, 24(7), pp.979-998.

Gambolati, G., Teatini, P. and Gonella, M., 2002. GIS simulations of the inundation risk in the coastal lowlands of the Northern Adriatic Sea. *Mathematical and Computer Modelling*, 35(9), pp.963-972.

Ghobarah, A., Saatcioglu, M. and Nistor, I., 2006. The impact of the 26 December 2004 earthquake and tsunami on structures and infrastructure. *Engineering structures*, 28(2), pp.312-326.

Guidoboni, E. and Comastri, 2005. A.: *Catalogue of earthquakes and tsunamis in the Mediterranean Area from the 11th to the 15th century*, ISBN: 88-85213-10-3, Istituto Nazionale di Geofisica e Vulcanologia, Italy.

Guidoboni, E., Comastri, A. and Traina, G., 1994. *Catalogue of Ancient Earthquakes in the Mediterranean Area up to the 10th Century (Vol. 1)*. Istituto Nazionale di Geofisica, Rome.

Gürer, Ö.F., Kaymakçı, N., Çakır, Ş. and Özburan, M., 2003. Neotectonics of the southeast Marmara region, NW Anatolia, Turkey. *Journal of Asian Earth Sciences*, 21(9), pp.1041-1051.

Hart, D.E. and Knight, G.A., 2009. Geographic information system assessment of tsunami vulnerability on a dune coast. *Journal of Coastal Research*, pp.131-141.

Hébert, H., Schindele, F., Altinok, Y., Alpar, B. and Gazioglu, C., 2005. Tsunami hazard in the Marmara Sea (Turkey): a numerical approach to discuss active faulting and impact on the Istanbul coastal areas. *Marine Geology*, 215(1), pp.23-43.

Heidarzadeh, M., Krastel, S. and Yalçiner, A.C., 2014. The state-of-the-art numerical tools for modeling landslide tsunamis: a short review. In *Submarine Mass Movements and Their Consequences* (pp. 483-495). Springer International Publishing.

Imamura, F., 1996. Review of tsunami simulation with a finite difference method. *Long-wave runup models*, pp.25-42.

IMM, 2015, Jeoloji Haritası, retrieved from http://www.ibb.gov.tr/tr-TR/SubSites/DepremSite/Documents/EK2_Jeoloji_Haritasi_1440x910_25000_300DPI.pdf, last visited on September, 2014

IMM, İstanbul Mikro bölgeleme Projesi, Avrupa Yakası, 2007. İstanbul Metropolitan Municipality (IMM)

Ismail, H., Wahab, A.A., Amin, M.M., Yunus, M.M. and Sidek, F.J., 2012. A 3-tier tsunami vulnerability assessment technique for the north-west coast of Peninsular Malaysia. *Natural hazards*, 63(2), pp.549-573.

Jenkins, L., 2000. Selecting scenarios for environmental disaster planning. *European Journal of Operational Research*, 121(2), pp.275-286.

Joerin, F., Thériault, M. and Musy, A., 2001. Using GIS and outranking multicriteria analysis for land-use suitability assessment. *International Journal of Geographical information science*, 15(2), pp.153-174.

Kuran, U. and Yalçiner, A.C., 1993. Crack propagations, earthquakes and tsunamis in the vicinity of Anatolia. In *Tsunamis in the World* (pp. 159-175). Springer Netherlands.

Leone, F., Lavigne, F., Paris, R., Denain, J.C. and Vinet, F., 2011. A spatial analysis of the December 26th, 2004 tsunami-induced damages: Lessons learned for a better risk assessment integrating buildings vulnerability. *Applied Geography*, 31(1), pp.363-375.

Liu, P.L., Woo, S.B. and Cho, Y.S., 1998. Computer programs for tsunami propagation and inundation. Cornell University.

Liu, P.L.F., Cho, Y.S., Yoon, S.B. and Seo, S.N., 1995. Numerical simulations of the 1960 Chilean tsunami propagation and inundation at Hilo, Hawaii. In *Tsunami: progress in prediction, disaster prevention and warning* (pp. 99-115). Springer Netherlands.

Malczewski, J. and Rinner, C., 2015. *Multicriteria decision analysis in geographic information science*. New York, NY, USA: Springer.

Malczewski, J., 1996. A GIS-based approach to multiple criteria group decision-making. *International Journal of Geographical Information Systems*, 10(8), pp.955-971.

Malczewski, J., 1999. *GIS and multicriteria decision analysis*. John Wiley & Sons.

Malczewski, J., 2000. On the use of weighted linear combination method in GIS: common and best practice approaches. *Transactions in GIS*, 4(1), pp.5-22.

Manyena, S.B., 2006. The concept of resilience revisited. *Disasters*, 30(4), pp.434-450.

- Marinoni, O., 2004. Implementation of the analytical hierarchy process with VBA in ArcGIS. *Computers & Geosciences*, 30(6), pp.637-646.
- Martin, N.J., Onge, B.S. and Waaub, J.P., 1999. An integrated decision aid system for the development of Saint Charles River alluvial plain, Quebec, Canada. *International Journal of Environment and Pollution*, 12(2-3), pp.264-279.
- McHarg, I.L. and Mumford, L., 1969. *Design with nature* (pp. 7-17). New York: American Museum of Natural History.
- Mercier, J.L., Sorel, D., Vergely, P. and Simeakis, K., 1989. Extensional tectonic regimes in the Aegean basins during the Cenozoic. *Basin research*, 2(1), pp.49-71.
- Murthy, M.R., Usha, T., Pari, Y. and Reddy, N.T., 2011. Tsunami vulnerability assessment of Cuddalore using numerical model and GIS. *Marine Geodesy*, 34(1), pp.16-28.
- NAMI DANCE (2016). *NAMI DANCE Manual*. Ankara, Turkey: METU. Available online at <http://namidance.ce.metu.edu.tr/pdf/NAMIDANCE-version-5-9-manual.pdf>.
- Omira, R., Baptista, M.A., Miranda, J.M., Toto, E., Catita, C. and Catalao, J., 2010. Tsunami vulnerability assessment of Casablanca-Morocco using numerical modelling and GIS tools. *Natural hazards*, 54(1), pp.75-95.
- Onat, Y. and Yalçiner, A.C., 2013. Initial stage of database development for tsunami warning system along Turkish coasts. *Ocean Engineering*, 74, pp.141-154.
- OYO-IMM, O. a. (2008). *Project report on simulation and vulnerability analysis of Tsunamis affecting the İstanbul Coasts*. İstanbul: OYO Int. Co. (Japan) for İstanbul Metropolitan Municipality (IMM)
- Özçiçek, B., 1996. 18 Eylül 1963 Doğu Marmara depremi etüdü, *Jeofizik*, 1(2), 49-69, (in Turkish).
- Ozer, C. and Yalçiner, A.C., 2011. Sensitivity study of hydrodynamic parameters during numerical simulations of tsunami inundation. *Pure and applied geophysics*, 168(11), pp.2083-2095.
- Ozer, C., 2012. *Tsunami Hydrodynamics in Coastal Zones* (Doctoral dissertation, PhD. Thesis, Middle East Technical University, Ankara, Turkey).
- Özgül N., Özcan İ., Akmeşe İ., Üner K., Bilgin İ., Korkmaz R., Yıldırım Ü., Yıldız Z., Akdağ Ö., Tekin M., 2011. *İstanbul İl Alanının Jeolojisi*, İstanbul Büyükşehir Belediyesi, İstanbul.
- Öztin, F. and Bayülke, N., 1990. *Historical earthquakes of Istanbul, Kayseri, Elazığ*. Ankara: Earthquake Research Department, General Directorate of Disaster Affairs, Ministry of Public Works and Settlement Report, pp.85-95.

Papadopoulos, G.A., 1993, August. Seismic faulting and nonseismic tsunami generation in Greece. In Proc. IUGG/IOC International Tsunami Symposium, pp. 23-27.

Papadopoulos, G.A., Gràcia, E., Urgeles, R., Sallares, V., De Martini, P.M., Pantosti, D., González, M., Yalçiner, A.C., Mascle, J., Sakellariou, D. and Salamon, A., 2014. Historical and pre-historical tsunamis in the Mediterranean and its connected seas: geological signatures, generation mechanisms and coastal impacts. *Marine Geology*, 354, pp.81-109.

Papathoma, M. and Dominey-Howes, D., 2003. Tsunami vulnerability assessment and its implications for coastal hazard analysis and disaster management planning, Gulf of Corinth, Greece. *Natural Hazards and Earth System Science*, 3(6), pp.733-747.

Papathoma, M., Dominey-Howes, D., Zong, Y. and Smith, D., 2003. Assessing tsunami vulnerability, an example from Herakleio, Crete. *Natural Hazards and Earth System Science*, 3(5), pp.377-389.

Pereira, J.M. and Duckstein, L., 1993. A multiple criteria decision-making approach to GIS-based land suitability evaluation. *International Journal of Geographical Information Science*, 7(5), pp.407-424.

Reese, S., Cousins, W.J., Power, W.L., Palmer, N.G., Tejakusuma, I.G. and Nugrahadi, S., 2007. Tsunami vulnerability of buildings and people in South Java—field observations after the July 2006 Java tsunami. *Natural Hazards and Earth System Sciences*, 7(5), pp.573-589.

Saaty. T.L., 1980, *The Analytic Hierarchy Process*, McGraw-Hill

Santos, A., Fonseca, N., Pereira, S., Zezere, J.L. and Koshimura, S., 2012. Tsunami risk assessment at Figueira da Foz, Portugal. 15 WCEE.

Şengör A.M.C., Görür, N., Şaroğlu, F., 1985. Strike–slip faulting and related basin formation in zones of tectonic escape: Turkey as a case study. In: Biddle, K.T., Christie-Blick, N. (Eds.), *Strike–Slip Deformation, Basin Formation and Sedimentation*, Special Publication Society of Economic Paleontology and Mineralogy No. 37, pp. 227–264.

Sinaga, T.P., Nugroho, A., Lee, Y.W. and Suh, Y., 2011. GIS mapping of tsunami vulnerability: Case study of the Jembrana Regency in Bali, Indonesia. *KSCE Journal of Civil Engineering*, 15(3), pp.537-543.

Smith, A.D., Taymaz, T., Oktay, F., Yüce, H., Alpar, B., Başaran, H., Jackson, J.A., Kara, S. and Şimşek, M., 1995. High-resolution seismic profiling in the Sea of Marmara (northwest Turkey): Late Quaternary sedimentation and sea-level changes. *Geological Society of America Bulletin*, 107(8), pp.923-936.

Soloviev, S. L., Solovieva, O. N., Go, C. N., Kim, K. S., and Shchetnikov, N. A., 2000. *Tsunamis in the Mediterranean Sea 2000 B.C.– 2000 A.D.*, Kluwer Academic Publishers, Netherlands, pp. 237.

Soysal, H., 1985. Tsunami (deniz taşması) ve Türkiye kıyılarını etkileyen tsunamiler. *Istanb. Univ. Bull. Mar. Sci. Geogr.* 2, 59-67

Soysal, H., Sipahioglu, S., Kolcak, D. and Altinok, Y., 1981. *Türkiye ve Cevresinin Tarihsel Deprem Katalogu MO 2100-MS 1900*. TUBITAK project Tbag, 341.

Sozdinler, C.O., Yalçiner, A.C. and Zaytsev, A., 2015. Investigation of Tsunami Hydrodynamic Parameters in Inundation Zones with Different Structural Layouts. *Pure and Applied Geophysics*, 172(3-4), pp.931-952.

Steinitz, C., Parker, P. and Jordan, L., 1976. Hand drawn overlays: their history and prospective uses. *Landscape architecture*, 66(5), pp.444-455.

Suppasri, A., Charvet, I., Macabuag, J., Rossetto, T., Leelawat, N., Latcharote, P. And Imamura, F., 2015. Building Damage Assessment and Implications for Future Tsunami Fragility Estimations. In: Esteban, M., Takagi, H. and Shibayama, T. eds., 2015. *Handbook of coastal disaster mitigation for engineers and planners*. Butterworth-Heinemann, pp 147-178.

Tadepalli, S. and Synolakis, C.E., 1996. Model for the leading waves of tsunamis. *Physical Review Letters*, 77(10), p.2141.

Tarbotton, C., Dominey-Howes, D., Goff, J.R., Papatoma-Kohle, M., Dall'Osso, F. and Turner, I.L., 2012. GIS-based techniques for assessing the vulnerability of buildings to tsunami: current approaches and future steps. *Geological Society, London, Special Publications*, 361(1), pp.115-125.

Thomas, L.S., 1980. *The analytic hierarchy process*. McGraw-Hill International.

Thywissen, K., 2006. Core terminology of disaster reduction: A comparative glossary. *Measuring vulnerability to natural hazards: Towards disaster resilient societies*, pp.448-496.

Tinti, S., Maramai, A. and Graziani, L., 2001. A new version of the European tsunami catalogue: updating and revision. *Natural Hazards and Earth System Science*, 1(4), pp.255-262.

Titov, V.V. and Synolakis, C.E., 1998. Numerical modeling of tidal wave runup. *Journal of Waterway, Port, Coastal, and Ocean Engineering*, 124(4), pp.157-171.

Tufekci, S., 1995. An integrated emergency management decision support system for hurricane emergencies. *Safety Science*, 20(1), pp.39-48.

UNISDR, 2009: Terminology on Disaster Risk Reduction. United Nations International Strategy for Disaster Reduction, Geneva, Switzerland. unisdr.org/eng/library/lib-terminology-eng.htm.

Usha, T., Murthy, M.R., Reddy, N.T. and Mishra, P., 2012. Tsunami vulnerability assessment in urban areas using numerical model and GIS. *Natural hazards*, 60(1), pp.135-147.

Villagrán De León, J.C., 2004. Manual para la estimación cuantitativa de riesgos asociados a diversas amenazas. Acción contra el Hambre. Oficina de Asuntos Humanitarios de la Comunidad Europea (ECHO). Villa Tek. Guatemala. Coordinadora Nacional para la Reducción de Desastres. sfsl.

Wikipedia. 2015. Türkiye'nin coğrafi bölgeleri. [ONLINE] Available at: https://tr.wikipedia.org/wiki/T%C3%BCrkiye%27nin_co%C4%9Frafii_b%C3%B6lgeleri. [Accessed 24 August 2016]

Wikipedia. 2016. Bakırköy. [ONLINE] Available at: <https://en.wikipedia.org/wiki/Bak%C4%B1rk%C3%B6y>. [Accessed 24 August 2016].

Wisner B., Blaikie P., Cannon T., Davis I., 2004. At risk: natural hazards, people's vulnerability and disasters. Routledge, 2nd edn. p 284

Wood, N. and Stein, D., 2001. A GIS-based vulnerability assessment of Pacific Northwest ports and harbours to tsunami hazards. In Proceedings of International Tsunami Symposium (ITS 2001), Session (Vol. 1, pp. 1-13).

Wood, N., 2009. Tsunami exposure estimation with land-cover data: Oregon and the Cascadia subduction zone. *Applied Geography*, 29(2), pp.158-170.

Wood, N.J. and Good, J.W., 2004. Vulnerability of port and harbor communities to earthquake and tsunami hazards: The use of GIS in community hazard planning. *Coastal Management*, 32(3), pp.243-269.

Wood, N.J., 2002. Vulnerability of port and harbor communities to earthquake and tsunami hazards in the Pacific Northwest. Unpublished PhD dissertation, Department of Geosciences, Oregon State University

Yalçiner, A.C., 1999. 1999 İzmit Tsunamisi. TÜBİTAK, Bilim Tek. 383, 34-39

Yalçiner, A.C., Alpar, B., Altınok, Y., Özbay, İ. and Imamura, F., 2002. Tsunamis in the Sea of Marmara: Historical documents for the past, models for the future. *Marine Geology*, 190(1), pp.445-463.

Yalçiner A. C. and Aytöre B., 2012. Presentations in the "Training Course on Tsunami Hazard Assessment for Nuclear Power Plants", organized by IAEA, Vienna, August, 2012.

Yalçiner, A.C., Gülkan, P., Dilmen, D.I., Aytore, B., Ayca, A., Insel, I. and Zaytsev, A., 2014. Evaluation of tsunami scenarios for western Peloponnese, Greece. *Bollettino di Geofisica Teorica ed Applicata*, 55(2).

Yalçiner, A.C., Ozer, C., Karakus, H., Zaytsev, A. and Guler, I., 2011. Evaluation of coastal risk at selected sites against Eastern Mediterranean tsunamis. *Coastal Engineering Proceedings*, 1(32), p.10.

Zaytsev, A.I., Pelinovsky, E.N., Kurkin, A.A., Kostenko, I.S. and Yalçiner, A., 2016. The possibility of tsunami in the Sea of Okhotsk caused by deep-focus earthquakes. *Izvestiya, Atmospheric and Oceanic Physics*, 52(2), pp.217-224.

Zhu, X. and Dale, A.P., 2001. JavaAHP: a web-based decision analysis tool for natural resource and environmental management. *Environmental Modelling & Software*, 16(3), pp.251-262.